Predicting Retention of Diluted Bitumen in Marine Shoreline Sediments, Southeastern Vancouver Island, British Columbia, Canada

by

Lee Allen Sean Britton

B.Sc. University of Victoria, 2015

A Thesis Submitted in Partial Fulfilment of the

Requirements for the Degree of

MASTER OF SCIENCE

in the Department of Geography

Supervisory Committee

Predicting Retention of Diluted Bitumen in Marine Shoreline Sediments,

Southeastern Vancouver Island, British Columbia, Canada

by

Lee Allen Sean Britton

B.Sc. University of Victoria, 2015

Supervisory Committee

Dr. John R. Harper (Department of Geography)
(Co-Supervisor)

Dr. Dan. J. Smith (Department of Geography)
(Co-Supervisor)

Dr. James Gardner (Department of Geography)
(Committee Member)

Supervisory Committee

Dr. John R. Harper (Department of Geography)
(Co-Supervisor)

Dr. Dan. J. Smith (Department of Geography)
(Co-Supervisor)

Dr. James Gardner (Department of Geography)
(Committee Member)

Abstract

Canada has become increasingly economically dependent on the exportation of bitumen to trans-oceanic international markets. As the export of Alberta bitumen from ports located in British Columbia increases, oil spill response and readiness measures become increasingly important. Although the frequency of ship-source oil spills has dramatically declined over the past several decades, they remain environmentally devastating when they occur. In the event of a marine spill, great lengths of shoreline are at risk of being contaminated. Once ashore, oil can persist for decades if shoreline hydraulic conditions are correct and remediation does not occur. Most commonly transported oils (e.g., fuel oils, Bunker C, crude oil, etc.) have been thoroughly studied, and their fate and behaviour in the event of a marine spill is well understood. In contrast, because diluted bitumen has been historically traded in relatively low quantities and has almost no spill history, there is a sizable knowledge gap regarding its effects and behaviour in the marine environment and on coastal shorelines.

The intent of this thesis was to develop a classification scheme to identify marine shorelines of high and low diluted bitumen (dilbit) retention for southeastern Vancouver Island,

British Columbia. This study builds upon the outcome of former laboratory bench top dilbit and sediment research known as Bitumen Experiments (Bit_Ex). Bit_Ex investigated dilbit penetration and retention in six engineered sediment classifications ranging from coarse sand to very large pebble in accordance with the Wentworth Classification scheme. This research used Bit_Ex findings to predict dilbit retention in poorly sorted *in-situ* beach sediments found on shorelines representative of the southern coast of Vancouver Island, British Columbia, Canada.

Field and laboratory measurements were conducted to document the occurrence of *in-situ* shoreline sediments and hydraulic conditions and were used to predict dilbit retention by comparing such characteristics between Bit_Ex and unconsolidated *in-situ* beach sediments. Saturated hydraulic conductivity (Ks) was measured using a double-ring constant-head infiltrometer. Measured Ks values were then compared to predicted Ks values generated by five semi-empirical Ks equations. A modified version of the Hazen Approximation was selected as the most appropriate. Using measured and calculated metrics, sediments were grouped as having either low or high dilbit retention. When sediments were analysed as homogenous samples, the experimental results suggested two of ten shorelines were composed of a combination of low and high retention sections, while the remaining eight sites were of low retention. Upon the isolation of coarse surface strata, results indicated two shorelines were entirely veneered with high retention sediments, and four shorelines were a combination of high and low retention. The residual four shorelines were found to be entirely composed of low retention sediments. The results illuminate the

importance of shoreline stratification when predicting shoreline oil retention. This characteristic is a factor that current shoreline oil retention mapping techniques do not adequately consider. Additionally, the findings suggest that while sediments indicative of retaining weathered dilbit are relatively uncommon within Juan de Fuca and Harro Straits, high retention unweathered dilbit sediments are more common.

Table of Contents

List of Figures

List of Tables

List of Abbreviations

AWB	Access Western Blend
AWB W0	Unweathered Access Western Blend
AWB W2	Weathered Access Western Blend
Bit_Ex	Diluted Bitumen Experiments (Harper *et al.* 2016)
CEDD	Coastal Erosion and Dune Dynamics
CLB	Cold Lake Blend
CLB W0	Unweathered Cold Lake Blend
CLB W2	Weathered Cold Lake Blend
CRD	Capital Regional District
DCI	Double-Ring Constant-Head Infiltrometer
IFO 180	International Fuel Oil 180
Ks	Saturated Hydraulic Conductivity
MAE	Mean Absolute Error
SARA	Saturates Aromatics Resins Asphaltines
S1P2	Site 1 Plot 2
S1P14	Site 1 Plot 14
S1P14(s1)	Site 1 Plot 14 strata 1
S1P19-20	Site 1 Plot 19-20
S1P26	Site 1 Plot 26
S1P26(s1)	Site 1 Plot 26 strata 1
S2P4	Site 2 Plot 4
S2P14	Site 2 Plot 14
S2P16	Site 2 Plot 16
S2P16(s1)	Site 2 Plot 16 strata 1
S2P21	Site 2 Plot 21
S3P28	Site 3 Plot 28
S3Pn	Site 3 Plot nude beach
S4P8	Site 4 Plot 8
S4P17	Site 4 Plot 17
S5P2	Site 5 Plot 2
S5P9	Site 5 Plot 9
S5P9(s1)	Site 5 Plot 9 strata 1
S5P9(s2)	Site 5 Plot 9 strata 2
S5P9(s3)	Site 5 Plot 9 strata 3
S5P9(s4)	Site 5 Plot 9 strata 4
S5P9(s5)	Site 5 Plot 9 strata 5
S5P16	Site 5 Plot 16
S6P10	Site 6 Plot 10
S6P10(s1)	Site 6 Plot 10 strata 1
S6P10(s2)	Site 6 Plot 10 strata 2
S6P56	Site 6 Plot 56
S6P144	Site 6 Plot 144

S6P156	Site 6 Plot 156
S6P156(s1)	Site 6 Plot 156 strata 1
S6P174	Site 6 Plot 174
S7P7	Site 7 Plot 7
S7P12	Site 7 Plot 12
S8P10	Site 8 Plot 10
S8P10(s1)	Site 8 Plot 10 strata 1
S8P10(s2)	Site 8 Plot 10 strata 2
S8P14	Site 8 Plot 14
S8P22	Site 8 Plot 22
S9P1	Site 9 Plot 1
S9P1(s1)	Site 9 Plot 1 strata 1
S9P6	Site 9 Plot 6
S9P6(s1)	Site 9 Plot 6 strata 1
S10P1	Site 10 Plot `
S10P1(s1)	Site 10 Plot 1 strata 1
TMEP	Trans Mountain Expansion Project

Acknowledgements

My ability to complete this thesis was directly related to the people who have encouraged and supported me throughout this process and in my life. I am indebted to many, but I must first start with my sister and mentor Catharine Galbrand. Catharine is someone that I have continually admired for as long as I can remember. Catharine is ten years my senior and showed me, through example, the importance of setting goals and how persistence, tenacity, and independence makes achieving those goals that much sweeter. She continues to be the most reliable, encouraging, and accepting person in my life; for that I will never be able to thank her enough.

To Dr. John Harper, this entire endeavor would never have come to fruition if it was not for your confidence in my ability to play with oil and sand. I cannot thank you enough for your encouragement, support, and mentorship. I feel honored to have had you as part of my committee. I look forward to many more journeys aboard the Golden Dawn and others, all of which should be complemented by Fat Tug or some other more enjoyable beer.

I am very thankful to Brian House at Moran Coastal & Ocean Resources (MCORI) and Moran Environmental Recovery (MER) for his continued support throughout my Masters. Brian is located in Boston, MA and although he is across the continent, he has taken great interest in not only this project but in me and my success. I am very thankful to be considered part of the MER team and for his constant mentorship.

Dr. Dan Smith, I feel it is rare to come across a seasoned academic that is as accepting and flexible as you are. You welcomed me into the UVTRL with no reservations and included me in your many adventures deep into the mountains and far away from where my research was conducted. Thank you for making me feel so welcomed in your lab, for your support, and most importantly, for asking relevant questions at the end of my defense.

If there is one person's life that I would love to mimic it would be Dr. James Gardner's. He has spent his life exploring, understanding, and teaching people about the world in which we live. He finds secrets to discover intrigue in the most unexpected places and dives in with no apprehensions. I truly admire him and am thankful to have had him on my committee.

Less formally, I would like to thank my friends. Completing this thesis did not come without support from the people I love and admire. I feel lucky to have spent even a fraction of my life getting to know them. Firstly, the numerous friends and colleagues at the University of Victoria. The UVTRL was full of gems. Thanks to BJ Mood, Anna Galbraith, Lauren Farmer (lowlow), Bethany Coulthard, and Jill Harvey. The former SEDD lab provided their fair share of moral and mental support. Thanks to Michael Grilliot, Alana Rader, Juan Felipe Gomez, and Alex Lausanne, and I truly hope this is not the last time our paths cross. To my closest friends, Al and Jeanny Britton, Calvin Stuckert, Brian Dalrymple, Sana Golden, Tommy Forss, Ashleigh Britton, Melanie Galbrand, Hayden Thomson, Sam Dalrymple, and Brian and Linda Stuckert. I am excited to adventure with you again more regularly. Finally, I'd like to thank Alexis Petrunia, Dr. Dave Atkinson, Dr. Dan Peters, Ben Bapsy, Mohammed Elgundi, and Jason Chalifour for their support and encouragement over the past two years, it did not go unnoticed.

I owe my current and future success to these people and many others that have helped me along the way. They have given me their patience, time, and respect. I hope to be a hybrid of all of you someday ☺.

1 Chapter One: Introduction

1.1 Introduction

When oil spills occur in coastal environments, the oil is likely to be stranded on shore by local winds and currents. If stranded above the swash line, shoreline hydraulics and the fluid property of the oil largely determine where and how much oil will be retained by unconsolidated sediments (Freeze and Cherry 1979, Etkin *et al.* 2008, Xia *et al.* 2010, Geng *et al.* 2014). Previous sediment oil retention research has focused on homogeneous light, medium, and heavy oil products (Harper *et al.* 1995, Peterson *et al.* 2003, Short *et al.* 2004, Owens *et al.* 2008, Alrodini 2015). Such research has improved our understanding of oil and sediment interactions, as well as the long-term environmental persistence of oil on shorelines although, a comparitively new prodict, diluted bitumen (dilbit), is yet to be is not yet well understood (Imhoff *et al.* 2003, Gerhard *et al.* 2007, Owens *et al.* 2008, Shigenaka 2011, Fingas 2015a, Muñoz *et al.* 2016).

The behaviour and consequences of dilbit spills on shorelines is relatively unknown. Consisting of a heterogeneous blend of hydrocarbons from Alberta's bitumen deposits (GOC 2013), dilbit is a blend of two refined hydrocarbon products: a low viscosity, highly volatile component (diluent) and a high viscosity relatively non-volatile component (bitumen) (GOC 2013, NRC 2013, Harper *et al.* 2016). The fluid properties of the two constituents vary independently once dilbit has been spilled (GOC 2013, Etkin *et al.* 2015), altering the way in which it interacts with shoreline sediments, as well as its impacts on

shorelines. The significance of dilbit weathering and its relationships to shoreline oil retention modelling remains largely unknown (Brown *et al.* 1991, GOC 2013, WO 2013, Harper *et al.* 2016).

The projected increase in dilbit transport and transoceanic exportation from Vancouver, British Columbia (Figure 1.1), resulting from the Trans Mountain Expansion project (TMEP), has been accompanied by a perceived increased risk of marine oil and dilbit spills

Figure 1.1 - Standard transportation route of ships carrying dilbit to transpacific ports (modified from LO 2013), highlighting the location of the Salish Sea (including the Juan de Fuca Strait) and the North Pacific Ocean surrounding southern Vancouver Island (modified from Google Inc. 2016, Worldatlas 2016)

(Winter and Haddad 2014, Joeckel *et al.* 2015). To address concerns about the impact of dilbit spills on coastal shorelines, the Government of Canada funded the Bit_Ex project (Harper *et al.* 2016). Designed as a labratory bench-top scale study, the experiment examined dilbit penetration and retention in uniform sediments in an experimental setting. Overall, Bit_Ex showed that fresh dilbit freely penetrates sediments composed of very coarse sand or larger sediments, while weathered dilbit freely penetrates granules and coaser sediments. Additionally, Bit_Ex found that when sediments were submerged (simulating high tide) in sea water, very coarse sand and granules retained the most unweathered dilbit, while granules to large pebbles retained the highest percentage of weathered dilbit (Harper *et al.* 2016). A recommendation arising from Bit_Ex was that an *in-situ* experiment be completed to assess the behaviour of weathered and unweathered dilbit in shoreline sediments in Pacific Canada.

1.2 Purpose and research objectives

The purpose of this research was to refine the current understanding of dilbit contamination on natural shorelines and to identify shorelines of high retention within the study region. The specific objectives of the research were:

Objective 1: To measure the hydraulic properties of shoreline sediments.

Objective 2: To evaluate the ability of *in-situ* sediments to transmit both unweathered (fresh state) and moderately weathered dilbit to describe retention.

Objective 3: To make recommendations to aid in emergency response planning and risk mapping for dilbit.

1.3 Study area

The study area encompasses the southeastern tip of Vancouver Island, British Columbia, Canada. Southeastern Vancouver Island is bordered on the west by the North Pacific Ocean, on the east by the Salish Sea, and to the south the Juan de Fuca Strait connects these two bodies of water (Figure 1.1). Sea cliffs and pocket beaches dominate coastlines within the region. Sea cliffs are considered to have low oil retention potential, and it is assumed that dilbit spills would have little lasting impact on such a coastline type. On the other hand, pocket beaches consisting of unconsolidated sand, gravel and cobble deposits are locations where spilled diblit is expected to have significant and long-lasting impacts and are the primary focus of this study.

1.4 Methods

The research was completed by first identifying pocket beaches within the study area by querying a dataset known as ShoreZone, which inventories shoreline geomorphic and biological variations, for representative unconsolidated sediment shorelines. Using random stratified sampling, random plots were selected on each beach for *in-situ* measurements and sampling. At each selected beach, sediment samples were obtained for laboratory analysis and *in-situ* hydraulic properties were measured by means of a double-ring constant-head infiltrometer. Saturated hydraulic conductivity (Ks) of the shoreline sediment was calculated and compared to measured Ks to select the most appropriate Ks model for predicting dilbit transmission through the sediment. *In-situ* dilbit Ks results, in conjunction with Bit_Ex findings, were then used to infer dilbit retention.

1.5 Thesis format

This thesis consists of five chapters. Following this chapter, Chapter 2 provides an overview of current scientific knowledge relating to oil and dilbit spill behaviour, associated environmental persistence, and a brief explanation of regional shoreline geomorphology. Chapter 3 describes the methods employed for site selection, field data collection, and laboratory analysis of data. Results are summarised in Chapter 4. Chapter 5 discusses the research findings, presents recommendations, and offers suggestions for further research.

2 Chapter Two: Literature Review

2.1 Introduction

Petroleum products are currently the world's largest traded commodity, with production and consumption forecasted to expand until at least 2035 (Santos *et al.* 2014). As of 2016, Canada was the fourth largest petroleum exporter in the world (IEA and OECD 2016). From 2009 to 2013 the Canadian oil industry nearly doubled in value, growing from 68.3 billion to 130.7 billion dollars (Brokaw 2012; ITC 2015; Workman 2015).

Crude oil is Canada's largest exported hydrocarbon (Al-Zyoud and Elloumi 2017). Although a relatively new product, dilbit is expected to soon equal crude oil in this regard (Mcknight *et al.* 2015). With an estimated 1.8 trillion barrels, Canada possesses the world's largest deposit of bituminous sediments and the third largest known petroleum reserves after Saudi Arabia and Venezuela (Chilingarian 2011; Banerjee 2012; AEUB 2015). Currently, the majority of Canadian dilbit is exported to the United States, although in the near future the Canadian petroleum industry will begin exporting dilbit to India and China (EIA 2014; Li and Amorelli 2016). Delivering bitumen to transoceanic markets firstly requires overland transport. To facilitate this, a diluent is added to the bitumen, changing bitumen to diluted bitumen or "dilbit".

In Canada, Kinder Morgan, Inc., received conditional approval to expand the existing pipeline connecting Alberta to Burnaby on the British Columbia coast with the TMEP (TC

2015). Using an existing right-of-way, the TMEP will expand the pipeline capacity from 300,000 to 890,000 barrels of dilbit per day (KM 2015). After arriving in Burnaby the dilbit will be transported by tanker to transoceanic markets through the Port of Vancouver, the Salish Sea, and Strait of Juan de Fuca to the North Pacific Ocean, passing several of the most densely populated regions in British Columbia, including the Vancouver Metropolitan area and the Victoria Capital Region District (CRD) (Foster *et al.* 2010; LO 2013).

Dilbit has been shipped in relatively small volumes over this route for approximately 40 years, with no recorded marine transportation-related spills to date (KM 2015, McKnight *et al.* 2015). The TMEP will increase the number of dilbit shipments from ~100 to ~300 ships per year (TC 2013). With such a significant increase in volume and traffic, there comes perceived long-term risks associated with accidental spills of dilbit (King *et al.* 2014).

Oil spills are damaging to the environment due to the toxic nature of oil's chemical constituents, their long-term environmental persistence (weeks to decades), and the invasive processes which are required for remediation (Doerffer 1992; Owens *et al.* 2008 Etkin 2015). Furthermore, oil spilled in marine environments disturbs human economic activities such as shipping, commercial fishing, and recreation. Marine oil spills also impact marine and terrestrial organisms and the habitats they occupy (Doerffer 1992; NRPG 2013).

With dilbit projected to become one of Canada's chief exports (Mcknight *et al.* 2015), it is vital to understand its behaviour and impacts if spilled in a marine environment. Such understanding will aid in the development of dilbit emergency response strategies and, therefore, may reduce the short- and long-term environmental impacts of spills.

2.2 The fate and behaviour of oil at sea

The fate and behaviour of oil spills in marine environments is determined by the oil type, air and water temperature, spill location, water turbidity, ocean currents, average wind direction, sea state, and the type of shoreline it will eventually become stranded upon (Wang *et al.* 2003; Fingas 2013; Etkin 2015). While the behaviour of oil spilled in the open sea is relatively well-studied and predictively modelled, less is known about the behaviour of oil once it is stranded onshore (Yapa 2013).

While the goal of oil spill responders is to mitigate shoreline stranding as much as possible, this objective is rarely entirely successful (Peterson *et al.* 2003). For example, immediately following the 1989 *Exxon Valdez* oil spill in Prince William Sound, Alaska, great effort was made to prevent oil from reaching the shoreline. Despite this effort, it is estimated that 40 to 45% of the oil spilled from the *Exxon Valdez* spread over 2,100 km of shoreline (Peterson *et al.* 2003, Michel *et al.* 2013). In 2010, the British Petroleum Deep Water Horizon spill resulted in oil residue reaching over 1,700 km of coastline in the Gulf of Mexico (Michel *et al.* 2013). Both incidents illustrate that despite substantial efforts to mitigate shoreline oiling, it readily occurs. Given that oil stranded on shore has ongoing consequences for shorelines, focused attention needs to be directed to understand how

dilbit will interact with unconsolidated *in-situ* sediments once stranded on shorelines in coastal British Columbia (French-McCay 2004; Etkin 2015).

2.2.1 Describing petroleum products

Each petroleum product is a heterogeneous mixture composed of thousands of hydrocarbon compounds. To differentiate oil types, science and industry commonly define each in regards to their broad hydrocarbon constituents: saturates, aromatics, resins, and, asphaltenes (SARA) (Figure 2.1) (Emmett *et al.* 2011; Fingas 2015a, 2015b; Hollebone 2015). Saturates, which have a carbon skeleton, take various shapes (chains, branch chains, and rings) and sizes, and are partially soluble in water (Emmett *et al.* 2011; Hollebone 2015). Aromatics have a single or double-ring structure composed of light end hydrocarbons and tend to be more volatile, toxic, and environmentally persistent (Etkin 2015; Hollebone 2015; PGLEC 2015). Resins and asphaltenes are larger, environmentally persistent compounds, composed of multiple rings that are dominated by hydrogen and

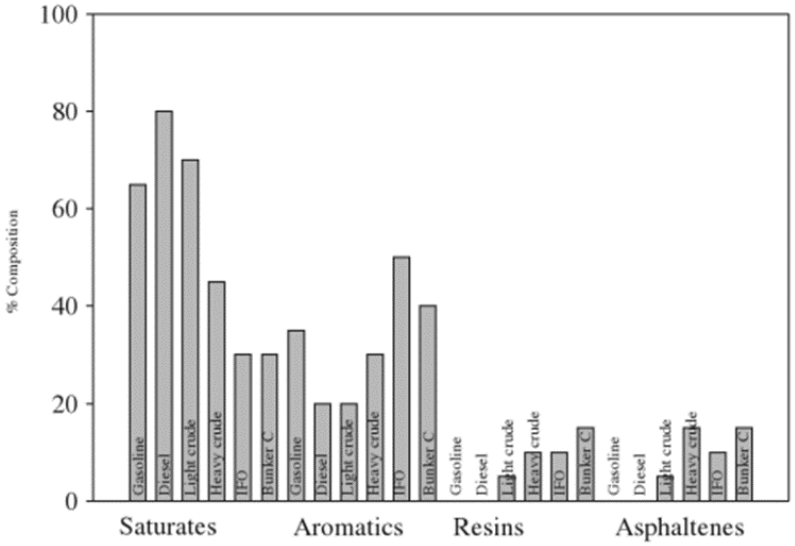

Figure 2.1- Expected SARA volumes for various hydrocarbons by percent composition (Fingas 2015c).

carbon but also contain oxygen, nitrogen, metals, and sulphur. Where resins are soluble in crude oil, asphaltenes are not (Etkin 2015; Fingas 2015b).

The ratio of each SARA component determines three important factors when considering oil spill behaviour: viscosity, specific gravity, and solubility (Hollebone 2015). Viscosity is defined as a fluid or fluid-like substance's resistance to flow (Barrow *et al.* 2004). Lower viscosity fluids will more readily flow and vice versa (Harper *et al.* 1995; Wang *et al.* 2003). The viscosity of a hydrocarbon product is determined by the ratio of lighter compounds such as saturates and aromatics present in contrast to heavier compounds such as resins and asphaltenes (Etkin *et al.* 2007; GOC 2013). Specific gravity (density) is the mass of a given volume of oil at 15 ^{o}C in comparison to water (Barrow *et al.* 2004; Hollebone 2015). Solubility, when referring to oil, describes the ability of a hydrocarbon (solute) to dissolve in water (solvent) although the percent mass lost through dissolution is a fraction of a percent (Doerffer 1992; Fingas 2015c). It is noteworthy, however, that aromatics and saturates which readily dissolve in water are particularly toxic to aquatic life, making them of particular concern in water bodies (Fingas 2015c).

Dilbit is a relatively equal combination of SARAs (Philibert *et al.* 2016). To render bituminous sediments into raw bitumen requires the application of heat and chemicals to release the entrained bitumen (Banerjee 2012). Through this process, saturates and aromatics are largely driven off, leaving the raw bitumen to be dominated by highly viscous and dense resins and asphaltenes. The addition of a low viscosity and density diluent,

dominated by saturates and aromatics, allows for the combination of diluent and bitumen to flow easier for transportation purposes (Fingas 2015b).

2.2.2 Weathering: A chemical and physical process

Environmental conditions during and after a spill, in combination with oil type, determine the weathering state of oil once it is stranded onshore (Doerffer 1992; Barrow *et al.* 2004). The process of weathering, which begins immediately after oil is released into the environment, is described as percent mass loss and is influenced by evaporation, temperature, biodegradation, natural dispersion, adhesion to materials, interaction with mineral fines, emulsification, dissolution, photooxidation, sedimentation, and tarball formation (Doerffer 1992; Moldestad *et al.* 2004; GOC 2013; Fingas 2015d). Although numerous factors contribute to weathering, it is largely controlled by time, mixing energy, and the ambient air and water temperature (Hollebone 2015).

Viscosity and density increases in response to volatile (aromatics and saturates) fractions of the hydrocarbon product being driven off during weathering processes (Figure 2.2) (Doerffer 1992; GOC 2013; Hollebone 2015). Environmental exposure time and higher temperature expedite the weathering process (Hollebone 2015). Evaporation of low viscosity hydrocarbons such as gasoline, diesel, or kerosene is very rapid due to their high ratio of volatile compounds (Figure 2.2) (Doerffer 1992). These products often evaporate entirely or dissolve from surface plumes within one to two days of a spill (Doerffer 1992; Etkin 2015). Conversely, heavier hydrocarbon compounds, such as bunker C, lubricant oil,

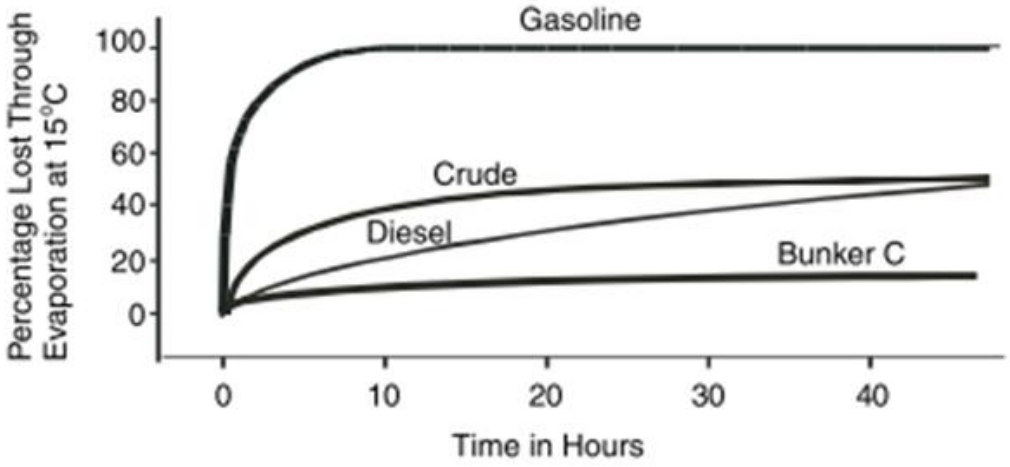

Figure 2.2 - Percent lost through evaporation at 15°C (Barrow et al. 2004: 92).

or bitumen, contain comparably low volumes of aromatics and high amounts of molecularly-heavy compounds (resins and asphaltenes). They are of high viscosity and change little throughout a spill event (Figure 2.2) (Fingas 2015b). The combination of these characteristics results in heavy oils being much more environmentally persistent, if not remediated, in comparison to lighter oils when spills occur (Polaris 2013; King *et al.* 2014).

In general, as a spill event temporally extends and hydrocarbon weathering continues, an increase in density, viscosity, and interfacial tension occurs in response to the loss of light fraction hydrocarbons. Over time this change results in the dominance of heavy fraction hydrocarbons which are more environmentally persistent (Fingas 2013; GOC 2013). As every oil is composed of varying combination of SARAs and, therefore, possesses slightly different viscosities and densities, each oil will weather differently based on the conditions into which it is released (Fingas 2013, 2015a) .

2.2.3 Environmental conditions and their impacts on a spill

The impact a spill can have on the environment is affected by the setting into which it is released (Etkin 2015, Fingas 2015a). In the marine environment, several oceanographic factors must be taken into consideration when predicting the effects and behaviour of a spill. These include hydrodynamic variables such as currents, tides, waves, current velocity, wind velocity and direction, water and air temperatures, and the type of shoreline substrate (Spaulding 1988; Harper *et al.* 1995; Beegle-Krause and Lehr 2015; Etkin 2015).

Current direction, velocity, and predominant wind direction will affect the way a spill travels and spreads across a water body. These factors can impact the rate of evaporation and dispersion by increasing the surface area of the spill, thereby increasing the rate of weathering, which ultimately affects an oil's behaviour once stranded ashore (Owens 1985; J. Harper *et al.* 1995; Barrow *et al.* 2004; Etkin 2015).

2.2.4 Oil sediment interactions and retention

Hydrocarbon adhesion to sediment is one of the main natural processes for removing oil from water once spilled (Yapa 2013). As oil is deposited onshore its density and viscosity, in combination with the receiving sediment characteristics, determine its ability to penetrate and be retained by the receiving sediment (Fingas 2006, Michel 2011, Harper *et al.* 2016). Light oils, such as diesel, gasoline, or kerosene, penetrate the sediment surface but remain above the water table (Doerffer 1992). In contrast, heavy oils, which slowly penetrate shoreline sediments, can become stranded on the sediment surface (Harper *et al.* 2016). This behavioural characteristic means that heavy oils tend to entrain sediments,

which increases its overall mass (Doerffer 1992, Owens *et al.* 2008, Etkin 2015, Lin 2015). Following this, the oil-covered sediments may be buried or re-deposited in the nearshore. Both light and heavy oils, which do not adhere to sediments, are prone to remobilization if deposited in the intertidal zone due to their density being less than salt water (Doerffer 1992).

Shoreline type (i.e. cliff/rock shores, estuary, or sand), oil type, weathering state, tidal cycle, and near shore wave energy all influence the fate of spilled oil once stranded on shoreline sediments (Harper *et al.* 1995; Sergy *et al.* 2003; Owens *et al.* 2008; Shigenaka 2011; Harper *et al.* 2015). For example, cliffs and rock shores have a very low oil penetration and retention when compared to marshland shorelines (Doerffer 1992, Barrow *et al.* 2004, Fingas 2013, 2015a, Etkin *et al.* 2015). In addition to an oil's weathering stage, coarse sediment shoreline oil retention is determined by the receiving sediment's hydraulic properties (porosity, permeability, hydraulic conductivity) as well as the initial oil loading (Humphrey and Harper 1993; Harper *et al.* 1995; Lee *et al.* 2003; Owens *et al.* 2008)

2.2.5 Comparing dilbit to heavy oil

There is a discussion in the literature regarding the validity of comparing spills involving dilbit and heavy oil related to the differing properties of these products (Brown *et al.* 1991; Cooper 2006; Polaris 2013). The most apparent differences are the hydrocarbon constituents of each product and their dynamic viscosities. Heavy oil is relatively homogeneous, being comprised predominantly of stable long-chain hydrocarbons that do not readily evaporate (Doerffer 1992). On the other hand, dilbit is a heterogeneous mixture

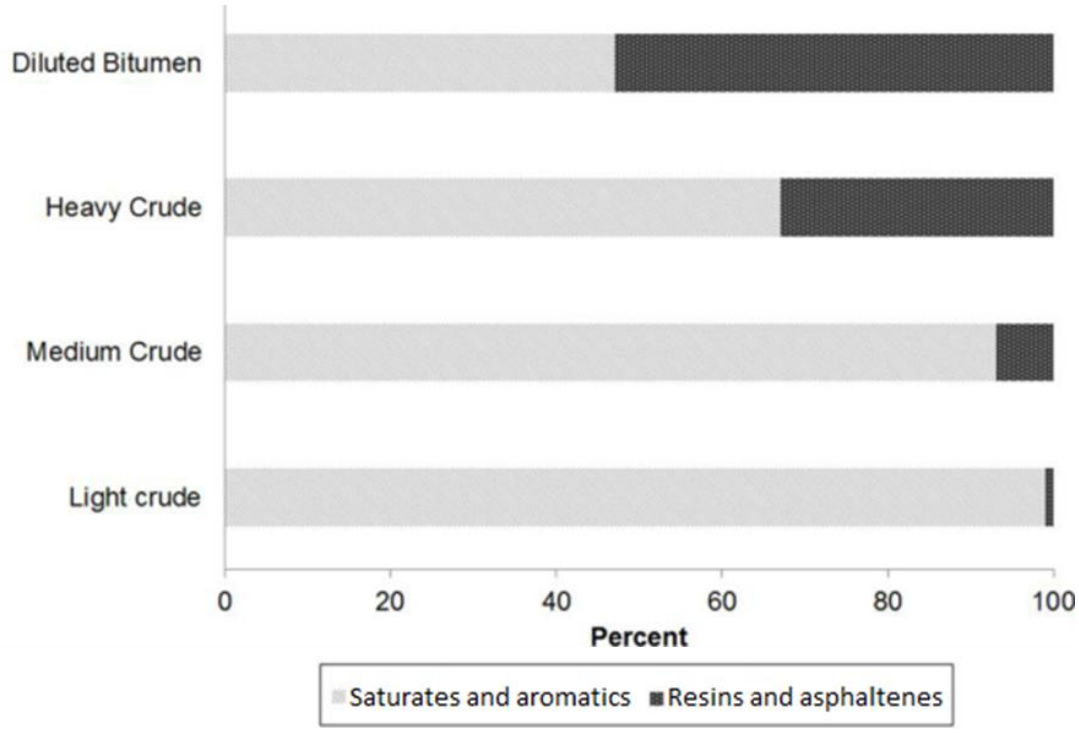

Figure 2.3 - Comparison of the percent composition of different oils. Light ends seen in gray and the environmentally persistent, heavier ends seen in black (McKnight *et al*. 2015).

of both long and short chain hydrocarbons, blended as high as 1:1 diluent to bitumen. These characteristics result in viscosity differences between the lighter dilbit and heavy oil in the order of 2 to 3 magnitudes (Figure 2.4) (Gunter 2009, Polaris 2013, Fingas 2015c). Heavy oil can be described as something between a coffee cream and olive oil, whereas dilbit is more akin to SAE 50 motor oil (Gunter 2009, WO 2013, HIFM 2015).

2.2.6 Comparative weathering

The evaporative qualities of the diluent component of dilbit cause rapid weathering within 6 to 12 hours of being spilled (Figure 2.5) (Brown *et al.* 1991; GOC 2013; Polaris 2013). This rapid weathering adds to the difficulty of comparing dilbit spills to a heavy oil spill

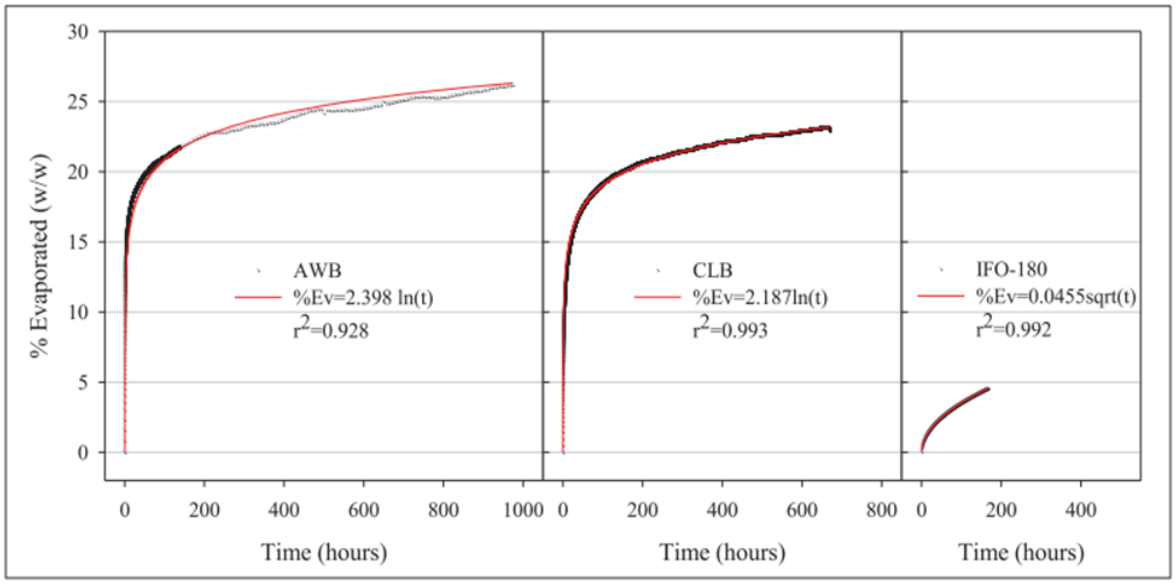

Figure 2.4 – Comparison of evaporation rate by percent mass of two dilbits and one crude oil (Access Western Blend (AWB), Cold Lake Blend (CLB), and Intermediate Fuel oil 180 (IFO-180). The AWB, CLB, and the IFO-180 experiments lasted ~950, ~650, and ~200 hours, respectively at 15ºC with little to no air disturbance (GOC 2013).

(Cooper 2006, Fingas 2015c). Given time and exposure, dilbit will revert, chemically and physically, to something akin to bitumen, whereas heavy oil will maintain relatively consistent fluid property throughout the weathering process (Figure 2.4) (GOC 2013, Polaris 2013, WO 2013). As each blend of dilbit contains a slightly different percent volume of diluent, each will react differently to a given set of environmental conditions (Fingas 2015a).

When comparing weathering rates between International Fuel Oil (IFO-180) and both dilbit blends, Access Western Blend (AWB) and Cold Lake Blend (CWB), the percent mass lost to evaporation was observed to be far greater and far more rapid in dilbit than in IFO-180 (Figure 2.4) (GOC 2013). This difference is largely associated with the loss of the volatile

condensate or diluent (Figures 2.3 and 2.4) (GOC 2013). This rapid loss of condensate acts to differentiate dilbit from fuel oil whereby, as dilbit weathering continues, the diluent component evaporates leaving a stable and environmental persistent bitumen-like product after 6 to 12 hours of environmental exposure (Figure 2.4) (GOC 2013). As the percent evaporation of dilbit increases, the density and dynamic viscosity also increase, altering the physical properties of the oil and how it interacts with water and sediment if stranded (Table 2.1).

Thus, dilbit and heavy oil possess similar viscosity and density characteristics when initially spilled but as the duration of the spill extends, the less they are alike. For this reason, the dilbit and heavy oil comparison is adequate in the initial stages of contingency planning. However, this approach is not adequate during later stages of weathering when the characteristics of dilbit change independently from those of heavy oils (Etkin *et al.* 2015, PGLEC 2015).

2.2.7 Research on dilbit fate and behaviour: Bit_Ex

An initial investigation of diluted bitumen and shoreline sediment interactions was the Bitumen Experiment (Bit_Ex) (Harper *et al.* 2015). Bit_Ex was a laboratory study designed to assess the penetration and retention of diluted bitumen in seven sediment size classifications. Eight oils were used in the experiment, six of which were dilbits. In addition, International Fuel Oil 180 (IFO180) and Bunker C were used to compare the Bit_Ex findings with previous similar experiments. Two variations of dilbit were used:

Table 2.1 - Density and dynamic viscosity of AWB, CLB, and IFO 180.

Oil type	Density(g/ml)	Dynamic viscosity (mPa•s)
CLB		
Unweathered at 15°C	.9249	285
W2 (~16.8%) at 15°C	.9816	0.000183
AWB		
Unweathered at 15°C	0.9353	347
W2 (~16.8%) at 15°C	0.9846	.000297
IFO 180		
Unweathered at 15°C C	.9664	1920

Modified from GOC (2013).

AWB and CLB at three weathering states (fresh <3%, moderate 15 to 17%, and heavily weathered 24 to 26%).

Based upon bulk sediment characteristics and the physical properties of dilbit, the dilbit would either fully penetrate (maximum of 15 cm) the sediment or it would not fully penetrate the sediment, in which case, dilbit penetration was measured. Bit_Ex revealed the finest sediment through which dilbit is able to freely penetrate, as any sediment finer will restrict fluid transmission and, therefore restrict penetration and retention (Table 2.2).

Another useful means of characterising dilbit and sediment interactions is through a sediment's ability retain oil once oil saturated sediment has been submerged in water (simulating a tidal cycle) (Table 2.3). The Bit_Ex results show that unweathered dilbit freely penetrates approximately very coarse sand to very large pebbles while weathered dilbit freely penetrates medium pebble to very large pebble (Harper *et al.* 2015). While

Table 2.2 - Average dilbit penetration in Bit_Ex test sediments in cm below datum.

Dilbit Type	Sediment Types						
	CS[1]	VCS[1]	Gran[1]	S. Peb[1]	M. Peb[1]	L. Peb[1]	V.L Peb
d10	0.53	1.09	2.80	4.82	8.75	16.38	32.46
CLB (15% weathered)	1.2	1.4	3.3	7.3	10.8	15	15
AWB (18% weathered)	1.3	2	3.7	7.9	14.9	15	15
CLB (fresh)	7.6	13.9	15	15	15	15	15
AWB(fresh)	5.7	14.7	15	15	15	15	15

[1]: CS refers to coarse sand, VCS very coarse sand, Gran granules, S. Peb small pebble, M. Peb. Medium pebble, L. Peb large pebble and VL Peb. very large pebble Source:

Notes:

1. modified from Harper *et al.* (2015).
2. Light grey indicates sediment that dilbit variation was able to flow through unrestricted

penetration was high (>14cm) in sediment sizes classified as medium pebble and above, there was very little observed retention. Conversely, in coarse sand and finer sediments, there was relatively little penetration in comparison to very coarse sand through to medium pebble, and these sediments did not release a significant amount of dilbit after a 24-hour soak (Table 2.4). Although the findings are yet to be published, the results show a significant relationship between dominant sediment grain size and dilbit retention and penetration.

Table 2.3 - % of Initial dilbit loading retained after 1-hour inundation.

Dilbit Type	Sediment Classification						
	CS	VCS	Gran	S.Peb	M.Peb	L.Peb	V.L.Peb
d10	0.53	1.09	2.80	4.82	8.75	16.38	32.46
CLB (15% weathered)	20	39	87	98	96	93	92
AWB (18% weathered)	16	70	65	96	94	90	70
CLB (fresh)	93	99	95	78	20	1	2
AWB(fresh)	61	98	87	15	3	5	2

Notes:

1. Modified from (Harper *et al.* 2015).
2. Light grey indicates sediment that dilbit variation was able to flow through unrestricted

Table 2.4 - % of Initial dilbit loading retained after 24-hour inundation.

Dilbit Type	Sediment Classification						
	CS	VCS	Gran	S.Peb	M.Peb	L.Peb	V.L.Peb
d10	0.53	1.09	2.80	4.82	8.75	16.38	32.46
CLB (15% weathered)	11	26	59	94	92	65	19
AWB (18% weathered)	10	53	48	94	89	37	14
CLB (fresh)	58	93	75	54	8	0	3
AWB(fresh)	37	89	63	10	1	3	1

Notes:

1. Modified from (Harper *et al.* 2015).
2. Light grey indicates sediment that dilbit variation was able to flow through unrestricted

2.2.8 Considering sediments of mixed grain size

While Bit_Ex advanced understanding of dilbit-sediment interactions in sediments of uniform grain size, this is a condition that rarely occurs in nature (Davidson-Arnott *et al.* 2005). Sediments with uniform grain size will have fluid mechanics that differ from those of sediments of mixed grain sizes (Green and Ampt 1911; Hazen 1911; Detmer 1995; Blott and Pye 2001; Argyrokastritis and Kerkides 2003; Nimmo 2004; Knödel et. al. 2007; Deck 2010; Onur 2014). Salarashayeri and Siosemarde (2012) investigated the relationship

between grain diameters (derived from a particle size distribution (PSD) curve) and the ability of saturated sediments to transmit fluids (saturated hydraulic conductivity (Ks)). They determined that particle diameters at 10% of the mass of the sample (effective grain size or d_{10}) was a significant parameter for determining Ks from a PSD curve. Sperry and Peirce (1995) found the effective grain size of a sediment accounts for 69% of Ks variability. Similar findings are reported by Bear (1972), Sperry and Peirce (1995), Jury and Horton (2004), Hazen (2011) and Cabalar and Akbulut (2016).

A relationship between Ks and PSD exists because variations in particle diameter and the resulting void spaces (pore throat and body) alter the way in which a fluid is transmitted through a medium (Dullien 1979; Alyamani and Şen 1993; Svensson 2014). Pore throats are points of constriction and, therefore, act to restrict fluid flow (Bear 1972). Pore bodies are voids which act as reservoirs for fluids. As mean grain size is reduced, pore throats and bodies become smaller and surface area increases, resulting in a higher frictional resistance that acts to limit fluid transmission (Bear 1972; Rawle 2011).

The d_{10} value is commonly presented as describing the threshold responsible for restricting fluid flow. When integrated into semi-empirical equations, such as the Kozeny-Carmen, Hazen, Slichter, Zamarin, and the Kozeny equations, it is found to be a significant factor in increasing the accuracy of Ks predictions (Bear 1972; Freeze and Cherry 1979; Svensson 2014). Such equations have been modified to predict the migration of not only water but viscous fluids such as oil (Bear 1972).

2.2.9 Saturated hydraulic conductivity as a predictor of retention

The use of Ks to predict dilbit retention requires a sound understanding of sediment hydraulics. As a fluid travels through sediments consisting of a small effective grain size and, therefore small pore throats, pore bodies, and more grain-to-grain contacts, it follows a longer travel path that equates to slower fluid transmission rates. Such sediments can be described as being of high tortuosity and low Ks (Vereecken *et al.* 2006). Alternatively, as effective grain size increases, the pore throats and pore bodies increase in size, resulting in less grain-to-grain contacts and faster rates of fluid transmission. Such sediment can be described as having low tortuosity and therefore high Ks (Vereecken *et al.* 2006).

Sediment oil saturation does not occur immediately, but rather slowly once the oil has already entered the sediment. As dilbit penetrates the sediment surface, it is initially held at the grain-to-grain contacts by means of capillary pressure gradients which act to draw fluids into small passages (pore throats) between grains forming small menisci around the particle contact points (Harper *et al.* 1995, Owens *et al.* 2008). It is in the grain-to-grain contacts where oil is most tenaciously held due to the capillary forces and the fluid properties of the oil (Owens 1985, Harper *et al.* 1995, 2016). As the grain-to-grain contacts reach their holding capacity, oil then floods into pore bodies where it is most easily liberated from and where it can travel in response to pressure gradients within the sediment (i.e. redistribution and remobilization) (Bear 1972, Freeze and Cherry 1979, Hudak 2005). The permeating fluid properties are a vital consideration when predicting Ks. A significant difference found between unweathered and weathered dilbit penetration and retention

which likely can be attributed to a difference in fluid properties. As weathered dilbit penetrates a sediment surface, it does so more slowly when compared to an unweathered dilbit. Given the same grain size distribution and d_{10}, the attenuation of unweathered dilbit from the sediment occurs more rapidly as its fluid properties allow for ease of remobilization. If unweathered and weathered dilbit penetrates to the same depth, weathered dilbit will remain in higher concentrations when compared to unweathered dilbit (e.g. a thin veneer/stratum gravels or granule over silt or clay).

2.2.10 Brief dilbit spill history

While accidental discharges of oil products have declined globally during the past 50 years, they continue to be commonplace (ITOPF 2015). Examples of recent spills in Canada include: the 2016 North Battleford Pipeline Spill in Saskatchewan, with an estimated 200,000 litres of discharge; the 2015 MV *Marathassa* spill in 2015 in British Columbia, with an estimated discharge 2,700 litres; the 2013 Lac-Mégantic derailment in Quebec, with an estimated discharge of 7,700,000 litres; the 2012 Red Deer River spill in Alberta, with an estimated discharge 460,000 litres; and, and the 2011Little Buffalo Spill in Alberta, with an estimated discharge 4,500,000 litres (GOC 2013; TSBC 2014; Hossain 2016;). Such information highlights the frequency of sizeable spills in Canada.

In North America there have been two well-documented dilbit spills: the 2007 Burnaby Mountain spill in Burnaby, British Columbia, and the 2010 Kalamazoo River spill in Marshall, Michigan (McKnight *et al.* 2015; MOE 2015). The Burnaby Mountain spill occurred following the puncture of a charged dilbit transport line by an excavator (MOE

2015). Approximately 234,000 litres of dilbit was released, with the majority travelling through storm sewer lines to Burrard Inlet where it covered approximately 1,200 m of shoreline (MOE 2015). The Kalamazoo River spill, also known as the Marshall spill, occurred after a pipeline operated by Enbridge Energy ruptured (King *et al.* 2014). An estimated 3,193,000 litres of dilbit flowed into the river and onto the surrounding floodplain. After several days the dilbit began to sink below the river surface due to high turbidity and sediment loading in the Kalamazoo River at the time of the event (McGowan *et al.* 2016, Etkin *et al.* 2015). After the dilbit had sunk, it became increasingly difficult to remove as the remediation techniques employed were intended for buoyant oil (Crosby *et al.* 2013). Soluble condensates were found to be more than the lethal concentration 50 within the Kalamazoo River as soluble fractions readily dissolved into the river water (McKnight *et al.* 2015). Lethal concentration 50 describes the chemical concentration that kills 50% of test subjects.

Accidents such as the Kalamazoo River Spill showcase the sensitivity of dilbit to variations of environment conditions and its currently unpredictable nature (Dew *et al.* 2015). At the time of the Kalamazoo River Spill it was widely accepted that dilbit, being less dense than water, would not sink in either freshwater or marine environments. However, this was not the case (Short 2013, Dew *et al.* 2015). In 2014, the United States Environmental Protection Agency estimated 303,000 litres of weathered dilbit remained on the Kalamazoo River stream bed (McKnight *et al.* 2015). In contrast, dilbit from the Burnaby Mountain

spill acted as assumed and remediation efforts resulted in the successful recovery of most of the floating dilbit (McKnight *et al.* 2015).

2.3 Coastal geomorphology in the Salish Sea

Shoreline sediments are an important consideration when understanding the way in which fluid is transmitted through such sediments. Glacial advances of the Cordilleran Ice Sheet during the Fraser Glaciation were responsible for stripping the landscape of southern Vancouver Island of much of its accretional features deposited during previous glacial episodes and for creating the deep steep-walled fjords that characterise the shorelines of today (Terich 1987). As such, bedrock dominates large sections of the coastline, although small coarse-sediment beaches with narrow sandy intertidal zones and steep pebble-cobble beach berms are frequent and are the primary focus in this study (Harper 1980; Downing 1983; Terich, 1987; Scheffers *et al.* 2015).

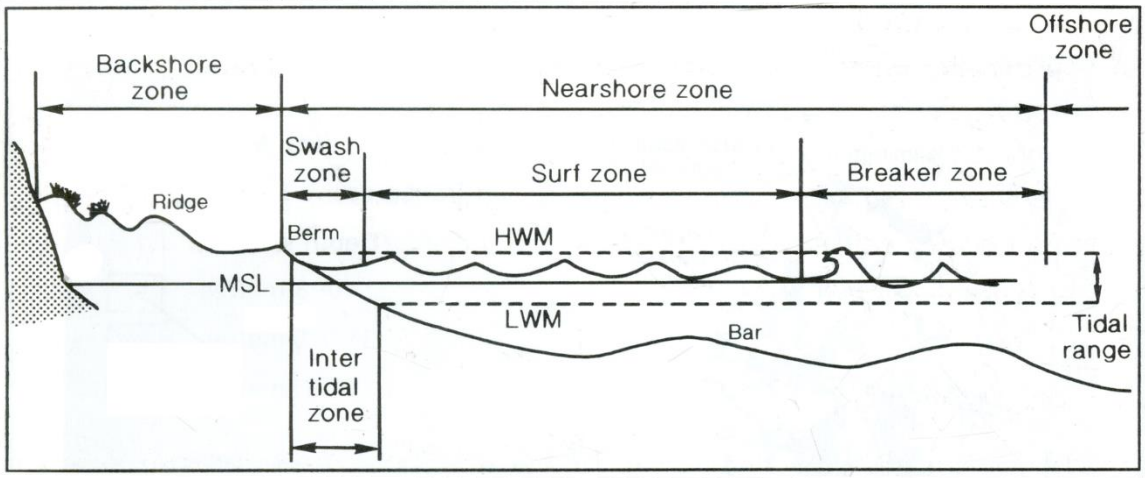

Figure 2.5 - Shorezone nomenclature, modified from Terich (1987). HWM is high water mark, MSL is mean sea line, and LWM is low water mark.

Shorelines in the region (Figure 1.1) are indicative of a storm-dominated and relatively immature coast in response to recent glaciation, sea level fluctuations, and high tidal variations (>4m) (Davies 1972, Masselink and Hughes 2003). During the Fraser Glaciation maximum, an estimated 1900 m of ice blanketed the region, resulting in over 150 m (possibly as much as 300 m) of glacio-isostatic depression (Yorath 2005; Mosher and Hewitt 2004). Concurrent eustatic sea level changes affecting global sea levels also impacted the region (Clark and Mix 2002), and the combination of these changes influenced the local shoreline position until some 6,200 years ago (Yorath 2005; James *et al.* 2009). With a relatively short period of time for coastal processes to modify the southern coastline of Vancouver Island, shorelines in the region are dominated by pocket beaches composed of unconsolidated material contained within rock headlands.

2.3.1 Regional shoreline processes

Glacial retreat and relative sea level provide context for ongoing progradation and contemporary beach processes in the Salish Sea and Strait of Juan da Fuca region (Harper 1980; Terich 1987). With sea level maintaining a relatively stable position since ~6,200 years before present, shorelines have developed in response to waves and tides, as well as their associated processes (Downing 1983; Ametepe 1991;). Waves, in particular, have mobilised and sorted sediments by weight, shape and availability, from the shorezone. Sediments are then transported either offshore or alongshore to lower-energy, quiescent waters and deposited (Bascom 1964)(Figure 2.6).

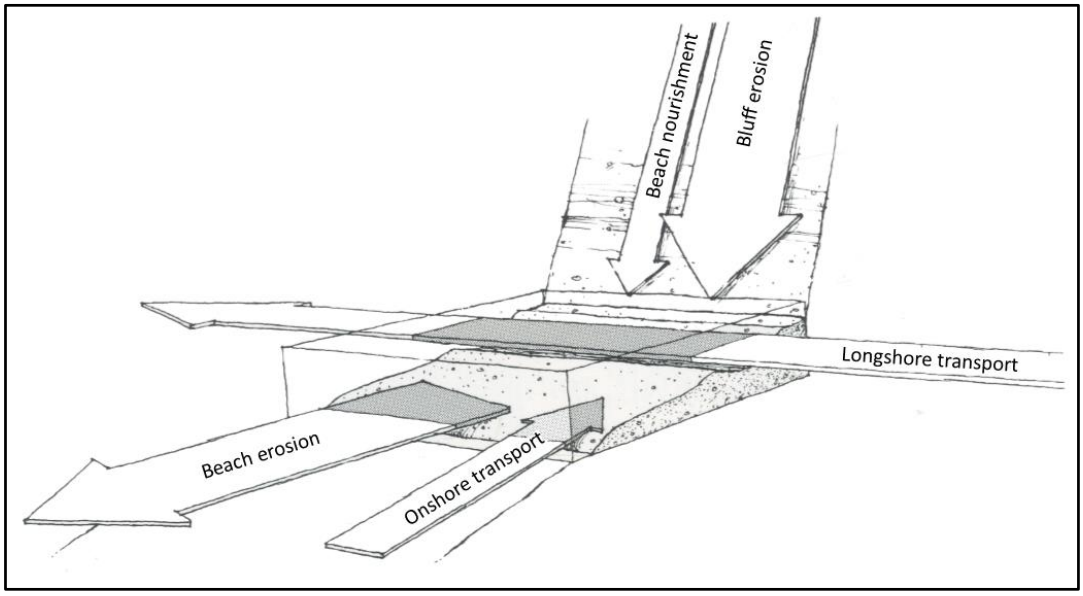

Figure 2.6 - Sediment supply and transport common to the Salish Sea and the Juan de Fuca Strait, modified from Downing (1983).

2.3.2 Regional tides

Tides play a significant role along the coast of southern Vancouver Island. The Salish Sea experiences two high and two low tides, known as semi-diurnal tides, per 24-hour period (Thomson 1981, Terich 1987). The basin geometry in the Johnstone Strait to the north, and the Juan de Fuca Strait to the south, channelize tidal energy and create tidal currents which play an important role in the regional shoreline geomorphology (Thomson 1981). As tidal fluctuations occur, water is quickly flushed through the Juan de Fuca Strait, creating continual tidal currents parallel to the shoreline. Such tidal currents, in concert with waves, are responsible for the majority of longshore transportation of sediment (Masselink and Hughes 2003).

2.3.3 Waves

Shorelines undergo constant change in response to local wave regimes (Bascom 1964; Harper 1980). Although aeolian, biological (e.g. vegetation growth) and fluvial erosion processes are active, their role in shaping local coastlines is much less pronounced (Viles and Spencer 1995). Wind waves are generated in response to wind speed, wind duration, and fetch distance (area over which wind can generate waves) (Bascom 1964). As the wind travels over the surface of the water, friction generates waves, with large fetch distances creating larger more powerful waves while the inverse being true for smaller fetches (Bascom 1964; Terich 1987). Because land masses constrain most of the Salish Sea and the eastern region of the Strait of Juan da Fuca, the region is defined as a fetch-limited system whereby the maximum wave height is constrained by fetch (Davies 1972; Terich 1987).

Fundamental to beach geomorphology, wave energy is expressed as:

$$WE = H^2 \qquad \text{(Equation 2.1)}$$

where WE is wave energy and H is the height of the wave measured from trough to crest (Bascom 1964, Masselink and Hughes 2003). As wave energy is calculated by raising wave height to the power of two, it becomes apparent that slight increases in wave height result in dramatic increases in wave energy (Steers 1969). Hence, most sediment movement occurs during stochastic high-energy events which generate the most powerful waves.

Because waves mobilise sediment, as wave energy increases, as does the size of the sediment it can mobilise when waves break ashore.

2.3.4 Seasonal variations

On shorelines where sediments are available, beaches undergo constant erosion and deposition. When discussing shoreline morphology, two main terms are broadly employed: constructive and destructive processes. Calmer, low-energy waves with long wavelengths, which break slowly over larger distances and generate low wave heights, are referred to as constructive waves. As constructive waves, indicative of the summer months, move towards shore, they contact the seabed at greater depths, mobilising sediments from the nearshore and transporting it shoreward (Figure 2.3). Over time, the continual deposition of sediment drives seaward progradation of the shoreline, changing the dominant sediment type and reducing the beaches gradient or profile (Laing *et al.* 1998; Floor 2000;). Comparatively, destructive waves, characteristic of the winter months, develop in response to high winds or currents and have shorter wavelengths. These waves move ashore and exert a considerably greater amount of energy over smaller distances in comparison to constructive waves. As destructive waves plunge into shallow nearshore waters, they mobilise sediments. They then move via longshore transport or by offshore currents (Bascom 1964; Ametepe 1991) (Figure 2.3). Shorelines in the Salish Sea and the Juan de Fuca Strait undergo continuous deposition, erosion, and sediment transportation. Constructive processes are primarily responsible for deposition and destructive processes being responsible for erosion.

2.3.5 Sediment transport

Once a sediment has been mobilised into the intertidal and shallow nearshore zone, its movement on a beach is overwhelmingly governed by longshore transport (Figure 2.6) (Bascom 1964; Chardón-Maldonado *et al.* 2015). Longshore transport takes place through two primary means: the back and forth swashing of waves which mobilise and carry sediment, and longshore currents which develop in the surf zone and move sediment perpendicular to the shoreline (Terich 1987; Thomas 1990). Alternatively, sediments may also be carried out of the swash zone and deposited into the offshore environment by offshore currents. Consistent unidirectional longshore and offshore currents sort sediments, whereby coarser fractions occur in regions of a shoreline with high wave energy and become finer distal from such a point (Steers 1969).

In the Salish Sea the direction of sediment transportation is largely driven by prevailing wind direction. As such, longshore drift can switch orientation as winter southeasterly winds become summer northwesterlies (Harper 1980). This is a pattern which can cycle sediment on a single beach allowing for both destructive and constructive processes to occur simultaneously (Harper 1980).

As little time has passed since the Fraser Glaciation, the beaches of the Salish Sea are predominantly immature and are dominated by sediment ranging from boulders to sands.

As such, shoreline development is an ongoing process, through which wave energy continually sorts and redistribute sediment.

2.4 Chapter summary

The current understanding of dilbit effects and behaviour on marine shorelines is inadequate. Shortcomings in knowledge and communication are highlighted when responding to dilbit spills, such as the Marshall Spill, where prolonged clean-up times and resultingextended exposure to contamination resulted. The application of heavy oil response strategies to fresh dilbit may be adequate if a response does not exceed 6 to 12 hours, which is the period during which dilbit behaves similarly to heavy oil (Figures 2.3 and 2.5). Beyond this period, however, such measures may no longer be adequate, as the fluid properties of the dilbit change as it weathers, giving rise to new fluid characteristics and physical properties. Efforts have been made to understand the interactions between shoreline sediments and dilbit in Bit_Ex, where experiments were conducted in a laboratory scale on uniform sediments. However, further research is needed to apply findings to *in-situ* shorelines composed of non-uniform sediment which are indicative of the southeastern coast of Vancouver Island.

3 Chapter Three: Methods

This chapter presents the methods and approaches used for field site and plot selection; double-ring constant-head infiltrometer installation; calculating measured Ks; obtaining sediment samples; sediment processing and analysis (grain size distribution analysis (GSD)); and the selection of semi-empirical equations to predict Ks.

3.1 Field site and plot selection

Study sites were selected using a combination of GIS software (QGIS) to examine ShoreZone data and Google Earth (2016) to corroborate findings. ShoreZone is a shoreline mapping dataset which inventories cross-shore and longshore geomorphic variations in British Columbia, Alaska and Oregon (Harper and Morris 2014). The ShoreZone dataset was initially queried for shorelines composed of high retention sediments as described by Bit_Ex (see Chapter 2 Table 2.3) (Harper *et al.* 2016). Preliminary site selection was based upon shoreline type, substrate, exposure (fetch distance), shore component information, and shoreline sensitivity index. This assessment resulted in the identification of 12 potential study sites, of which ten were selected for analysis primarily based upon site accessibility (Figure 3.1; Table 3.1).

Table 3.1 - List of all field sites.

Site 1: Muir Creek, Sooke	Site 2: Aylard Farm Beach, Sooke
Site 3: Witty's Lagoon, Metchosin	Site 4: Loon Bay, Victoria
Site 5: Arbutus Cove Beach, Victoria	Site 6: Island View Beach, Saanichton
Site 7: Resthaven Park, Sidney	Site 8: Chalet Beach, Sidney
Site 9: Glencoe Cove-Kwartsech Park North, Victoria	Site 10: Glencoe Cove-Kwartsech Park South, Victoria

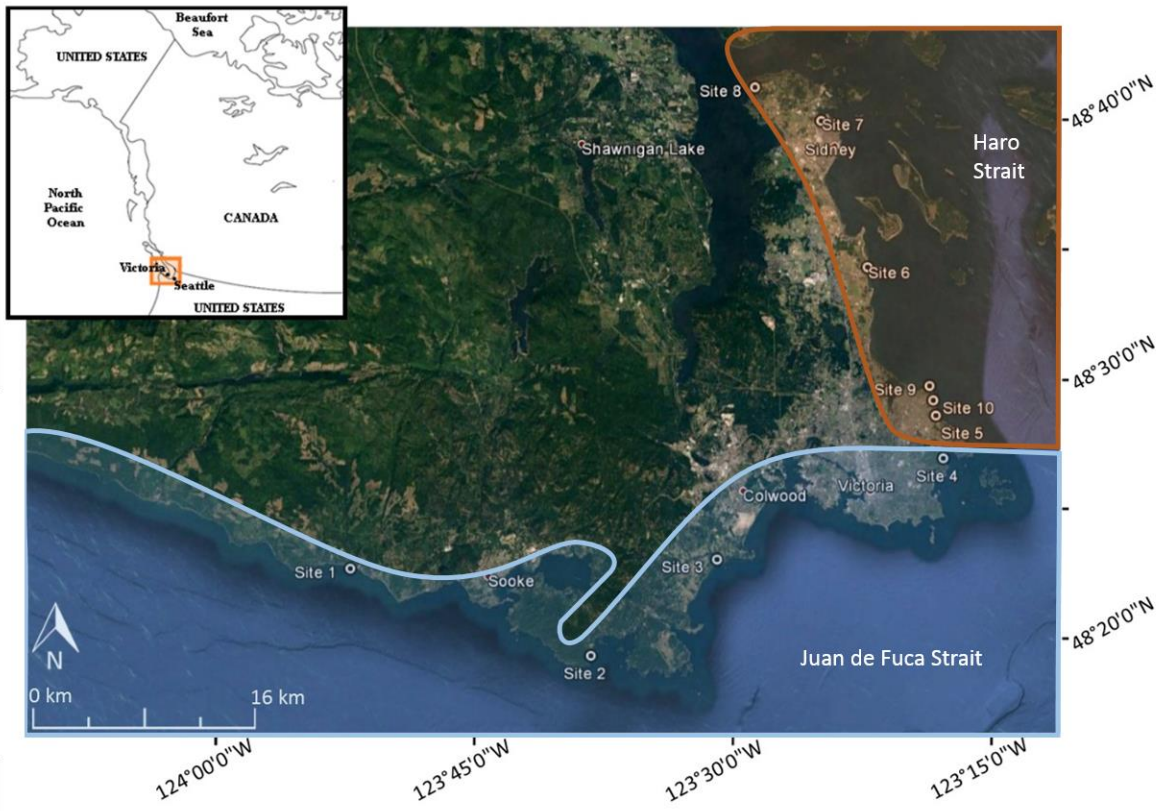

Figure 3.1 - Field site locations (modified from Google Inc., 2016). Blue line indicates site found in Juan de Fuca Strait and the orange line illustrates those located in Haro Strait.

3.1.1 Plot selection

Due to the alongshore and cross-shore variations in sediments at each site, zones above the high water line were isolated and broken into three areas: proximal to headlands; central; and, distal from headlands (Figure 3.2). Each area was divided into approximately 20 m sections and assigned a unique ID number (Figure 3.2). Using a random number generator, one plot from each of the three areas was randomly selected for experimental analysis. Similar stratified random sampling procedures have been used in both shoreline and oil spill monitoring programs (COE 1956, Short *et al.* 2004).

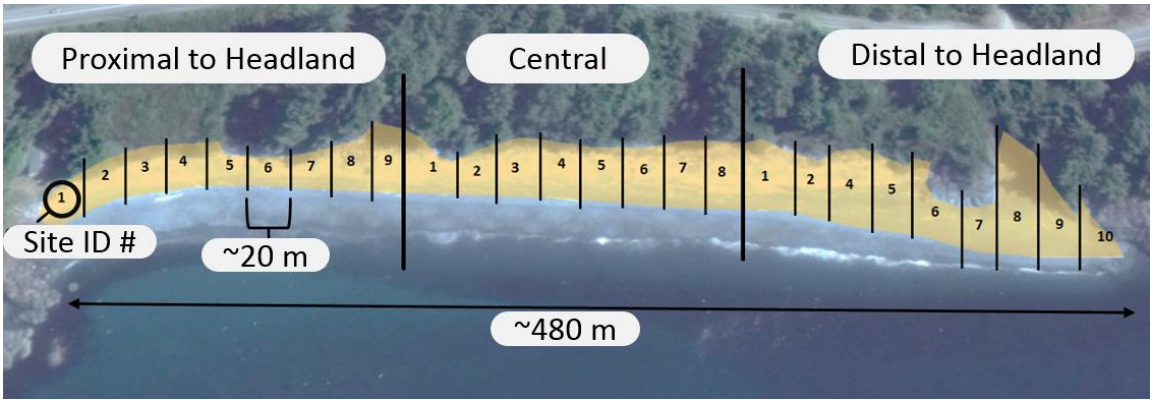

Figure 3.2 - Example beach delineation (imaged modified from Google Inc. 2016).

Each site was divided lengthwise into three areas with the exception of sites 6, 9 and 10. Site 6 (Island View Beach), the longest of the ten selected sites spanning 3.9 km of non-linear shoreline, was divided into five areas to capture longshore variations in sediment that otherwise might not have been obtained in three areas. Sites 9 and 10 (Glencoe Cove-Kwartsech Park North and South) are relatively small beaches (ca. 120 and 40 m in length) with little observed surficial spatial variation of sediments. Consequently, both sites were divided into 20 m plots, with identical methodology then being applied (i.e. randomly selected plot followed by visual inspection).

3.2 Field Measurements

The manner in which a fluid (both water and contaminant) transmits through or is retained in a sediment is determined partly by its fluid properties and partly by the sediment hydraulic properties (Etkin *et al.* 2008). Saturated hydraulic conductivity (Ks) is a measure of a porous medium's ability to transmit fluid when all void space are flooded (Jury and Horton 2004), and is used to predict retention. Ks is particularly useful in the context of this research because it minimises the influence of micropores, pore space geometry,

preferential flow paths, and capillary forces, and isolates gravity as the primary driving force for fluid transmission. In addition, the ability of Ks to reduce the impact of antecedent conditions allows for the isolation of saturated flow rates (Dingman 2002, Jury and Horton 2004, Vereecken *et al.* 2006, Deck 2010).

Many approaches and methodologies exist to indirectly and directly measure Ks (Bear 1972, Folk 1974, Freeze and Cherry 1979, Mohanty *et al.* 1994, Svensson 2014). Given that this research focuses on shore sediments in the Strait of Juan De Fuca and Harro Strait regions where the beaches consist primarily of sands, pebbles, cobbles and/or boulders, a double-ring constant-head infiltrometer (DCI) was selected for the direct field measurement of Ks (Figure 3.3). The DCI was chosen due to its ability to deliver large volumes of water to the sediment surface for prolonged periods, thereby allowing for saturation to be achieved and Ks to be measured. Additionally, its simple construction and its reputation for accurately predicting K_S in coarse-grained unconsolidated sediments contributed to its selection for use in this study. (Johnson 1963, Melalia 1993, Bloomquist 2001, ASTM:D5126/D5126M-90 2010, ASTM:D3385-09 2016).

3.2.1 Direct measurement of Ks

Various instruments exist to obtain *in-situ* Ks values. Each comes with advantages and disadvantages, and these are thoroughly discussed in the broader hydrogeology, ground water hydrology, and environmental science literature (Bloomquist 2001, Hammecker *et al.* 2005, Knödel *et al.* 2007, Nimmo *et al.* 2009, Deck 2010, Philips and Kitch 2011). Although the DCI instrument employed in this study can directly measure a variety of *in-situ* sediment properties, in this instance it is used to measure vertical or uni-directional Ks.

3.2.2 Double-ring constant-head infiltrometer installation

To measure saturated hydraulic conductivity (Ks), a DCI was installed at or above the high tide or high wrack line at each randomly selected plot (Figure 3.3). Specific test locations were visually identified as representative of both the plot and the beach as a whole. If plots contained obstructions such as logs, boat ramps, debris, or if plots were deemed unrepresentative, then the next randomly selected plot was used (Figure 3.4).

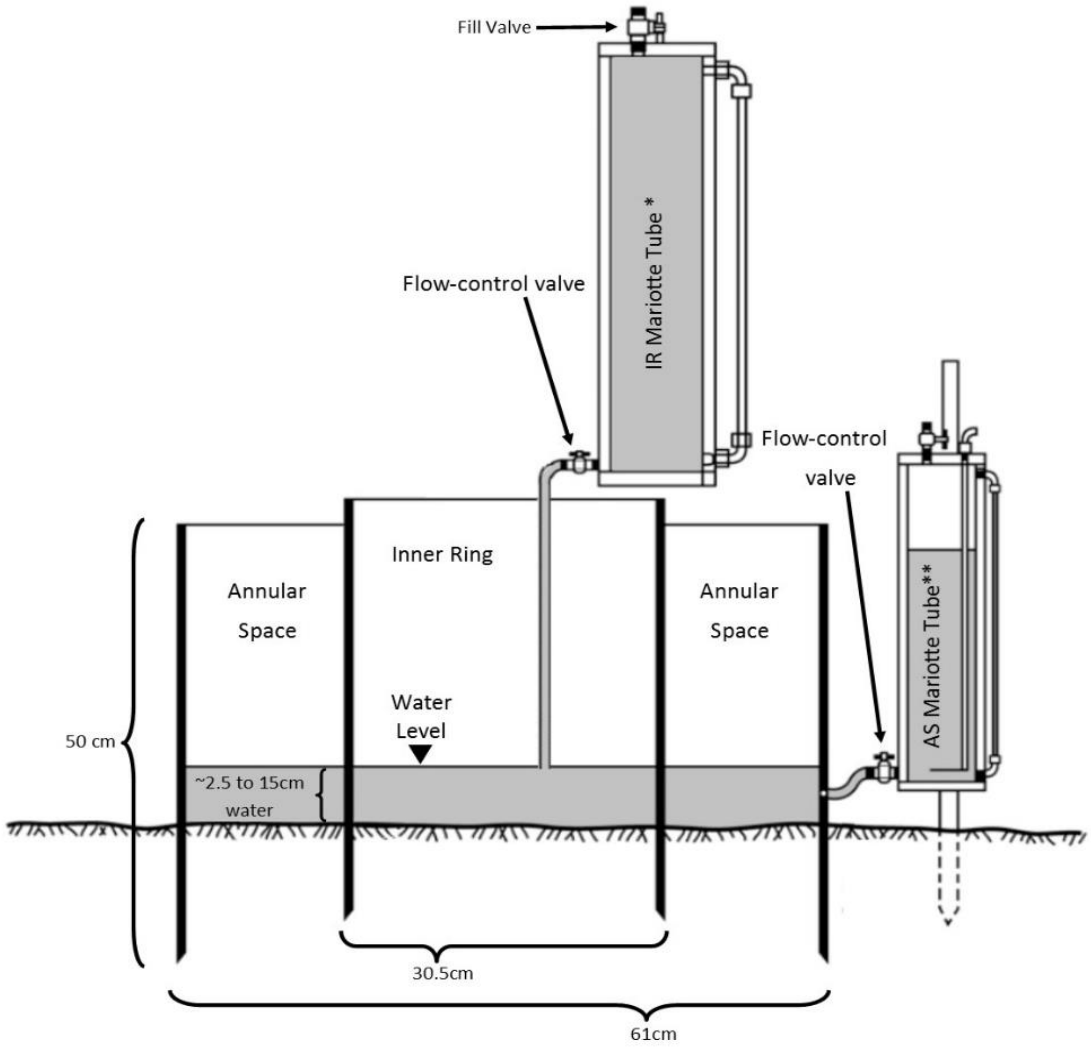

Figure 3.3 - Diagram of double-ring constant-head infiltrometer installation. Modified from ASTM:D3385-09 (2016).

DCI *in-situ* installation requires the insertion of two concentric cylinders into the sediment to a maximum depth of 20 cm, or until an impenetrable stratum is met (i.e. bedrock or consolidated sediments) (Johnson, 1963). Once both rings are inserted to approximately the same depth, water is delivered to both the inner ring and the annular space (the area between the inner and outer ring) (Figure 3.3). Water depths in both rings are maintained using Mariotte tubes to supply water continually and to sustain head pressure throughout the duration of the experiment. The downward flow of water from the annulus acts to mitigate lateral migration of water from the inner ring during the testing, inducing unidirectional flow in the inner ring and increasing the accuracy of measured Ks values.

3.2.3 DCI obtained data and Ks calculation

To obtain Ks, water levels were recorded at 5 to 10 minute intervals from the calibrated Mariotte Tube delivering fluid to the inner ring. As water was continually supplied to the inner ring, sediments approach saturation, infiltration rates stabilise, and K_S could be

Figure 3.4 - Example DCI installation location at Site 10. The shaded area indicates the region within which the DCI could have been installed within this plot.

approximated (Fetter 2001, Gregory *et al.* 2005, Vereecken *et al.* 2006, Knödel *et al.* 2007, Deck 2010). Once infiltration rates stabilise, K_S was assumed to have been achieved, and the DCI tests were concluded.

Using Microsoft Excel (2013), K_S was generated in accordance with the ASTM standard D3385-09. K_S was calculated using the following formula:

$$\mathbf{V_{IR} = \Delta V_{IR}/(A_{IR} \cdot \Delta t)} \qquad \textbf{Equation 3.1}$$

where V_{IR} represents the incremental infiltration velocity (cm/sec), ΔV_{IR} represents the volume of liquid required to maintain water depth in the inner ring (cm^3), A_{IR} represents the area of the inner ring (cm_2), and Δt indicates the change in time (ASTM:D3385-09 2016).

The rate at which a measured volume of water transmits through a finite surface can be described as V_{IR}. V_{IR} is initially variable, although, as V_{IR} approaches Ks the infiltration rates becomes increasingly stable and are representative of Ks once steady state infiltration has occurred.

3.2.4 Sediment samples

Sediment samples were obtained directly beside each DCI test location and were mechanically sorted and analysed for grain size distribution (GSD). Bulk sediment samples were acquired using a Barrel Sampler (10 cm diameter; 20 cm length) that obtained approximately 1500 g of sediment per sample when fully driven into the sediment (ASTM:D4700-15 1999, Knödel *et al.* 2007). In instances where the barrel sampler could not be driven into the sediment, samples were taken using a small shovel. Additionally, for

plots where sediment stratification was prominent, samples of each stratum were taken for GSD analysis. Once obtained, samples were placed in plastic bags and labelled with identification numbers for laboratory analysis at the Coastal Erosion and Dune Dynamics (CEDD) Laboratory, University of Victoria.

3.3 Laboratory analysis

3.3.1 Sediment processing

Samples were weighed using a Kilo Tech KCS301 scale (accurate to 1g) and were oven dried using a Fisher Scientific Isotemp Oven for ~8 to 10 hours at 110 ± 5°C as per ASTM Standard D6913-04 (2009). Once dry, samples were then re-weighed to calculate percent moisture by dividing the sample weight before drying by sample weight post-drying (Folk 1974). Following this, a subsample of 200 g was obtained using an ELE International 'Riffel Box' sample splitter. Each subsample was then mechanically sorted with an ELE International Rota Sift equipped with dry seives following the ASTM standard D6913−04 (2009). Sorting, skewness, kurtosis, and particle diameter percentile metrics were obtained using the Microsoft Excel package GRADISTATS (Blott and Pye 2001, Hubbard and Glasser 2005, Dunning 2006, Prins *et al.* 2007, Rodríguez and Uriarte 2009, Bernier *et al.* 2014).

3.3.1.1 Sorting

Sorting nomenclature was developed by Folk and Ward (1957) to describe the degree of uniformity of particle size in a sediment. Classifications within the Folk and Ward (1957) nomenclature are: very well sorted; well sorted; moderately well sorted; moderately sorted; poorly sorted; very poorly sorted; or, extremely poorly sorted. Each category is designated by the statistical variance of the particle sizes within a sample (Blott and Pye 2010).

3.3.1.2 Skewness

Skewness aids in the conceptualization of a sediment particle size distribution (Folk and Ward 1957). It describes the symmetry, or lack thereof, within a sample and in what direction, if any, it is distorted. There are five main classifications of skewness: very finely skewed; finely skewed; symmetrical; coarsely skewed; or, very coarsely skewed (Folk and Ward 1957, Folk 1974, Blott and Pye 2010).

3.3.1.3 Kurtosis

When sediment samples are analysed in terms of a GSD, the graphical representation of the statistical distribution (assuming normal distribution) can be described in terms of its peakedness or flatness in six classifications: very platykurtic; platykurtic; mesokurtic; leptokurtic; very leptokurtic; or, extremely leptokurtic (Folk and Ward 1957; Blott and Pye 2001). Platykurtic describes a shallow, flat distribution with large standard deviations. Mesokurtic characterises a normal distribution, and leptokurtic describes small tails and a tall central peak, with low standard deviation and more clustering around the mean (Folk and Ward 1957, Blott and Pye 2001, Dunning 2006, Rodríguez and Uriarte 2009).

3.3.1.4 Percentiles

Percentiles describe the particle diameter as a specific percent at which the remaining sediment is coarser, or the particle size in which 10% of the mass of the sample is finer than the sample (Blott and Pye 2001, ASTM:D422−63 2007, Hajek *et al.* 2010, Rawle 2011). GRADISTAT (2010) provides, among others, particle diameters at the 10^{th}, 50^{th}, and 90^{th} percentiles, although, for the purpose of this research, only the particle diameter at the 10^{th} percentile (d_{10}) of the sample's mass was required (Blott and Pye 2001).

Each of these statistical measures was used to characterise and inventory the sediment present at each site. The combination of such statistical measures aids in the understanding of sediment-fluid transmission and allows for the comparison of plots, beaches, and Bit_Ex sediments.

3.3.1.5 Bulk density & porosity

Bulk density describes a sediment sample's dry weight in relation to its volume (Knödel *et al.* 2007). Given the known dimensions of the Barrel Sampler, once the sediment sample had been dried and weighed, bulk density was calculated by:

$$\boldsymbol{\rho b = \frac{M_s}{V}} \qquad \textbf{Equation 3.2}$$

where ρb is bulk density, M_s is dry soil weight (g), and V is soil volume (cm^3) (Smith and Mullins 2000, Knödel *et al.* 2007).

Using ρb, porosity is then back-calculated and is a dimensionless quantity presented as a percentage or a fraction that describes the ratio of a sample's void space within a known volume (Johnson 1963, Bascom 1964, Brassington 2007). Represented as:

$$\boldsymbol{\phi = 1 - \frac{\rho_b}{\rho_p}} \qquad \textbf{Equation 3.3}$$

where ϕ signifies porosity, $\rho_b$is equal to bulk density, and ρ_p represents the density of the particles (Detmer 1995, Knödel *et al.* 2007). ρ_p was approximated at 2.65 g/cm^3 or equal to the density of quartz, as it is the dominant component in shoreline sediments in the Salish Sea and Juan De Fuca Strait (Downing 1983, Terich 1987, Detmer 1995, ASTM:D4700-15 1999, Knödel *et al.* 2007).

3.3.2 Semi-empirical Ks models

Directly measuring Ks is preferred, although not always feasible. For this reason, various empirical and semi-empirical formulas exist to estimate Ks based on the characteristics of the porous media and the properties of the permeating fluid. For the purpose of this research, five semi-empirical equations used for coarse-grained sediments were identified to estimate Ks: the Kozeny-Carmen, Hazen, Slichter, Zamarin, and the Kozeny equations (Table 3.2) (Carrier 2003, Pliakas and Petalas 2011, Salarashayeri and Siosemarde 2012, Svensson 2014). To select the best Ks model for this application, the predicted Ks was compared to the *in-situ* measured Ks (Freeze and Cherry 1979, Carrier 2003, Chapuis and Aubertin 2003, Cabalar and Akbulut 2016). As these Ks formulae are dimensionally standardised, they meet the necessary requirements for comparison (Pliakas and Petalas 2011, Cabalar and Akbulut 2016). Such expressions have been employed previously to predict Ks within both coarse and fine sediments (Hazen 1911, Chapuis and Aubertin 2003, Pliakas and Petalas 2011, Svensson 2014, Cabalar and Akbulut 2016).

Table 3.2 - Formulas employed to determine Ks for each site plot.

Equation	Name	Expression	Intended use
Equation 3.4	Kozeny-Carmen[1]	$K_s = \left(\frac{\rho g}{\mu}\right)\left[\frac{n^3}{(1-n)^2}\right]\left(\frac{d_{10}^2}{180}\right)$	For sediments which are composed of large grain sizes [4]
Equation 3.5	Hazen[2]	$Ks = \frac{g}{v} \cdot (6 \times 10^{-4}) \cdot [1 + 10(n - 0.26)] \cdot d_{10}^2$	For sediments that range from 0.1mm< d10 < 3 mm, n < 5 [2,3]
Equation 3.6	Slitcher [3]	$Ks = \frac{g}{v} \cdot 10^{-2} \cdot n^{3.287} \cdot d_{10}^2$	For sediments which have 0.01 mm < d10 < 5 mm[2,3]
Equation 3.7	Zamarin[3]	$Ks = \frac{g}{v} \cdot (8.2 \times 10^{-3}) \cdot \frac{n^3}{(1-n)^2} \cdot d_{10}^2$	For sediments which are composed of large-grain sands[2]
Equation 3.8	Kozeny[3]	$Ks = \frac{g}{v} \cdot (8.3 \times 10^{-3}) \cdot \frac{n^3}{(1-n)^2} \cdot d_{10}^2$	For sediments which are composed of large grain sediments [2]

[1]: (Bear 1972); [2]: (Cabalar and Akbulut 2016); [3]: (Pliakas and Petalas 2011); [4]: (Freeze and Cherry 1979). Where ρ represents fluid density, g is equal to gravity, $\mu$is dynamic viscosity of the fluid, n is characterizes porosity of the sediment, d_{10} denotes the particle diameter at 10% of the sediment samples mass, and v is equal to kinematic viscosity of the fluid.

4 Chapter Four: Results

This chapter presents the results from the field experiments and laboratory analyses. It includes site descriptions, summary statistics for grain size analysis, as well as measured and calculated saturated hydraulic conductivity (Ks) for all plots. Measured Ks were compared to predicted Ks using the Kozeny-Carmen, Hazen, Slichter, Zamarin, and the Kozeny equations with seawater as the permeant. A modified version of the Hazen Equation was used to model dilbit Ks for bulk plot sediment samples, sampled plot strata, and for Bit_Ex sediments. The chapter concludes with an assessment of the results intended to identify *in-situ* sediments of high dilbit retention.

4.1 Site environmental conditions and sediment characteristics

4.1.1 Site 1: Muir Creek

Muir Creek, Site 1 (Figure 4.1), is located approximately 36 km west of Victoria, Vancouver Island. The shoreline of Muir Creek was dominated by coarse surface sediments (Figure 4.2) with intermittent regions of sand. Below the coarse surface veneer there was a transition to finer sediments, producing a poorly sorted and multi-modal GSD analysis (Figures 4.3; 4.4; 4.5, and Table 4.1).

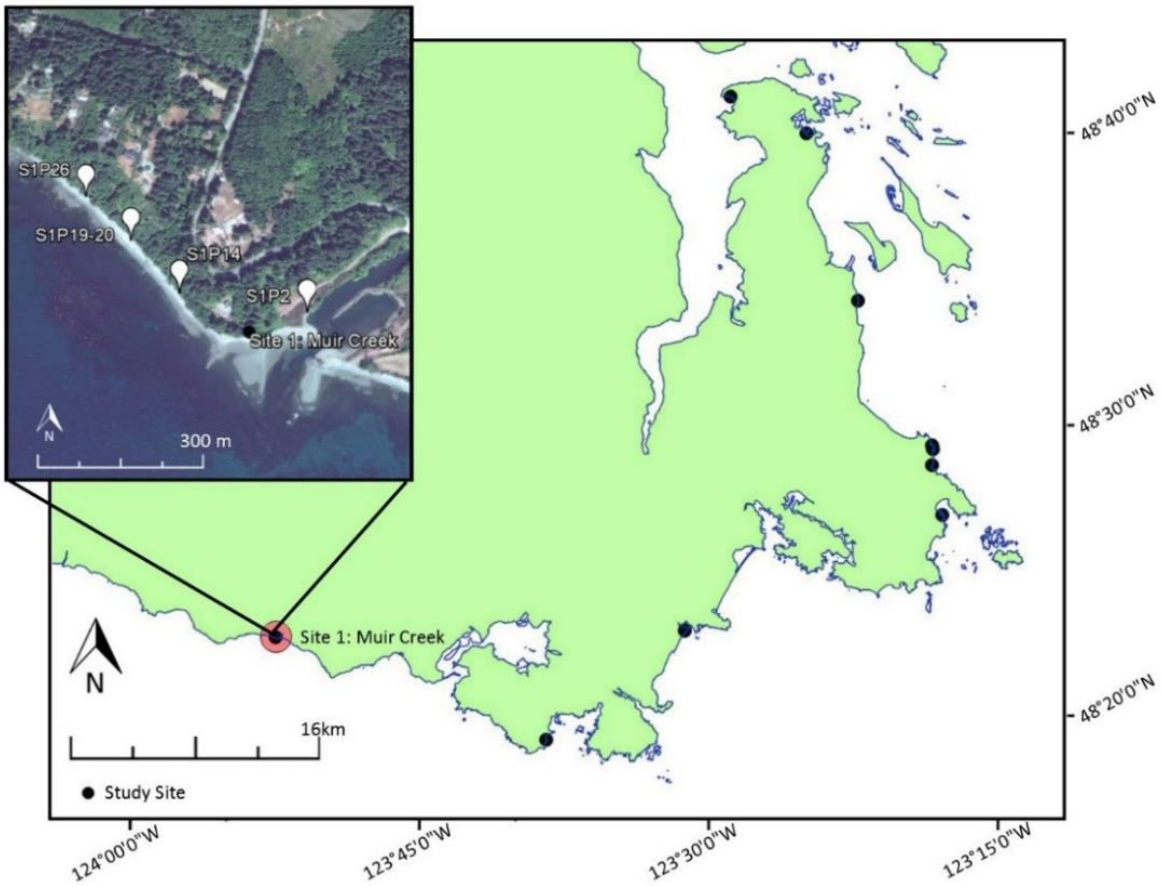

Figure 4.1 - Site 1: Muir Creek, B.C (Google Inc., 2015).

Figure 4.2 - Site 1 representative beach profile.

Table 4.1 - Site 1 environmental conditions, sediment description as per GRADISTAT (Version 8; Blott and Pye 2001).

Date Visited	August 11, 2016				
Environmental conditions					
Sky	Tidal Elevation	Avg. Air temperature	Avg. Water temperature	Avg. Ground temperature	Last Rain
Sunny	1.8m, rising	16°C	18°C	22°C	Aug. 7
Plot Sediment Characteristics					
Plot ID	S1P2	S1P14	S1P19-20	S1P26	
Lat (N)	48°22'48.36"	48°22'46.97"	48°22'49.34"	48°22'51.27"	
Long (W)	123°52'1.74"	123°52'14.23"	123°52'20.72"	123°52'26.77"	
Folk description[1]	sandy Gravel	sandy Gravel	sandy Gravel	Gravel	
Sorting[1]	Very Poorly Sorted	Very Poorly Sorted	Very Poorly Sorted	Poorly Sorted	
Skewness[1]	Coarse Skewed	Very Fine Skewed	Very Coarse Skewed	Symmetrical	
Kurtosis[1]	Very Platykurtic	Very Platykurtic	Very Platykurtic	Leptokurtic	
d_{10} Class[2]	Fine Sand	Medium Sand	Fine Sand	Very Coarse Sand	
d_{50} Class [2]	Very Coarse Sand	Very Fine Gravel	Very Coarse Sand	Medium Gravel	

[1]: Folk description, Sorting, Skewness, and Kurtosis described as per Folk and Ward (1957).
[2]: d_{10} and d_{50} represent the sediment particle diameter at 10 and 50% of a sample's mass and are described as per Folk and Ward (1957).

Figure 4.3 - S1P14. Profile pit dug to ~45 cm deep.

Figure 4.4 - S1P19-20 profile pit dug to ~45 cm deep.

Figure 4.5 - S1P26 profile pit dug to ~45 cm deep.

Note: No profile photo was taken for S1P2

4.1.2 Site 2: Aylard Farm Beach

Aylard Farm Beach, Site 2 (Figure 4.6), is located approximately 19 km west of Victoria, Vancouver Island. The shoreline of Aylard Farm Beach was predominately composed of fine sediments such as sand, although intermittent regions of granules and pebbles do occur (Figure 4.7). Below intermittent coarse surface veneer, there was a transition to finer sediments, producing a poorly sorted and multi-modal GSD analysis (Table 4.1 and Figures 4.8; 4.9; 4.10; 4.11). In regions where stratification was not apparent, the GSD analysis indicated a higher degree of uniformity indicative of well-sorted sediments (Table 4.2).

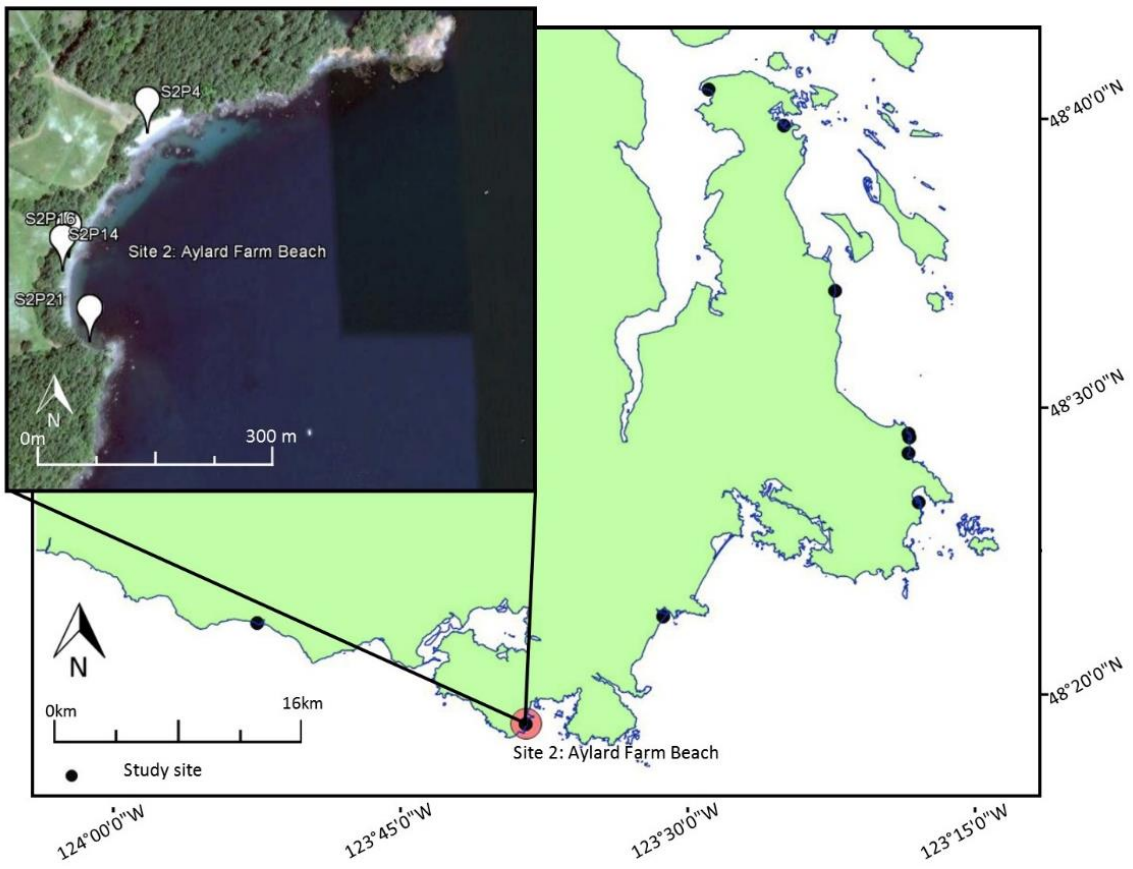

Figure 4.6 - Site 2: Aylard Farm Beach, Sooke (Google Inc., 2016).

Figure 4.7 - Site 2 representative beach profiles. Profile A is representative of S2P4 & S2P21 while profile B is representative of S2P14 & S2P16.

Table 4.2 - Site 2 environmental conditions and sediment description as per GRADISTAT (Version 8; Blott and Pye 2001).

Date Visited	August 17, 2016				
Environmental Conditions					
Sky	Tidal Elevation	Avg. Air temperature	Avg. Water temperature	Avg. Ground temperature	Last Rain
Sunny	0.6m, rising	12ºC	17ºC	24ºC	≥10 days
Plot Sediment Characteristics					
Plot ID	S2P4	S2P14	S2P16	S2P21	
Lat (ºN)	48°19'28.30"	48°19'22.57"	48°19'21.95"	48°19'18.74"	
Long (ºW)	123°38'7.06"	123°38'12.41"	123°38'12.82"	123°38'10.92"	
Folk description[1]	Sand	Sandy Gravel	Sandy Gravel	Slightly gravelly Sand	
Sorting[1]	Very Well Sorted	Very Poorly Sorted	Poorly Sorted	Moderately Well Sorted	
Skewness[1]	Coarse Skewed	Very Fine Skewed	Very Fine Skewed	Very Coarse Skewed	
Kurtosis[1]	Mesokurtic	Platykurtic	Leptokurtic	Mesokurtic	
d_{10} Class[2]	Very Fine Sand	Medium Sand	Medium Sand	Very Fine Sand	
d_{50} Class [2]	Fine Sand	Very Fine Gravel	Very Fine Gravel	Fine Sand	
[1]: Folk description, Sorting, Skewness, and Kurtosis described as per Folk and Ward (1957). [2]: d_{10} and d_{50} represent the sediment particle diameter at 10 and 50% of a sample's mass and are described as per Folk and Ward (1957).					

Figure 4.8 - S2P4 Profile pit dug to ~35 cm deep.

Figure 4.9 - S2P14 profile pit dug to ~32 cm deep. Note mud/clay at ~28 cm.

Figure 4.10 - S2P16 profile pit dug to ~32 cm deep. Note 5cm coarse strata at ~27 cm.

Figure 4.11 - S2P21 profile pit dug to ~23 cm deep. Note boulder/cobble at ~22 cm.

4.1.3 Site 3: Witty's Lagoon

Witty's Lagoon, Site 3 (Figure 4.12), is located approximately 13 km west of Victoria, Vancouver Island. The surficial shoreline sediment of Witty's Lagoon was primarily sand, although subsurface sediments vary widely in grain size. The sediments present at each plot show distinct characteristics when compared to each other, whereby, S3PN consists of considerably more uniform in contrast to S3P24 (Table 4.3 and Figures 4.14; 4.15).

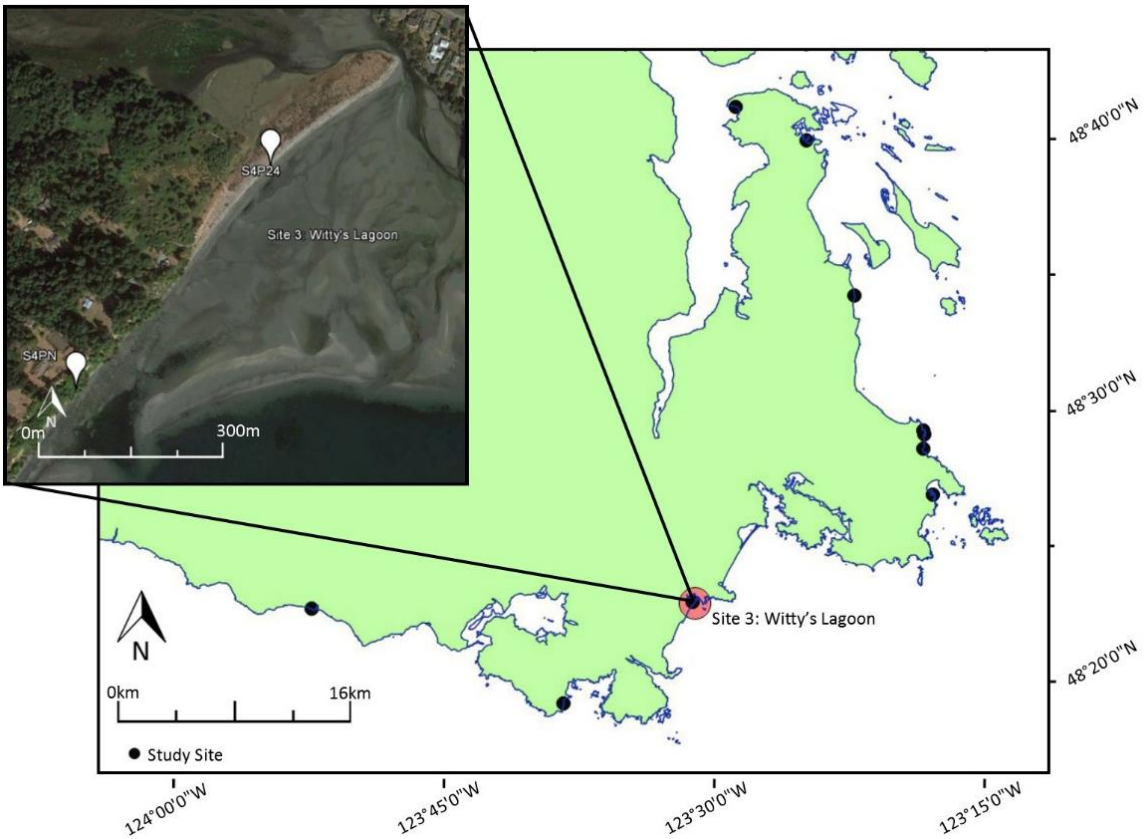

Figure 4.12 - Site 3, Witty's Lagoon, Sooke (Google Inc., 2016).

Figure 4.13 - Site 3 representative beach profile.

Table 4.3 - Site 3 environmental conditions and sediment description as per GRADISTAT (Version 8; Blott and Pye 2001).

Date Visited	Aug. 18. 2016				
Environmental Conditions					
Sky	Tidal Elevation	Avg. Air temperature	Avg. Water temperature	Avg. Ground temperature	Last Rain
Sunny	0.6m, rising	20°C	19°C	21°C	≥10 days
Plot Sediment Characteristics					
Plot ID	S3PN		S3P24[3]		
Lat (N)	48°22'52.76"		48°23'5.24"		
Long (W)	123°31'5.85"		123°30'49.44"		
Folk description[1]	Slightly gravelly Sand		Sandy Gravel		
Sorting[1]	Well Sorted		Very Poorly Sorted		
Skewness[1]	Symmetrical		Fine Skewed		
Kurtosis[1]	Mesokurtic		Very Platykurtic		
d_{10} Class[2]	Fine Sand		Fine Sand		
d_{50} Class [2]	Fine Sand		Coarse Sand		

[1]: Folk description, Sorting, Skewness, and Kurtosis described as per Folk and Ward (1957).
[2]: d_{10} and d_{50} represent the sediment particle diameter at 10 and 50% of a sample's mass and are described as per Folk and Ward (1957).
[3]: A bimodal distribution of sediment at site S3P24 resulted in the larger fractions of the sediments (cobble gravel) to be underrepresented in sediment statistics. Additionally, the sediment sampling tube's diameter did not allow for cobble size clasts to be obtained.

Figure 4.14 - S3PN. Profile pit dug to ~34 cm deep. Note coarse strata at 13 cm.

Figure 4.15 - S3P24 profile pit dug to ~45 cm deep.

4.1.4 Site 4: Loon Bay

Loon Bay, Site 4 (Figure 4.16), is located approximately 6 km east of Victoria, Vancouver Island. Regions of the Loon Bay shoreline was composed of a vegetated region, which extends to the high-water line, as well as regions of sand, which extend into the intertidal zone (Figure 4.17), both regions composed of sediment were dominated by sand (Table 4.4). Sediments were generally uniform in nature with no visual stratification (Figures 4.18; 4.19).

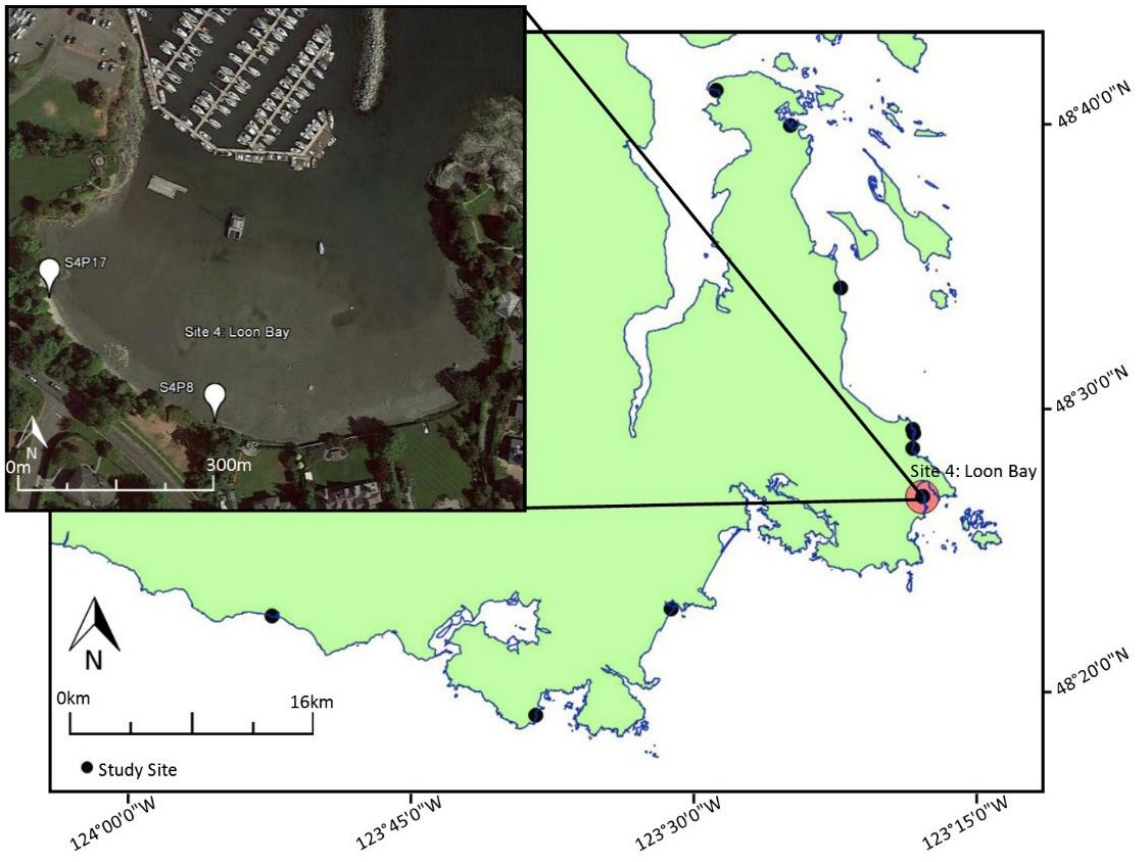

Figure 4.16 - Site 4. Loon Bay Victoria (Google Inc., 2016).

Figure 4.17 - Site 4 representative beach profile.

Table 4.4 - Site 4 environmental conditions and sediment description as per GRADISTAT (Version 8; Blott and Pye 2001).

Date Visited	Aug. 2, 20126				
Environmental Conditions					
Sky	Tidal Elevation	Avg. Air temperature	Avg. Water temperature	Avg. Ground temperature	Last Rain
Sunny	2.3m, rising	12ºC	18ºC	19ºC	≥10 days
Plot Sediment Characteristics					
Plot ID	S4P8		S4P17		
Lat (N)	48°26'59.22"		48°27'1.40"		
Long (W)	123°17'41.14"		123°17'45.51"		
Folk description[1]	sandy Gravel		Sand		
Sorting[1]	Very Poorly Sorted		Moderately Well Sorted		
Skewness[1]	Symmetrical		Symmetrical		
Kurtosis[1]	Very Platykurtic		Leptokurtic		
d_{10} Class[2]	Fine Sand		Fine Sand		
d_{50} Class [2]	Very Coarse Sand		Fine Sand		

[1]: Folk description, Sorting, Skewness, and Kurtosis described as per Folk and Ward (1957).
[2]: d_{10} and d_{50} represents the sediment particle diameter at 10 and 50% of a sample's mass and are described as per Folk and Ward (1957).

Figure 4.18 - S4P17 profile pit dug to ~33 cm deep.

Figure 4.19 - S4P8. Profile pit dug to ~15 cm deep.

4.1.5 Site 5: Arbutus Cove Beach

Arbutus Cove Beach, Site 5 (Figure 4.20), is located approximately 8 km northeast of Victoria, Vancouver Island. The shoreline of Arbutus Cove was dominated by sand, although regions of coarser sediments, such as granules and small pebble were common below the high-water line (Figure 4.21). The GSD analysis (Table 4.6) broadly indicated multi-modal distribution, although stratification was not visually present within profile pits dug at each plot (Figures 4.22; 4.23; 4.24)

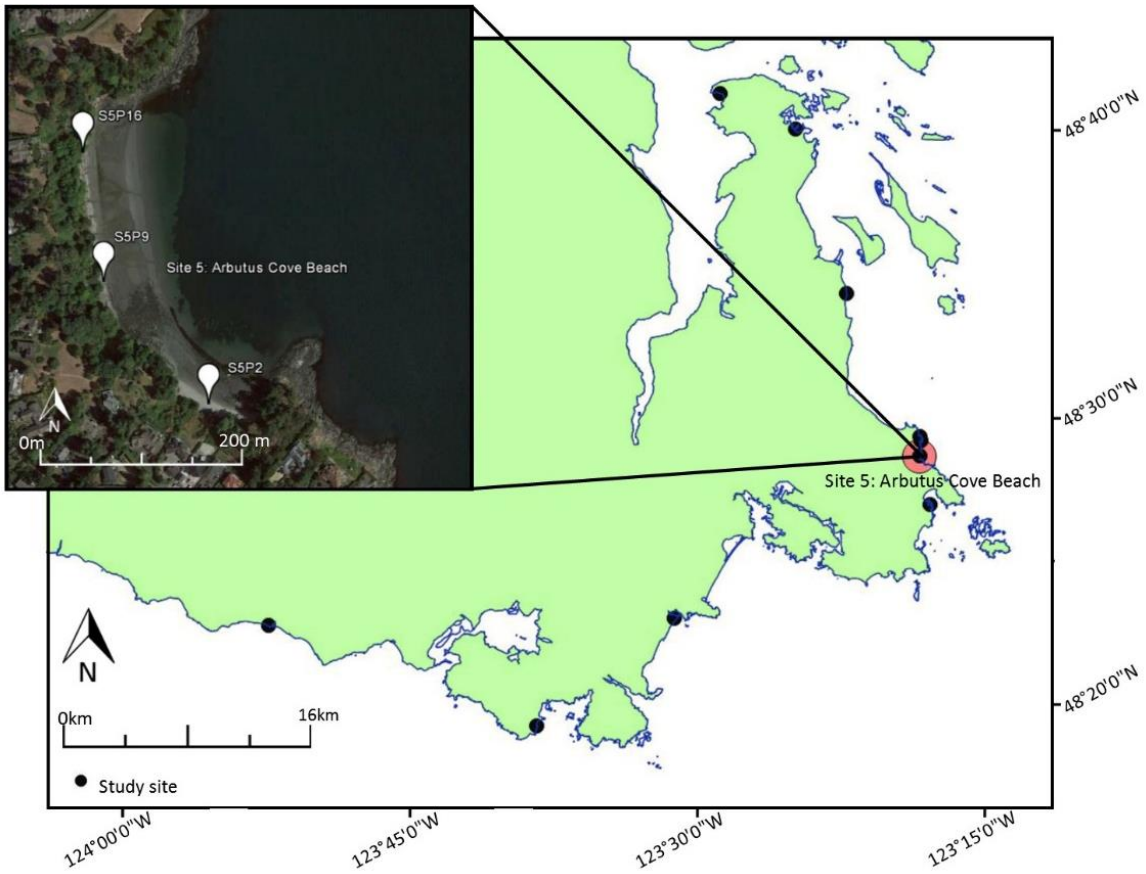

Figure 4.20 - Site 5. Arbutus Cove Beach, Victoria (Google Inc. 2016).

Figure 4.21 - Site 5 representative beach profile.

Table 4.5 - Site 5 environmental conditions and sediment description as per GRADISTAT (Version 8; Blott and Pye 2001).

Date Visited	July 19, 20, and 28, 2016				
Environmental Conditions					
Sky	Tidal Elevation	Avg. Air temperature	Avg. Water temperature	Avg. Ground temperature	Last Rain
Sunny	rising	18ºC	18ºC	24ºC	≥10 days
Plot Sediment Characteristics					
Plot ID	S5P2		S5P9	S5P16	
Lat (N)	48°28'33.14"		48°28'37.39"	48°28'41.87"	
Long (W)	123°18'5.75"		123°18'11.26"	123°18'12.28"	
Folk description[1]	Sand		gravelly Sand	sandy Gravel	
Sorting[1]	Very Well Sorted		Poorly Sorted	Very Poorly Sorted	
Skewness[1]	Coarse Skewed		Very Coarse Skewed	Very Fine Skewed	
Kurtosis[1]	Platykurtic		Very Leptokurtic	Very Platykurtic	
d_{10} Class[2]	Fine Sand		Fine Sand	Medium Sand	
d_{50} Class [2]	Fine Sand		Medium Sand	Very Fine Gravel	

[1]: Folk description, Sorting, Skewness, and Kurtosis described as per Folk and Ward (1957).
[2]: d_{10} and d_{50} represent the sediment particle diameter at 10 and 50% of a sample's mass and are described as per Folk and Ward (1957).

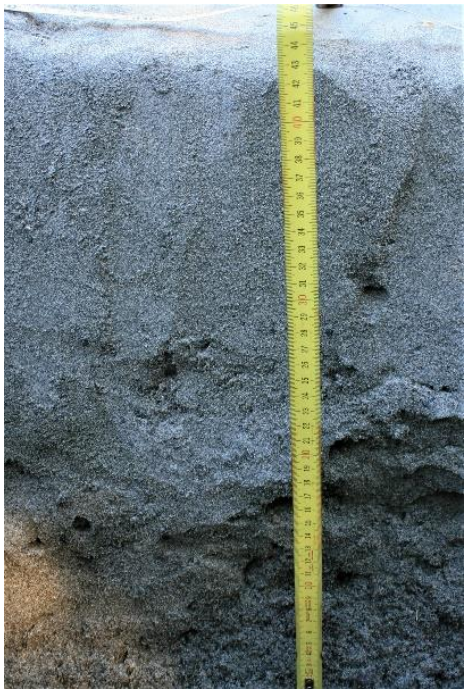

Figure 4.22 - S5P2. Profile pit dug to ~44 cm deep

Figure 4.23 - S5P9 profile pit dug to ~50 cm deep. Note coarser strata from 21 cm to 30 cm.

Figure 4.24 - S5P16 profile pit dug to ~26 cm deep.

4.1.6 Site 6: Island View Beach

Island View Beach, Site 6 (Figure 4.25), is located approximately 15 km north of Victoria, Vancouver Island. The shoreline of Island View Beach was dominated by sand, although regions of coarser sediments, such as granules and small pebble were common (Figure 4.26). Sediments were generally poorly sorted and skewed towards finer grain sizes (Table 4.6). The GSD analysis (Table 4.6) broadly indicated multi-modal distribution due to stratification which can be seen in Figures 4.27; 4.28; 4.29; 4.30.

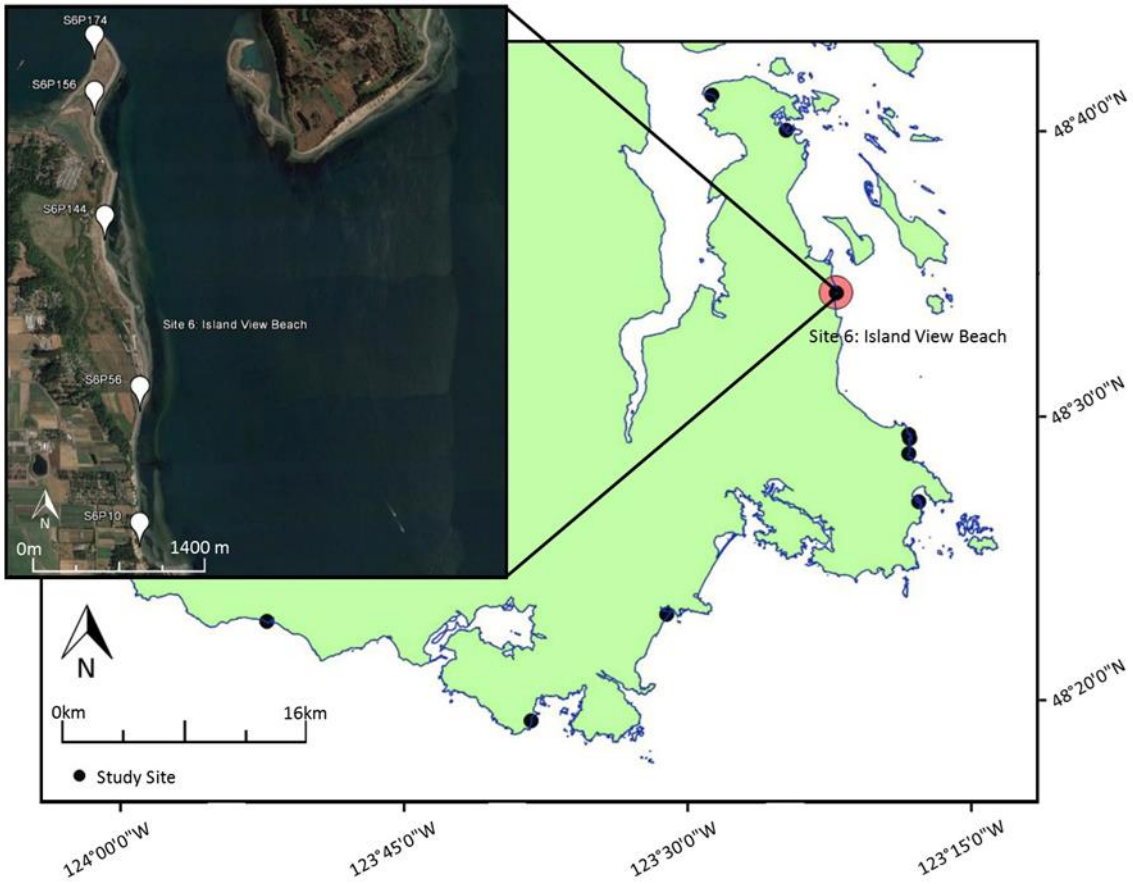

Figure 4.25 - Site 6. Island View Beach, Saanichton (Google Inc. 2016).

Figure 4.26 - Site 6 representative beach profiles. Photo A -S6P10; photo B - S6P56, and photo C - S6P156.

Table 4.6 - Site 6 environmental conditions and sediment description as per GRADISTAT (Version 8; Blott and Pye 2001).

Date Visited	Aug. 3, 9, 10, and 23 2016				
Environmental Conditions					
Sky	Tidal Elevation	Avg. Air temperature	Avg. Water temperature	Avg. Ground temperature	Last Rain
Sunny	Rising	18°C	17.5°C	21°C	Aug. 10
Plot Sediment Characteristics					
Plot ID	S6P10		S6P56	S6P144	
Lat (N)	48°33'36.10"		48°34'12.84"	48°34'59.11"	
Long (W)	123°22'2.16"		123°22'2.14"	123°22'16.63"	
Folk description[1]	gravelly Sand		gravelly Sand	sandy Gravel	
Sorting[1]	Poorly Sorted		Poorly Sorted	Poorly Sorted	
Skewness[1]	Very Coarse Skewed		Very Coarse Skewed	Very Fine Skewed	
Kurtosis[1]	Very Leptokurtic		Very Platykurtic	Very Platykurtic	
d_{10} Class[2]	Fine Sand		Fine Sand	Medium Sand	
d_{50} Class [2]	Medium Sand		Coarse Sand	Very Fine Gravel	

Table 4.6 continued			
Plot ID	S6P156	S6P174	
Lat (N)	48°35'32.92"	48°35'48.30"	
Long (W)	123°22'20.95"	123°22'21.00"	
Folk description[1]	Sandy Gravel	Sand	
Sorting[1]	Poorly Sorted	Very Well Sorted	
Skewness[1]	Fine Skewed	Symmetrical	
Kurtosis[1]	Very Platykurtic	Mesokurtic	
d_{10} Class[2]	Medium Sand	Medium Sand	
d_{50} Class [2]	Very Coarse Sand	Medium Sand	
[1]: Folk description, Sorting, Skewness, and Kurtosis described as per Folk and Ward (1957). [2]: d_{10} and d_{50} represent the sediment particle diameter at 10 and 50% of a sample's mass and are described as per Folk and Ward (1957).			

Figure 4.27 - S6P10. Profile pit dug to ~27 cm. Note coarse strata at ~10cm in addition to an underlying clay/silt layer at 27 cm.

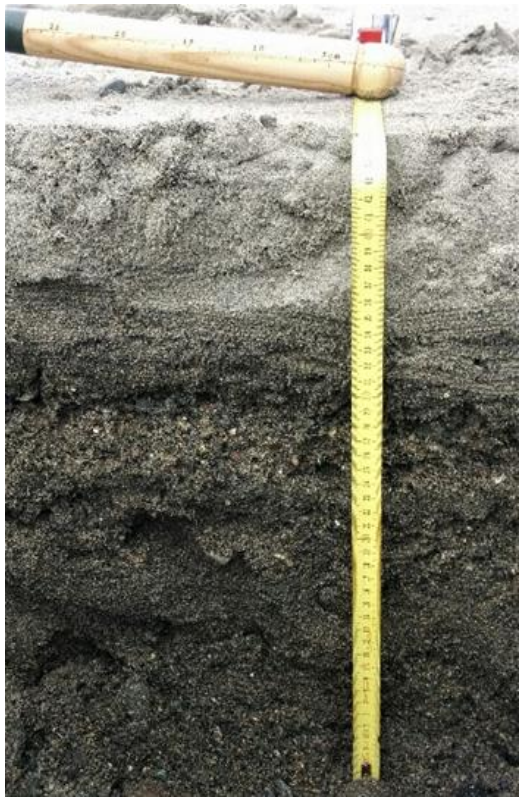

Figure 4.28 - S6P56 profile pit dug to ~45 cm. Note coarser strata from ~24 cm.

Figure 4.29 - S5P156 profile pit dug to ~45 cm.

Figure 4.30 - S6P144 profile pit dug to ~35 cm.

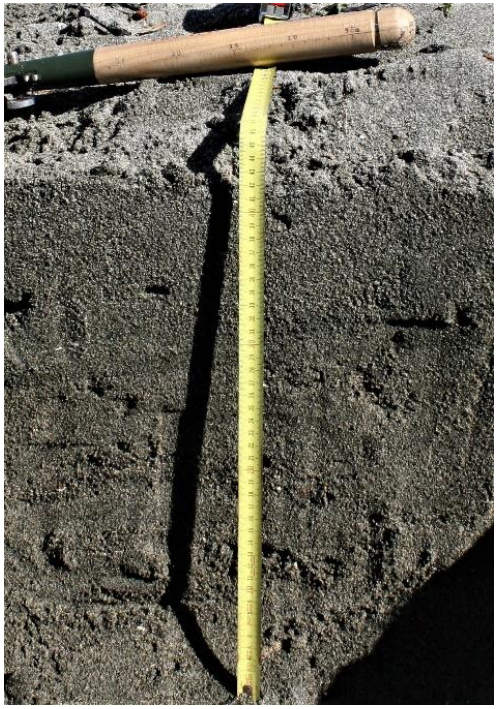

Figure 4.31 - S6P174 profile pit dug to ~45 cm.

4.1.7 Site 7: Resthaven Park

Resthaven Park, Site 7 (Figure 4.32), is located approximately 27 km north of Victoria, Vancouver Island. The shoreline of Resthaven Park was predominately finer sediments such as silts, clays, and fine sands, although coarse sediment (pebbles) were sparsely present within the shoreline sediment matrix (Figure 4.33). The presence of coarse sediment within the silts, clay, and sand matrix produced a poorly sorted and multi-modal GSD analysis, while sediment samples were visually dominated by the finer grain sizes (Table 4.7 and Figures 4.34; 4.35).

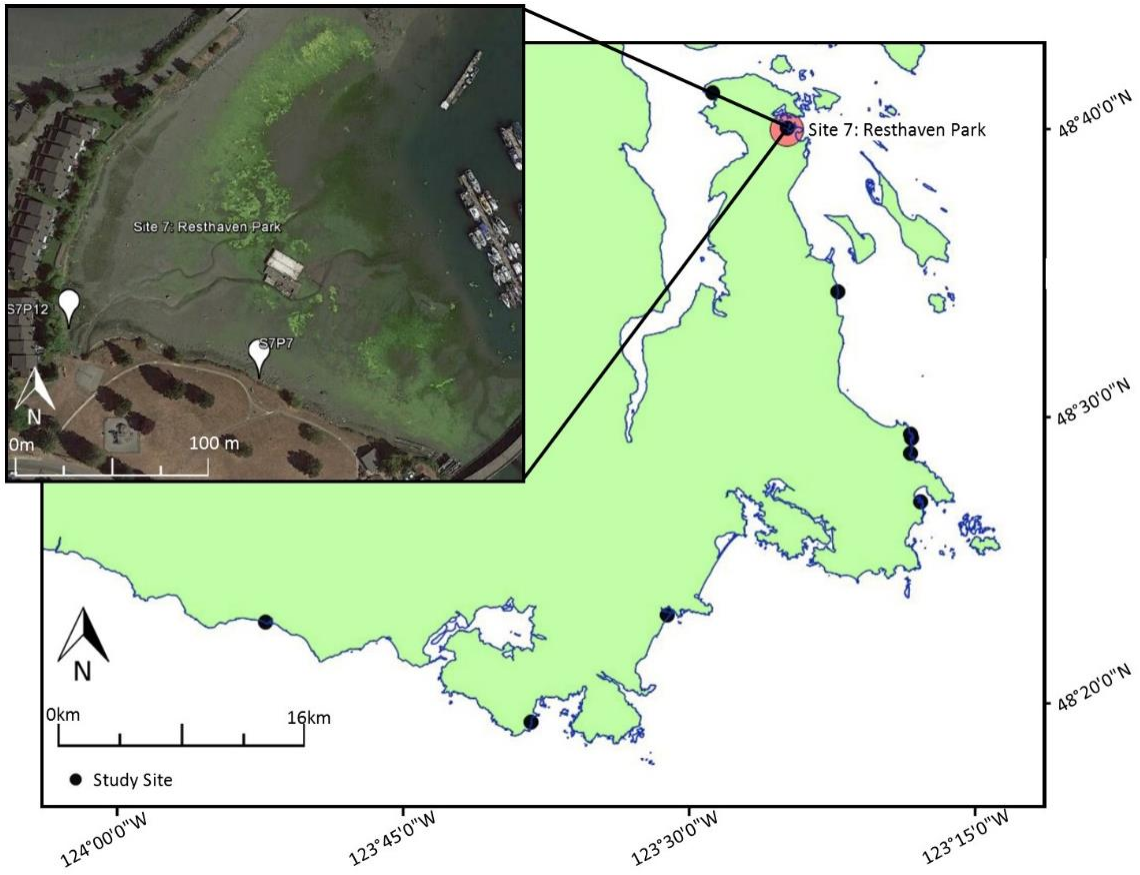

Figure 4.32 - Site 7. Resthaven Park, Sidney (Google Inc. 2016).

Figure 4.33 - Site 7 representative beach profiles. Photo A is representative of P7S7 and photo B is representative of S7P12.

Table 4.7- Site 7 environmental conditions and sediment description as per GRADISTAT (Version 8; Blott and Pye 2001).

Date Visited	Aug. 21, 2016				
Environmental Conditions					
Sky	Tidal Elevation	Avg. Air temperature	Avg. Water temperature	Avg. Ground temperature	Last Rain
Sunny	0.9 m, rising	22°C	18°C	19°C	≥10 days
Plot Sediment Characteristics					
Plot ID	S7P7		S7P12		
Lat (N)	48°39'59.71"		48°40'0.56"		
Long (W)	123°24'37.57"		123°24'42.55"		
Folk description[1]	muddy sandy Gravel		gravelly muddy Sand		
Sorting[1]	Very Poorly Sorted		Very Poorly Sorted		
Skewness[1]	Very Coarse Skewed		Very Coarse Skewed		
Kurtosis[1]	Very Platykurtic		Very Platykurtic		
d_{10} Class[2]	Fine Silt		Fine Silt		
d_{50} Class [2]	Fine Sand		Medium Sand		

[1]: Folk description, Sorting, Skewness, and Kurtosis described as per Folk and Ward (1957).
[2]: d_{10} and d_{50} represent the sediment particle diameter at 10 and 50% of a sample's mass and are described as per Folk and Ward (1957).

Figure 4.34 - S7P7. Profile pit dug to ~23 cm deep.

Figure 4.35 - S7P12 profile pit dug to ~33 cm deep. Note coarser strata from 27 cm to 33 cm.

4.1.8 Site 8: Chalet Beach

Chalet Beach, Site 8 (Figure 4.36), is located approximately 31 km north of Victoria, Vancouver Island. The shoreline of Chalet Beach was veneered by coarse surface sediments ranging from granules to coarse pebbles (Figure 4.37). Directly below the coarse surface stratum there were fine sediments such as silts, clays, and fine sand. Such conditions produce a poorly sorted and multi-modal GSD analysis (Table 4.8 and Figures

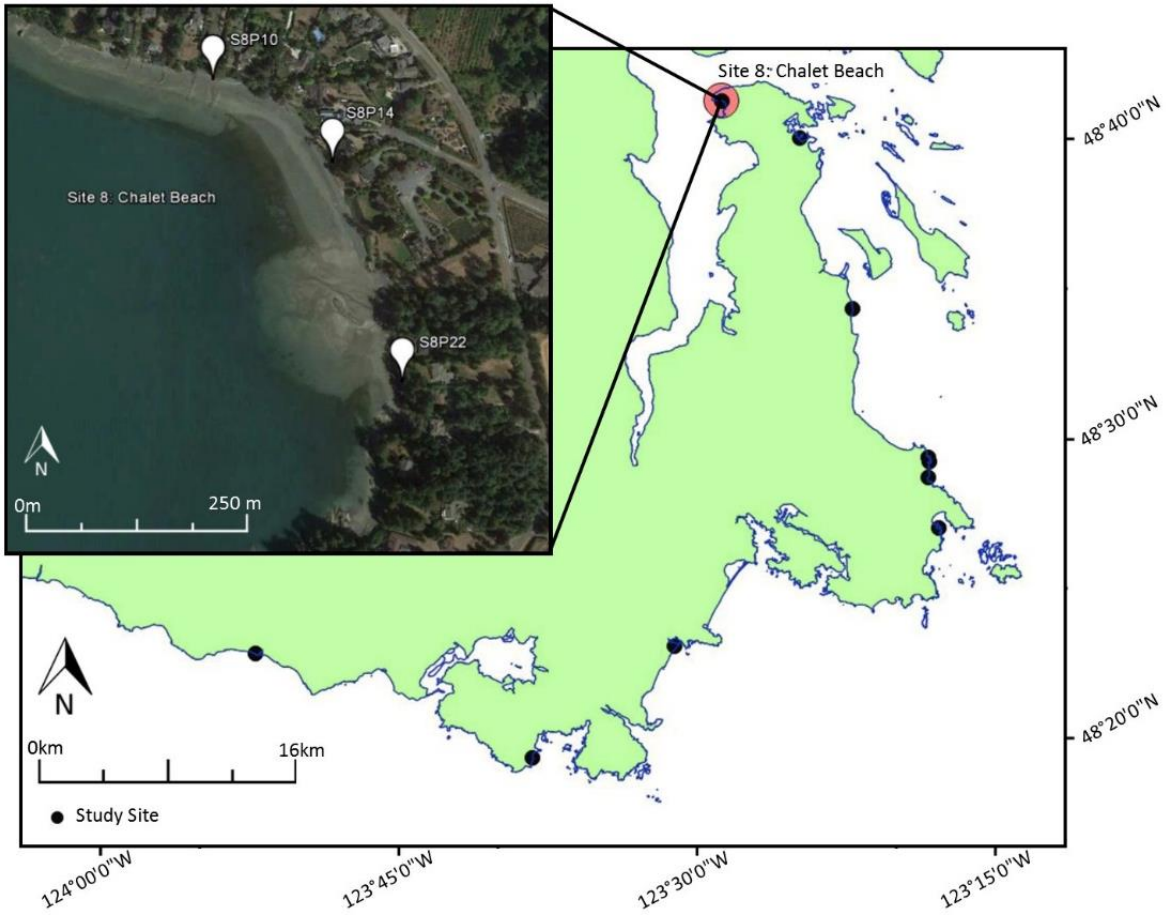

Figure 4.36 - Site 8. Chalet Beach, Sidney (Google Inc. 2016).

4.38; 4.39; 4.40).

Figure 4.37 - Site 8 representative beach profiles. Photo A taken at S8P10 and photo B taken at S8P14.

Table 4.8 - Site 8 environmental conditions and sediment description as per GRADISTAT (Version 8; Blott and Pye 2001).

Date Visited	July 22, 2016				
Environmental Conditions					
Sky	Tidal Elevation	Avg. Air temperature	Avg. Water temperature	Avg. Ground temperature	Last Rain
Sunny	0.5m, rising	24°C	23°C	32°C	≥10 days
Plot Sediment Characteristics					
Plot ID	S8P10		S8P14	S8P22	
Lat (N)	48°41'18.47"		48°41'15.44"	48°41'7.49"	
Long (W)	123°28'33.68"		123°28'27.12"	123°28'23.26"	
Folk description[1]	sandy Gravel		sandy Gravel	sandy Gravel	
Sorting[1]	Poorly Sorted		Poorly Sorted	Poorly Sorted	
Skewness[1]	Very Coarse Skewed		Very Fine Skewed	Symmetrical	
Kurtosis[1]	Mesokurtic		Platykurtic	Very Platykurtic	
d_{10} Class[2]	Coarse Silt		Fine Sand	Coarse Sand	
d_{50} Class [2]	Very Fine Gravel		Very Fine Gravel	Very Fine Gravel	
[1]: Folk description, Sorting, Skewness, and Kurtosis described as per Folk and Ward (1957). [2]: d_{10} and d_{50} represent the sediment particle diameter at 10 and 50% of a sample's mass and are described as per Folk and Ward (1957).					

Figure 4.38 - S8P10. Profile pit dug to ~11 cm. Note underlying silt/clay.

Figure 4.39 - S8P14 profile pit dug to ~8 cm. Note underlying silt/clay.

Figure 4.40 - S8P22 profile pit dug to ~16 cm. Note underlying silt/clay.

4.1.9 Site 9: Glencoe Cove-Kwartsech Park North

Glencoe Cove-Kwartsech Park North, Site 9 (Figure 4.41), is located approximately 9 km northeast of Victoria, Vancouver Island. The shoreline of Glencoe Cove-Kwartsech Park North was dominated by coarse surface sediments ranging between granules and small pebbles (Figure 4.42). A coarse surface veneer approximately 7cm thick quickly transitioned to finer sediments, producing a poorly sorted and multi-modal GSD analysis (Table 4.9 and Figures 4.43; 4.44).

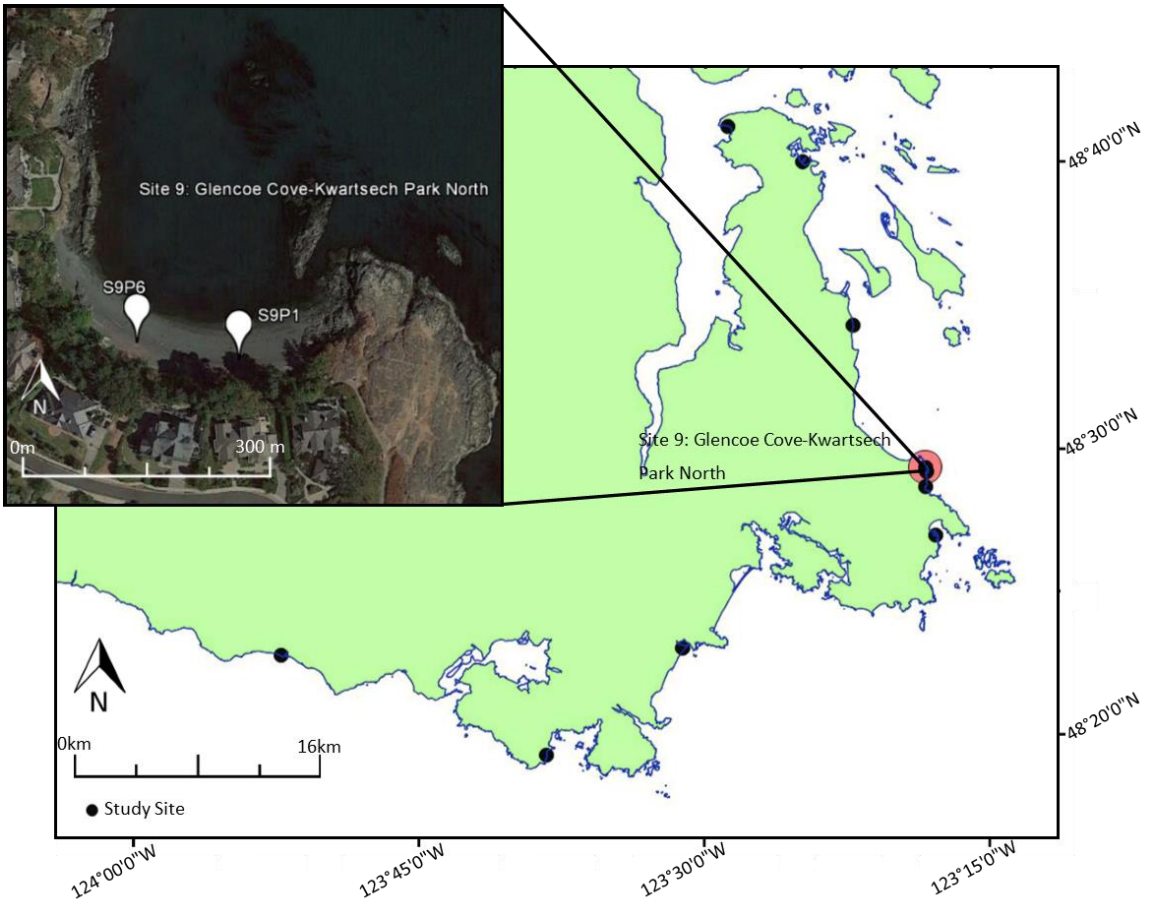

Figure 4.41 - Site 9. Glencoe Cove-Kwartsech Park North, Victoria (Google Inc. 2016).

Figure 4.42- Site 9 representative beach profiles.

Table 4.9 - Site 9 environmental conditions and sediment description as per GRADISTAT (Version 8; Blott and Pye 2001).

Date Visited	Aug. 25, 2016				
Environmental Conditions					
Sky	Tidal Elevation	Avg. Air temperature	Avg. Water temperature	Avg. Ground temperature	Last Rain
Sunny	2.0m, rising	18ºC	14ºC	14ºC	≥10 days
Plot Sediment Characteristics					
Plot ID	S9P3		S9P6		
Lat (N)	48°29'23.78"		48°29'24.01"		
Long (W)	123°18'10.34"		123°18'12.62"		
Folk description[1]	sandy Gravel		sandy Gravel		
Sorting[1]	Poorly Sorted		Poorly Sorted		
Skewness[1]	Very Fine Skewed		Very Fine Skewed		
Kurtosis[1]	Leptokurtic		Leptokurtic		
d_{10} Class[2]	Medium Sand		Medium Sand		
d_{50} Class [2]	Very Fine Gravel		Very Fine Gravel		

[1]: Folk description, Sorting, Skewness, and Kurtosis described as per Folk and Ward (1957).
[2]: d_{10} and d_{50} represent the sediment particle diameter at 10 and 50% of a sample's mass and are described as per Folk and Ward (1957).

Figure 4.43 - S9P3. Profile pit dug to ~36 cm. Note coarse strata from ~29 to ~36 cm and the underlying silt/clay.

Figure 4.44 - S9P6 profile pit dug to ~36 cm. Note coarse strata from ~29 to ~35 cm and the underlying silt/clay

4.1.10 Site 10: Glencoe Cove-Kwartsech Park South

Glencoe Cove-Kwartsech Park South, Site 10 (Figure 4.45), is located approximately 9 km northeast of downtown Victoria, Vancouver Island. The shoreline of Glencoe Cove-Kwartsech Park South was dominated by coarse surface sediments such as granules and small pebbles (Figure 4.46). The coarse surface strata (~8 cm thick) transitions to finer sediments, producing a poorly sorted and multi-modal GSD analysis (Table 4.10 and Figure 4.47).

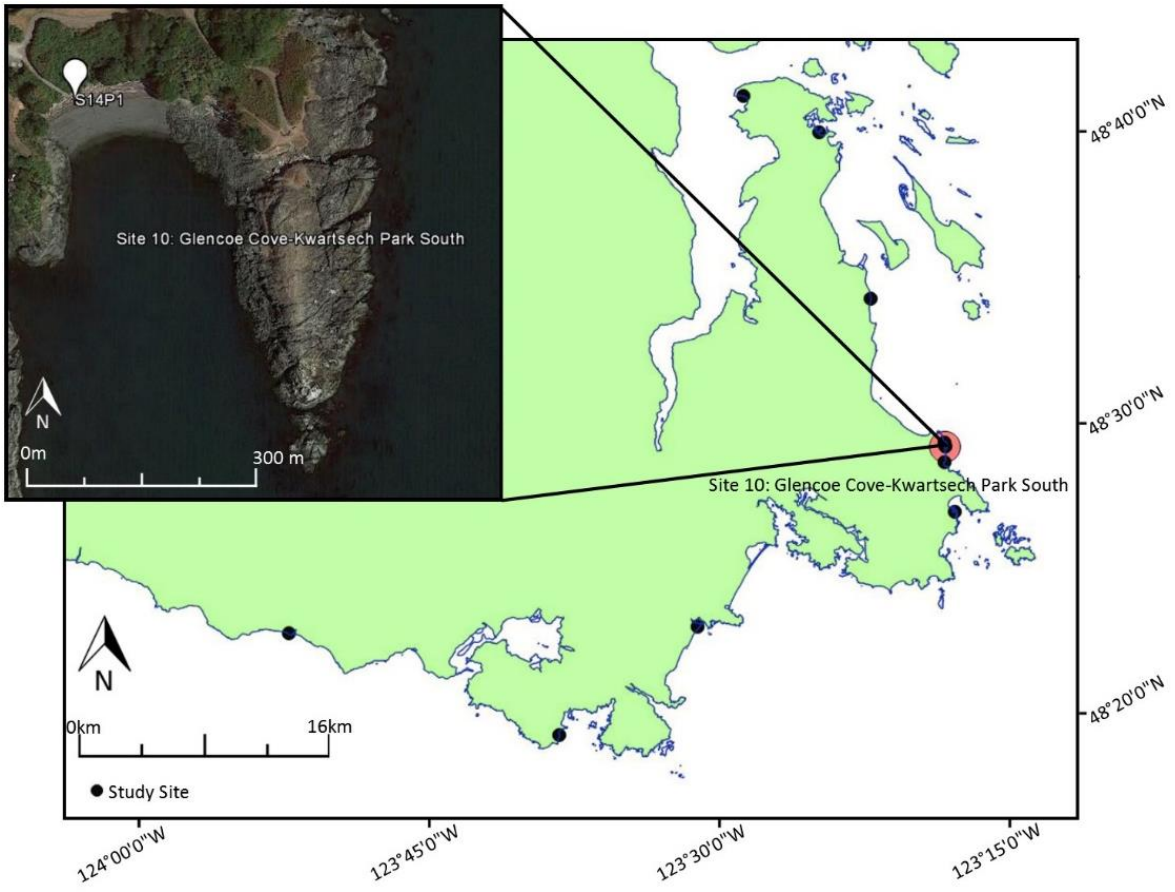

Figure 4.45 - Site 10. Glencoe Cove-Kwartsech Park South, Victoria (Google Inc. 2016).

Figure 4.46 - Site 10 representative beach profile.

Table 4.10 – Site 10 environmental conditions and sediment description as per GRADISTAT (Version 8; Blott and Pye 2001).

Date Visited	Aug. 25, 2016				
Environmental Conditions					
Sky	Tidal Elevation	Avg. Air temperature	Avg. Water temperature	Avg. Ground temperature	Last Rain
Sunny	2.0m, rising	18ºC	17ºC	19ºC	≥10 days
Plot Sediment Characteristics					
Plot ID	S10P1				
Lat (N)	48°29'15.14"				
Long (W)	123°18'8.24"				
Folk description[1]	sandy Gravel				
Sorting[1]	Poorly Sorted				
Skewness[1]	Very Fine Skewed				
Kurtosis[1]	Very Platykurtic				
d_{10} Class[2]	Medium Sand				
d_{50} Class [2]	Very Fine Gravel				
[1]: Folk description, Sorting, Skewness, and Kurtosis described as per Folk and Ward (1957). [2]: d_{10} and d_{50} represent the sediment particle diameter at 10 and 50% of a sample's mass and are described as per Folk and Ward (1957).					

Figure 4.47 - S10P1. Profile pit dug to ~37 cm. Note coarse strata from ~29 to ~37 cm.

4.2 Field results and model selection

4.2.1 Field results

The field campaign was designed to: (a) obtain *in-situ* Ks measurements; and, (b) obtain sediment samples representative of beaches on southeastern Vancouver Island. The effective grain size (d10) (Chapter 2, section 2.8) at the study sites ranges from 0.0073 mm (silt) to 2.12 mm (granules). Sand-sized particles (0.0062 to 0.2 mm) was the most common effective grain size for bulk sediment samples, occurring in 91% of plots. Measured porosities varied from 27% (S8P14; Figure 4.42) to 59% (S7P7; Figure 4.37), with the average porosity being 40% (Table 4.1). The maximum and minimum *in-situ* Ks values range from 237.24 (S5P156; Figure 4.27) to 4.25 (S7P7; Figure 4.3) m/day (Table 4.1). Bulk plot sediment samples were dominated by fine materials (silts and sand) and, therefore low Ks sediments are well represented at all the study sites. Large clast sediments (pebbles, cobbles, and boulders) are underrepresented at the sites, when the sediment samples are assessed as a homogeneous unit (Table 4.1).

In-situ Ks values for all sediments occur within the expected range given the dominance of sand within the samples. The results for *in-situ* Ks indicate sediments ranging from slightly below coarse sand (~9.9 m/day) to slightly above granules (~182.5 m/day) (Figure 4.1). In comparison, Bit_Ex sediments predicted Ks values that ranged from approximately 10 m/day to 11,900 m/day. To further contextualise and affirm both Bit_Ex and the sampled Ks results, Figure 4.1 shows the commonly accepted Ks values for pebble, sand, and silt presented by Freeze and Cherry (1979).

Table 4.11 - The d_{10} (mm), porosity (%), and measured Ks (m/day) for bulk sediment samples at each visited plots and Bit_Ex sediments.

Site Plot	d10 (mm)	Porosity	Measured Ks (m/day)	Site-Plot	d10 (mm)	Porosity	Measured Ks (m/day)
S1P14	0.27	0.36%	45.33	S5P16	0.27	0.37	237.24
S1P19-20	0.21	0.39%	145.60	S6P10	0.16	0.35	54.02
S2P4	0.11	0.43%	68.00	S6P56	0.18	0.37	148.81
S2P14	0.26	0.42%	27.69	S6P144	0.33	0.38	195.44
S2P21	0.12	0.45%	28.09	S6P156	0.38	0.30	121.62
S3P28	0.16	0.45%	72.93	S7P7	0.007	0.59	4.25
S3Pn	0.16	0.39%	38.01	S7P12	0.011	0.57	62.58
S4P8	0.15	0.47%	18.26	S8P14	0.64	0.27	137.43
S4P17	0.14	0.41%	70.81	S9P1	0.4	0.39	80.89
S5P2	0.18	0.39%	96.93	S9P6	0.5	0.40	42.16
S5P9	0.22	0.34%	156.92	S10P1	0.38	0.40	65.58
Bit_Ex Sediments				S. Peb	4.82	0.35%	733.93
CS	.53	0.36%	9.84	M. Peb	8.75	0.36%	2,050.97
VCS	1.09	0.36%	36.56	L. Peb	16.38	0.39%	11,895.07
Gran	2.80	0.37%	182.51	V. L. Peb	32.46	0.40%	52,945.53

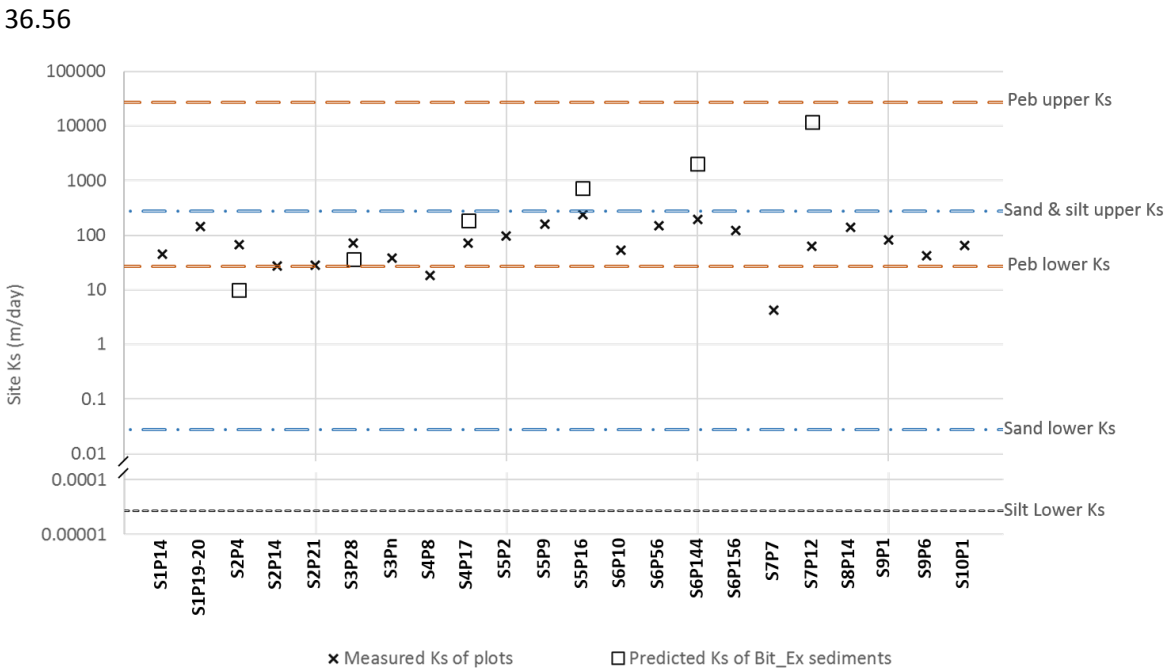

Figure 4.48 - Plot showing measured Ks for 22 plots accompanied by commonly accepted ranges of Ks for pebbles, sands, and silts. Bit_Ex sediments (coarse sand, very coarse sand, granules, small pebbles, medium pebbles, and large pebbles) Ks are plotted as squares for comparative purposes and were predicted using the Hazen Equation. Ks boundaries for pebbles, sand.

182.51

733.93

2,050.97

11,895.07

52,945.53

4.2.2 Model selection

Predicted Ks values were calculated using the Kozeny-Carmen, Hazen, Slichter, Zamarin, and Kozeny equations calibrated for seawater as the permeant. The predicted values were compared to measured values (Table 4.1) to select the most suitable model. Table 4.2 presents a summary of the results of this comparison.

The accepted variance for predicted Ks in the laboratory reported by Chapuis and Aubertin (2003) ranges from x*3 (three times) and x/3 (one-third), where x represents the mean measured Ks. Alternatively, Pliakas and Petalas (2011) determined model selection through the use of 95% confidence intervals, whereby mean predicted values were compared to mean measured values to select the best model. Given the expectations of the Chapuis and Aubertin (2003) and Pliakas and Petalas (2011) methodologies, in this instance, the Hazen Equation (Equation 3.5) was selected as the most suitable model for calculating saturated fluid transmission (Ks). The Hazen Equation produced the most precise results with the lowest mean absolute error (MAE) (67.8 m/day) and the lowest root mean squared error (RMSE) (86.27 m/day) (Table 4.2). Although the reported error values were relatively high, the predicted values occur within the accepted range described

by Chapuis and Aubertin (2003) and Pliakas and Petalas (2011). Figure 4.2 plots the results presented in Table 4.12

. **Table 4.12-** Shows summary statistics for both measured and predicted Ks. All results are shown in m/day. Standard deviation and confidence intervals are presented as a percentage.

	Measured	Kozeny-Carmen (Eqn. 5.4)	Hazen (Eqn. 5.5)	Slichter (Eqn. 5.6)	Zamarin (Eqn. 5.7)	Kozeny (Eqn. 5.8)
Number of plots	22	22	22	22	22	22
Mean Ks	87.2	41.1	67.5	21.1	60.7	61.4
MAE		69.4	67.8	70.9	71.6	71.7
RMSE		87.17	86.27	91.09	91.35	91.67
x*3 (upper)	261.6					
x/3 (lower)	29.1					
Lower 95% confidence	87.2					
Upper 95% confidence	112.7					

4.3 Application of the Hazen equation

The Hazen equation was selected as the most appropriate for modelling shoreline Ks. Section 4.4 presents the application of the Hazen equation to all sediment samples, as well as independent plot strata.

Ks was predicted using the properties of sea water at 15ºC as the permeant. The maximum predicted Ks was calculated to be 6823.1 m/day at s9p6(s1) (Figure 4.47) for surface sediment dominated by small gravel having an effective grain size of 5.31 mm, or the equivalent small pebbles in Bit_Ex's (Table 4.3; Figure 4.3). The lowest predicted Ks was 0.01 m/day (Table 4.3; Figure 4.3) at s7p7 (Figure 4.37) and was recorded in sediment dominated by silts and clays having an effective grain size much less than any of the sediments tested by Bit_Ex. Figure 4.3 shows predicted Ks values for all plots and strata compared to Bit_Ex sediments, as well as the accepted Ks values for pebble, sand, and silt as presented by Freeze and Cherry (1979).

Several plots were observed to be composed of highly stratified sediments, where a less permeable layer was found several centimeters below the surface of a coarser veneer (i.e. Figures 4.46 and 4.47). Stratification of sediments can affect the predicted Ks, as individual strata can have significantly different Ks values depending on their GSD (Barontini *et al.* 2005, Owens *et al.* 2008). Therefore, considering individual strata within a sediment profile is important when considering fluid retention in relation to Ks (Shwetha and Varija 2015). As such, plots that were highly stratified were analysed regarding both their bulk Ks and isolated strata Ks. Additionally, the isolation of and inclusion of coarse stratum (>coarse sand) sediments allows for such sediments to be considered within the study.

Table 4.13 - Measured d_{10}, porosity (%) and predicted Ks in m/day

Site plot (strata)	d10(mm)	Porosity (%)	Predicted Ks (m/day)
S1P2	0.2118	.23	14.6
S1P14	0.2713	.36	65.1
S1P14(s1)	2.1427	.22[1]	1110.7
S1P19-20	0.2053	.39	42.8
S1P26	1.5397	.39	2396.5
S1P26(s1)	0.3418	.27	57.3
S2P4	0.1147	.43	15.8
S2P14	0.2589	.42	77.0
S2P16	0.3450	.40	124.8
S2P16(s1)	1.6944	.23	932.4
S2P21	0.1168	.46	17.6
S3P28	0.1550	.45	30.3
S3Pn	0.1559	.39	24.1
S4P8	0.1550	.47	33.1
S4P17	0.1390	.41	21.4
S5P2	0.1836	.39	33.4
S5P9	0.2226	.34	39.5
S5P9(s1)	0.3108	.25[1]	39.4
S5P9(s2)	0.3038	.25[1]	37.6

Table 4.3 continued			
S5P9(s3)	0.3656	.25[1]	54.5
S5P9(s4)	0.3820	.25[1]	59.5
S5P9(s5)	0.4128	.25[1]	69.5
S5P16	0.2650	.37	64.6
S6P10	0.1576	.35	20.3
S6P10(s1)	0.1370	.56	33.2
S6P10(s2)	0.3476	.56	213.4
S6P56	0.1823	.36	31.4
S6P144	0.3273	.38	103.3
S6P156	0.3815	.30	91.9
S6P156(s1)	2.2194	.23	1599.7
S6P174	0.2887	.36	73.2
S7P7	0.0073	.47	0.1
S7P12	0.0113	.57	0.2
S8P10	0.0615	.31	2.5
S8P10(s1)	4.0668	.22[1]	4001.0
S8P10(s2)	0.0872	.56	13.4
S8P14	0.6407	.28	192.6
S8P22	0.7295	.44	654.3
S9P1	0.3967	.39	156.7
S9P1(s1)	3.8284	.22[1]	3545.7
S9P6	0.4983	.41	267.0
S9P6(s1)	5.3108	.22[1]	6823.1
S10P1	0.3801	.40	150.9
S10P1(s1)	2.1543	.28	2465.8

[1]: Porosity obtained from Freeze & Cherry (1979).
Note: Shaded boxes indicate isolated strata. Ks was predicted using the Hazen Equation.

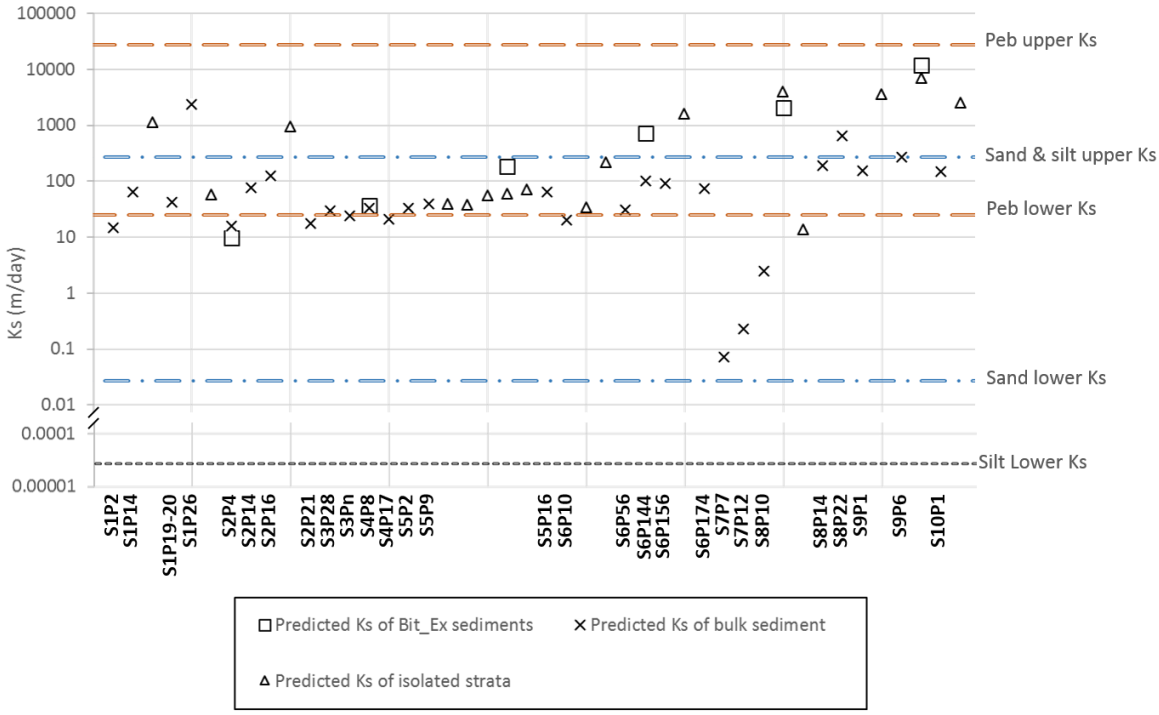

Figure 4.49 - Predicted Ks values for all plots and strata accompanied by predicted Ks values for Bit_Ex sediments.

4.3.1 Predicted Ks of dilbit in sampled sediments

Dilbit Ks was calculated for both bulk and individual strata samples using the Hazen Equation. Fluid properties for four variations of dilbit (Table 2.1) at 15^{o}C were used: Access Western Blend (AWB) and Cold Lake Blend (CLB), each at two weathering states, 0 % weathered (W0) and 16.9 % weathered (W2). Fluid properties were derived from a GOC (2013) report describing the properties and chemical composition of spilled dilbit in the marine environment.

The results from Bit_Ex were used to identify sediments of initial (1-hour high tide simulation) high retention (>50%) and remains >50% during the prolonged 24-hour soak for AWB (W0 and W2) and CLB (W0 and W2) (Tables 2.2 and 2.3). High retention

sediment data are shown in Figure 4.4 and 4.5 (A and B) as areas shaded in grey as derived from Harper *et al.* (2015). The findings indicate that: CLB W0 retention is highest in sediments ranging from very coarse sand to small pebbles, with an average retention of 91% (Table 2.1; Figure 4.4 (A)); CLB W2 retention is highest between granule and large pebble sediment with an average retention of 94% (Table 2.1; Figure 4.5 (A)); AWB W0 retention is highest in sediments ranging from coarse sand to granules with an average retention of 82% (Table 2.1; Figure 4.4 (B)); and AWB W2 retention is highest between very coarse sand to medium pebble with an average retention of 81% (Table 2.1; Figure 4.5 (B)). As discussed in Chapter 2 section 2.2.8 and 2.2.9, low retention sediments are caused by too many grain-to-grain contacts, as seen at Site 7 Plots 7 and 12 (Figures 4.34 and 4.35), which impeded fluid penetration and therefore retention. Sediments which have very few grain-to-grain contacts are of low retention due to its ability to freely penetrate sediment and be remobilized from it.

The Ks of dilbit through bulk sediment samples was predicted for AWB and CLB W0 and W2. Results indicate localised shoreline areas of high retention sediment. A localised region of high AWB W0, W2, and CLB W0 retention (Table 4.4; 4.5) was identified at Site 1 Plot 26 (Figure 4.8). Also, high retention AWB (W0) sediments were identified at Site 8 Plots 14 and 22 and CLB (W0) high retention sediments were identified at Site 8 Plots 14 and 22 as well as at Site 9 Plot 6 (Figures 4.42; 4.43, and 4.47, respectively).

Dilbit Ks was calculated for isolated coarse surface strata because few beaches were characterised by high retention sediments when bulk sediment samples were analysed.

Results indicated a surface stratum across Site 9 (Figure 4.46; 4.47) approximately 6.5 cm thick and composed of high retention with three dilbit variations tested (AWB W2, CLB W0, and CLB W2) (Table 4.4). Site 10's surface stratum, which was approximately 8 cm thick, was composed of high retention AWB W2, CLB W0, and CLB W2 sediments (Figure 4.4; 4.5; Table 4.4).

In addition to sites 9 and 10, which were characterised by beach-wide high retention surface strata, localised regions of high retention were identified at sites 1, 2, and 8. Two of the four plots at Site 1 Plot 14 (Figure 4.6) and Site 1 Plot 26 (Figure 4.8) were found to have high AWB W0, AWB W2, and CLB W0 retention. One of the four plots sampled at Site 2 Plot 16 (Figure 4.13) was comprised of a high AWB W0, AWB W2, and CLB W0 retention stratum, approximately 5 cm thick. Finally, Site 8 Plot 10 also possessed a single plot containing a high retention AWB W2, CLB W0, and CLB W2 stratum. All results for the analysis are presented in Figure 4.4 and 4.5, and Tables 4.4 and 4.5.

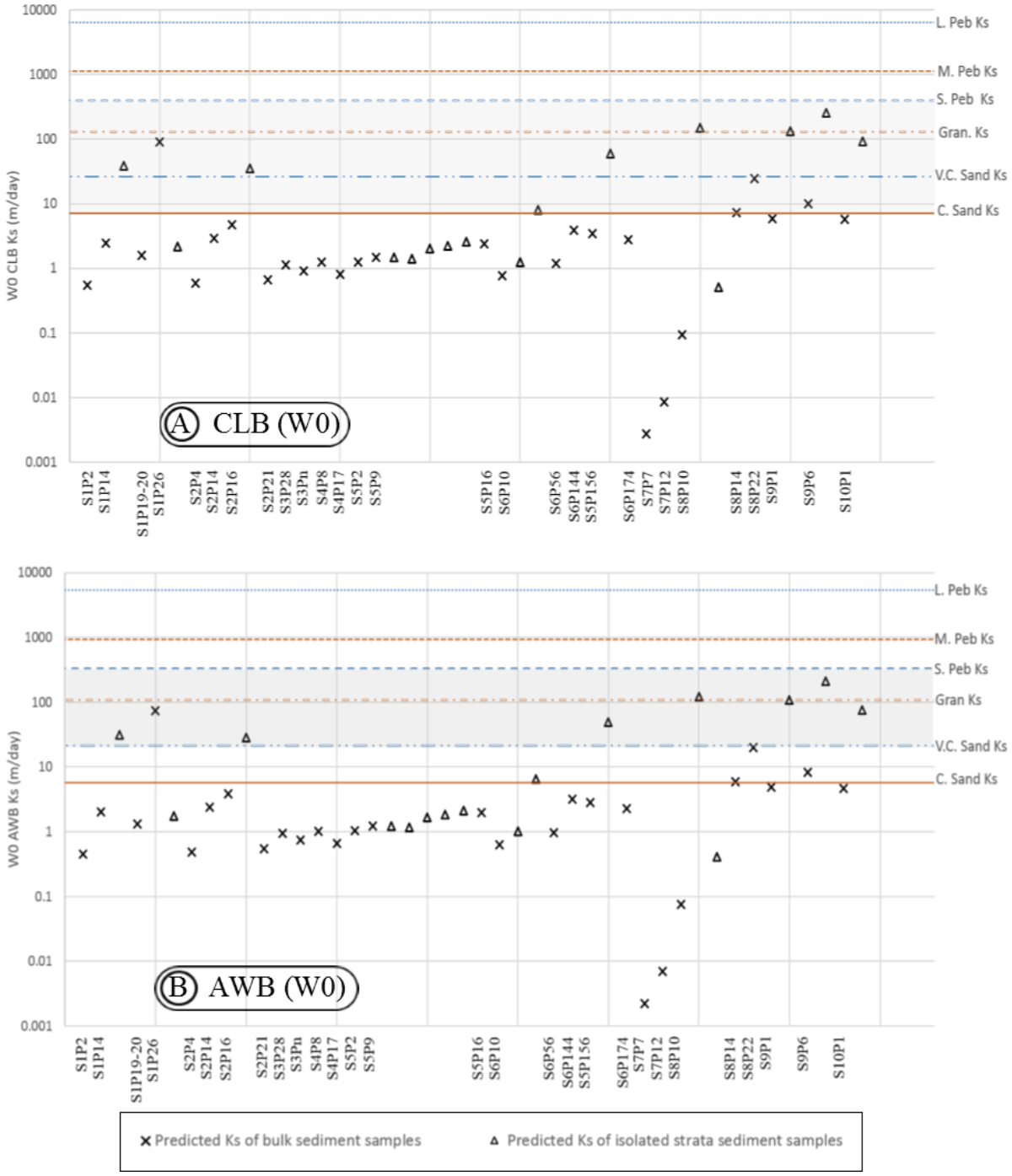

Figure 4.50 - Ks for AWB and CLB W0 for all plots and isolated strata. Plot A is CLB W0 and plot B is AWB W0. Dilbit Ks for Bit_Ex sediments was calculated with high retention sediments for each of the two oil types being shaded in grey. Where C. is coarse, V.C. is very coarse, Peb is pebble, and M. is medium.

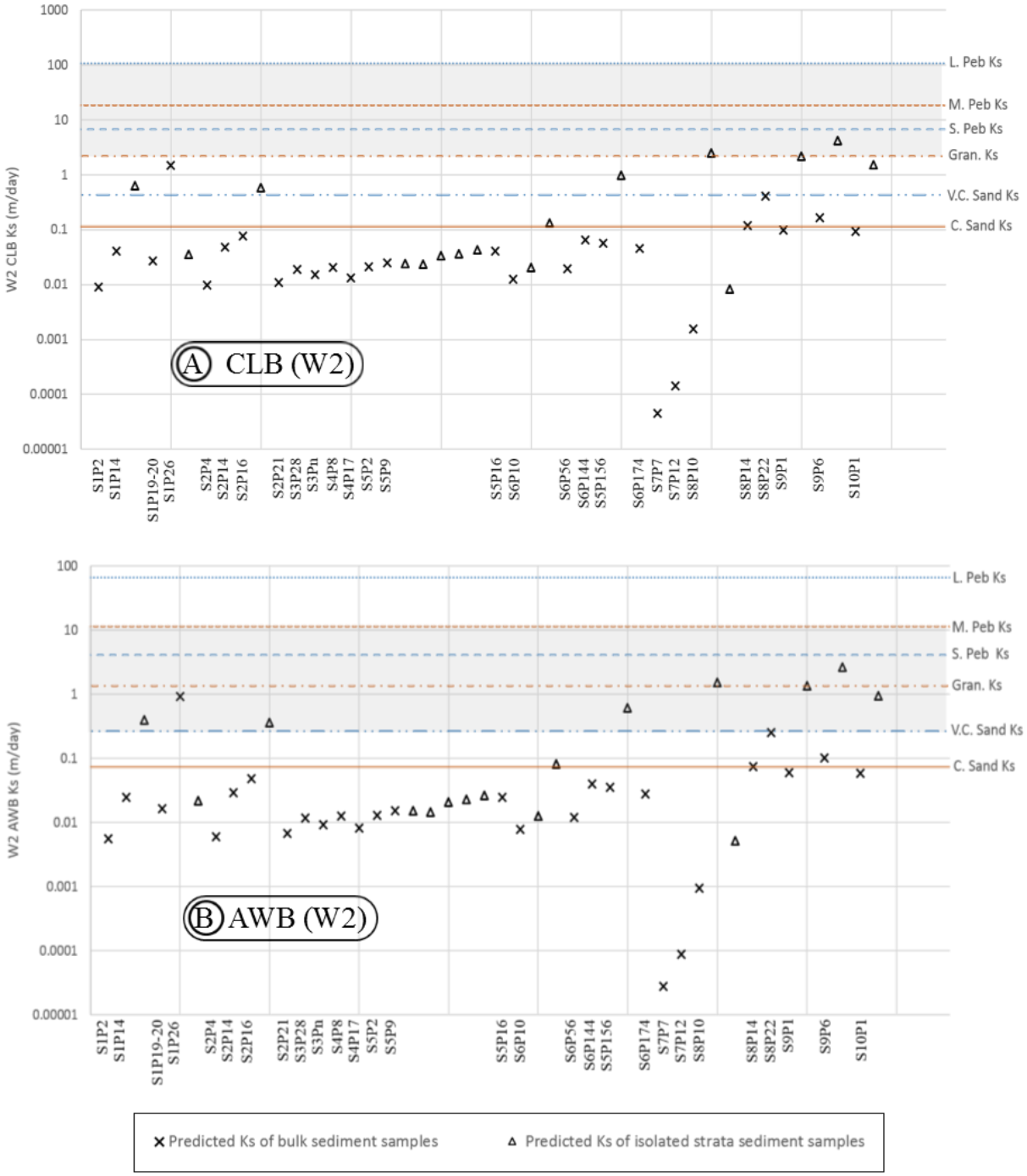

Figure 4.51 - The Ks for AWB and CLB W2 for all plots and isolated strata. Plot A is CLB W2 and plot B is AWB W2. Dilbit's Ks for Bit_Ex sediments was predicted with high retention sediments for each of the two oil types being shaded in grey. Where C. is coarse, V.C. is very coarse, Peb is pebble, and M. is medium.

Table 4.14 - Location of high retention sediment and predicted Ks of AWB W0 and W2 as well as CLB W0 and W2.

Site/Plot (strara)	d10 (mm)	Porosity (%)	CLB[1] (W0%) (m/day)	CLB[1] (W~17%) (m/day)	AWB[1] (W0%) (m/day)	AWB[1] (W~17%) (m/day)
CS	0.527	.36	7.1	0.1	5.8	0.1
VCS	1.09	.36	26.2	0.4	21.5	0.3
Gran	2.80	.37	130.7	2.2	107.4	1.3
S. Peb	4.82	.35	400.0	6.6	328.7	4.1
M. Peb	8.75	.36	1117.8	18.5	918.5	11.4
L. Peb	16.38	.39	4239.2	70.1	3483.3	43.3
V. L. Peb	32.46	.40	12156.8	200.9	9989.0	124.2
S1P2	0.2118	.23	0.54702	0.00904	0.44948	0.00559
S1P14	0.2713	.36	2.44292	0.04038	2.00730	0.02496
S1P14(s1)	2.1427	.22	38.5613	0.63736	31.6850	0.39392
S1P19-20	0.2053	.39	1.60763	0.02657	1.32096	0.01642
S1P26	1.5397	.39	89.9823	1.48727	73.93681	0.91920
S1P26(s1)	0.3418	.27	2.15145	0.03556	1.76780	0.02198
S2P4	0.1147	.43	0.59357	0.00981	0.48773	0.00606
S2P14	0.2589	.42	2.89016	0.04777	2.37479	0.02952
S2P16	0.345	.40	4.68657	0.07746	3.85087	0.04788
S2P16(s1)	1.6944	.23	35.0092	0.57865	28.76645	0.35763
S2P21	0.1168	.46	0.66253	0.01095	0.54439	0.00677
S3P28	0.155	.45	1.13757	0.01880	0.93472	0.01162
S3Pn	0.1559	.39	0.90670	0.01499	0.74502	0.00926
S4P8	0.155	.47	1.24445	0.02057	1.02254	0.01271
S4P17	0.139	.41	0.80260	0.01327	0.65949	0.00820
S5P2	0.1836	.39	1.25596	0.02076	1.03200	0.01283
S5P9	0.2226	.34	1.48331	0.02452	1.21880	0.01515
S5P9(s1)	0.3108	.25	1.47840	0.02444	1.21477	0.01510
S5P9(s2)	0.3038	.25	1.41256	0.02335	1.16067	0.01443
S5P9(s3)	0.3656	.25	2.04570	0.03381	1.68092	0.02090
S5P9(s4)	0.382	.25	2.23335	0.03691	1.83510	0.02281
S5P9(s5)	0.4128	.25	2.60801	0.04311	2.14295	0.02664
S5P16	0.265	.37	2.42602	0.04010	1.99341	0.02478
S6P10	0.1576	.35	0.76398	0.01263	0.62775	0.00780
S6P10(s1)	0.137	.56	1.24478	0.02057	1.02281	0.01272
S6P10(s2)	0.3476	.56	8.01331	0.13245	6.58438	0.08186
S6P56	0.1823	.38	1.17776	0.01947	0.96774	0.01203

Table 4.14 continued						
S6P144	0.3273	.38	3.88027	0.06414	3.18835	0.03964
S6P156	0.3815	.30	3.45189	0.05705	2.83635	0.03526
S6P156(s1)	2.2194	.23	60.0651	0.99279	49.35436	0.61359
S6P174	0.2887	.36	2.74664	0.04540	2.25686	0.02806
S7P7	0.007269	.47	0.00273	0.00005	0.00225	0.00003
S7P12	0.01126	.57	0.00859	0.00014	0.00705	0.00009
S8P10	0.0615	.31	0.09265	0.00153	0.07613	0.00095
S8P10(s1)	4.0668	.21	150.229	2.48306	123.4402	1.53464
S8P10(s2)	0.08722	.56	0.50453	0.00834	0.41456	0.00515
S8P14	0.6407	.26	7.23	0.11952	5.94148	0.07387
S8P22	0.7295	.44	24.56	0.40604	20.18526	0.25095
S9P1	0.3967	.38	5.88	0.09725	4.83450	0.06010
S9P1(s1)	3.8284	.21	133.1	2.20047	109.3920	1.35999
S9P6	0.4983	.40	10.02	0.16573	8.23894	0.10243
S9P6(s1)	5.3108	.21	256.19	4.23449	210.5018	2.61711
S10P1	0.3801	.39	5.66	0.09363	4.65454	0.05787
S10P1(s1)	2.1543	.28	92.58	1.53028	76.07499	0.94578

[1]: Fluid properties for AWB W0 and W2 as well as CLB W0 and W2 were derived from GOC (2013) are in Table 1.3.1. Lightly shaded Site-Plot (strata) indicate isolated strata. Dark shaded blocks indicate sediments of similar Ks and d10 to that of high retention sediments as indicated by Harper *et al.* (2016).

4.3.2 Categorization of high and low retention sediment

Given the above fluid and sediment interactions, sediments were divided into two categories for each dilbit weathering state (W0 and W2): high and low retention. A two-tailed paired means T-Test comparing weathered and unweathered dibit retention from Bit_Ex ($t(26) = 2.29$, $p < .05$ and $t(26) = 3.06$, $p < .05$, respectively) found a significant difference between the weathering states. Similar findings were described by Gundlach (1987) and Cheng *et al.* (2000) who comparing various unweathered and weathered petroleum products. For each weathering state, high retention sediments were identified through their percent dilbit retained after initial (1-hour) and long-term (24-hours) salt

Table 4.15 – High retention unweathered and weathered dilbit sediments.

Bit_Ex		Unweathered dilbit			
		CLB (W0		AWB (W0)	
Class	d_{10} (mm)	Ks_{dil} (m/day)	24 hr % Ret	Ks_{dil} (m/day)	24 hr % Ret
CS	0.527	7.1	.11%	5.8	.1%
VCS	1.09	26.2	.26%	21.5	.53%
Gran	2.80	130.7	.59%	107.4	.48%
S Peb	4.82	400.0	.94%	328.7	.94%
M Peb	8.75	1117.8	.92%	918.5	.89%
L Peb	16.38	4239.2	.65%	3483.3	.37%
VL Peb	32.46	12156.8	.19%	9989.0	.14%
		Weathered dilbit			
		CLB (W2)		AWB (W2)	
CS	0.527	0.1	.58%	0.1	.37%
VCS	1.09	0.4	.93%	0.3	.89%
Gran	2.80	2.2	.75%	1.3	.63%
S Peb	4.82	6.6	.57%	4.1	.1%
M Peb	8.75	18.5	.08%	11.4	.01%
L Peb	16.38	70.1	.00%	43.3	.03%
VL Peb	32.46	200.9	.03%	124.2	.01%

Grey shading indicates <50% retention after 24 hours of soaking while the bolded lines indicate the upper and lower boundaries for high and low retention sediments.

water immersion (tidal simulation) Table 4.15. Sediments with a high degree of initial retention (>50%) and which released <50% in the preceding 24 hours were deemed high retention, with all other sediments being designated as low retention (Figure 4.52).

4.3.2.1 Unweathered dilbit (W0)

Low W0 retention shorelines are characterised by very fine sediments and very coarse sediment (Table 4.15). Fine sediments impede fluid penetration and retention while coarse sediments allow for rapid penetration, rapid remobilization, and redistribution of stranded oil (Harper *et al.* 2016, Laforest *et al.* 2017). The results of a two-tailed paired means T-

test indicated a significant difference between Bit_Ex unweathered AWB and CLB W0 retention ($t(13) = 2.32$, $p < .05$) although, as CLB has a wider range of high retention sediments, its boundaries have been used to delineate AWB and CLB high retention sediments.

The range of sediments classified as high W0 retention, in accordance with Bit_Ex results, is bounded by small pebbles (W0 dilbit Ks ≈400 m/day; d10≈ 5.19 mm) for the upper limit, and coarse sand (W0 dilbit Ks ≈ 5.8 m/day; d10≈ 0.55 mm) for the lower limit (Figure 4.6 (A)). Within the high retention sediment classification, an average 60% of the initial oil was retained after oil latent sediments were submerged for one hour, releasing an additional 18% in the proceeding 24 hours (Table 2.3;2.4). Coarser sediments (small pebble to very large pebble), on average, showed lower percent retention at ~18% (Table 2.3) after 1 hour, 50% of which was remobilized within 24 hours (Table 2.4).

4.3.2.2 Weathered dilbit (W2)

The fluid properties of dilbit rapidly change in the first 6 to 12-hours post-spill (Chapter 2, section 2.6), ultimately changing the way dilbit interacts with shoreline sediments. As time progresses the diluent evaporates and weathered AWB and CLB behave in a similar fashion. A paired means T-Test indicated that was no significant difference between weathered dilbit retention within Bit_Ex sediments ($t(13) = 0.38$, $p < .05$). Given that no significant difference existed between dilbit variations, the lower boundary of high retention sediments is approximately equal very coarse sand and medium pebbles, while the upper boundary is confined by granules to large pebbles (Table 4.15). Sediments which were of high retention to either W2 CLB or W2 AWB were conservatively assumed to be

of high retention to both dilbit variations as there was no significant difference in retention between dilbits (Table 4.15).

The range of sediments classified as high retention for weathered dilbit (as indicated by Bit_Ex) is located between very coarse sand (W2 dilbit Ks ≈.4 m/day; d10≈ 1.06 mm) and large pebbles (W2 dilbit Ks ≈70 m/day; d10≈ 16.9 mm) (Figure 4.6 (B)). Bit_Ex indicates that such sediments initially retain 83% of dilbit (Table 2.3), releasing an average 17% of the remaining oil in the following 24 hours of seawater submergence. On average, coarser sediments (very large pebble) demonstrated high initial percent retention at ~81% (Table 2.3) after 1 hour, 65% of which was remobilized within 24 hours (Table 2.4). The lower threshold for weathered dilbit extends from coarse sand and finer showing an average of 20% initial retention and releasing an additional 15% post 24-hour soak.

Figure 4.52 presents the high retention sediments for unweathered (Figure 4.52(A)) and weathered (Figure 4.53(B)) dilbit as per the above description. Figure 4.52 (A) shows twelve plots of high retention W0, eight of which were isolated strata. Figure 4.52(B) shows eight plots of high W2 retention.

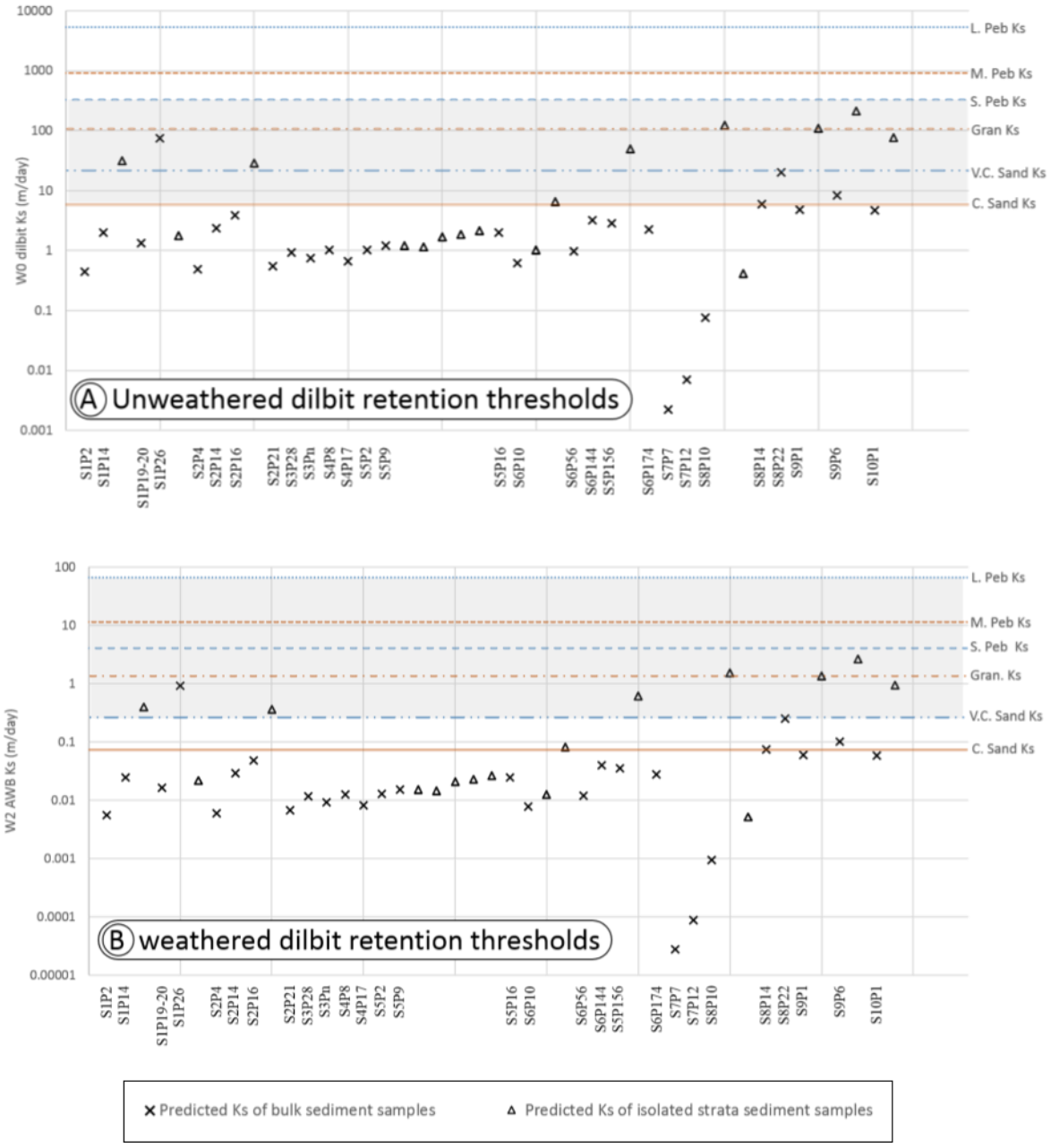

Figure 4.52 - Ks thresholds for sediments of high unweathered (A) and weathered (B) dilbit retention. Regions in grey indicate Ks and sediments indicative of high unweathered and weathered dilbit retention.

4.4 Summary

The results of these analyses show that all the study sites are characterised by the presence of sand, pebbles, or combinations of both. The measured Ks for all the plots occur within the expected range given the d_{10} of each plots sediment sample (Freeze and Cherry 1979). When comparing measured Ks to predicted Ks, a modified version of the Hazen Equation was found to be the most suitable semi-empirical equation to describe the saturated transmission rate of sea water through *in-situ* sediments. Using the Hazen Equation, the Ks of unweathered and weathered dilbit was predicted for all plots in addition to individual strata. When the sediments were analysed in bulk, four of the 28 plots were identified as having high dilbit retention. When the were analysed regarding both bulk sediments and coarse surface strata, twelve of the 28 plots were identified as having high dilbit retention capability.

5 Chapter Five:

Conclusions and Recommendations

This chapter summarises the research findings related to the four objectives of the thesis. It concludes with recommendations for application and further research.

5.1 Objective 1: To measure the hydraulic properties of shoreline sediments.

The measured hydraulic properties (Ks) of each plot fall within the expected range for such sediments when values were compared to standards presented by Freeze and Cherry (1979) (Table 4.11; Figure 4.41). The measurements assisted in model selection by allowing for comparisons between measured and predicted Ks values, with the Hazen Equation being identified as the most appropriate model. (Equation 3.5; Table 4.12).

5.2 Objective 2: To evaluate the ability of in-situ sediments to transmit both unweathered (fresh state) and moderately weathered dilbit to describe retention.

5.2.1 Shoreline dilbit retention

In general, shorelines within the study region were classified as not having high retention potential for both unweathered or weathered dilbit. The Ks values of shoreline sediments were lower, and effective grain sizes were smaller, than that of high retention sediments. However, stratification within the sediments is important. When individual shoreline sites were assessed, additional ones were found to be composed of stratified high and low retention sediments as well as those composed entirely of high retention sediments.

5.2.2 Unweathered dilbit retention

The Ks values of shorelines within the Strait of Juan de Fuca and Haro Strait were not indicative of sites having high unweathered dilbit retention potential. High retention W0 dilbit sediments, with effective grain size between 0.55 and 5.20 mm, have Ks values from 6.4 to 364.3 m/day. The Ks values and effective grain sizes measured on shorelines were predominately of lower Ks and of finer grain size than that of high retention sediments when samples were treated as a uniform. Such characteristics act to mitigate unweathered dilbit penetration and, therefore, retention. Four plots, Site 1 Plot 26, Site 8 Plot 14, Site 8 Plot 22, and Site 9 Plot 6 were identified as being of high retention.

Stratification of shoreline sediments was assessed, resulting in an increase in identified high retention shorelines. At six of the ten shorelines (Sites 1, 2, 6, 8, 9, and 10) stratified sediments were found to have a mix of high and low retention characteristics (Figure 4.1). Two sites (9 and 10) were veneered with high retention sediments (Figure 4.1).

The lower grain size limit for high retention sediments was not identified during Bit_Ex, but may be finer than coarse sand. During Bit_Ex, high initial retention of unweathered dilbit was observed within coarse sand with moderate remobilization. However, given that the weathering process immediately begins upon the release of dilbit into the marine environment, it is unlikely to come ashore in a completely unweathered state (SLRoss 2012, Harper *et al.* 2016, Laforest *et al.* 2017). In such a scenario, the lower grain size limit of the high retention sediments would vary, being skewed towards coarser sediments.

5.2.3 Weathered dilbit retention

The sediment composition and Ks values of shorelines in Juan de Fuca and Haro Strait were also not indicative of high weathered dilbit retention potential. For shorelines with an effective grain size between 0.55 and 8.67 mm to be regarded as of high W2 dilbit retention, their Ks values should range from 0.094 to 14.95 m/day. The sediments analysed as a uniform sample in the study area commonly had Ks values below those considered to be of high retention for weathered dilbit. Site 1 Plot 26 was the only high retention sediment identified.

Stratification of shoreline sediment was critical in consideration of retention. The number of high retention shorelines increased from one to six once individual strata at the sample Plots were assessed, indicating that sediment stratification plays an important role in determining shoreline oil retention. All identified high retention W2 shorelines were also identified as being of high W0 retention, although, regions of high W2 retention were less frequent across such shorelines.

Given the rapid pace at which dilbit weathering occurs, and the accepted spill response time for the region (minimum 18 hours (WCMRC 2012)), it is likely that responders would encounter dilbit in a W2 state (Harper *et al.* 2016). Given this, shorelines composed of large clast sediments should be monitored for dilbit retention as a spill temporally extends.

5.2.4 Shoreline Stratification

Shoreline sediment stratification was found to be an important consideration as suggested by Short *et al.* (2004). With only three of the ten shorelines being identified as having high

retention sediment based on analysis of a uniform sample (Sites 1, 8, 9), the identification of individual strata within a sample became increasingly important. Shoreline stratification was visually present in nine of the twenty-seven sampled plots (Sites 1, 2, 6, 8, 9, and 10), although stratification alone did not suggest the presence of high retention sediments.

When shoreline surface strata composed of coarse grains were independently analysed, the Ks values of several additional shorelines were identified as having localised areas of high W0 and W2 retention (Figure 4.49; Table 4.13). The results also indicate that two shorelines were veneered entirely by high retention sediment (site 9 and 10) (Figure 4.43-4.45).

On shorelines with stratified high and low retention sediments, fine-grained strata would minimise dilbit penetration resulting in its remobilization and redistribution. Given the observed mosaic of high and low retention sediments, dilbit would remain in high concentration in localised patches on the shoreline while easily being remobilized from others. As dilbit stranding and remobilization continues, so does the weathering process, altering the fluid properties of the dilbit and consequentially the sediments with high retention (Fingas 2015e).

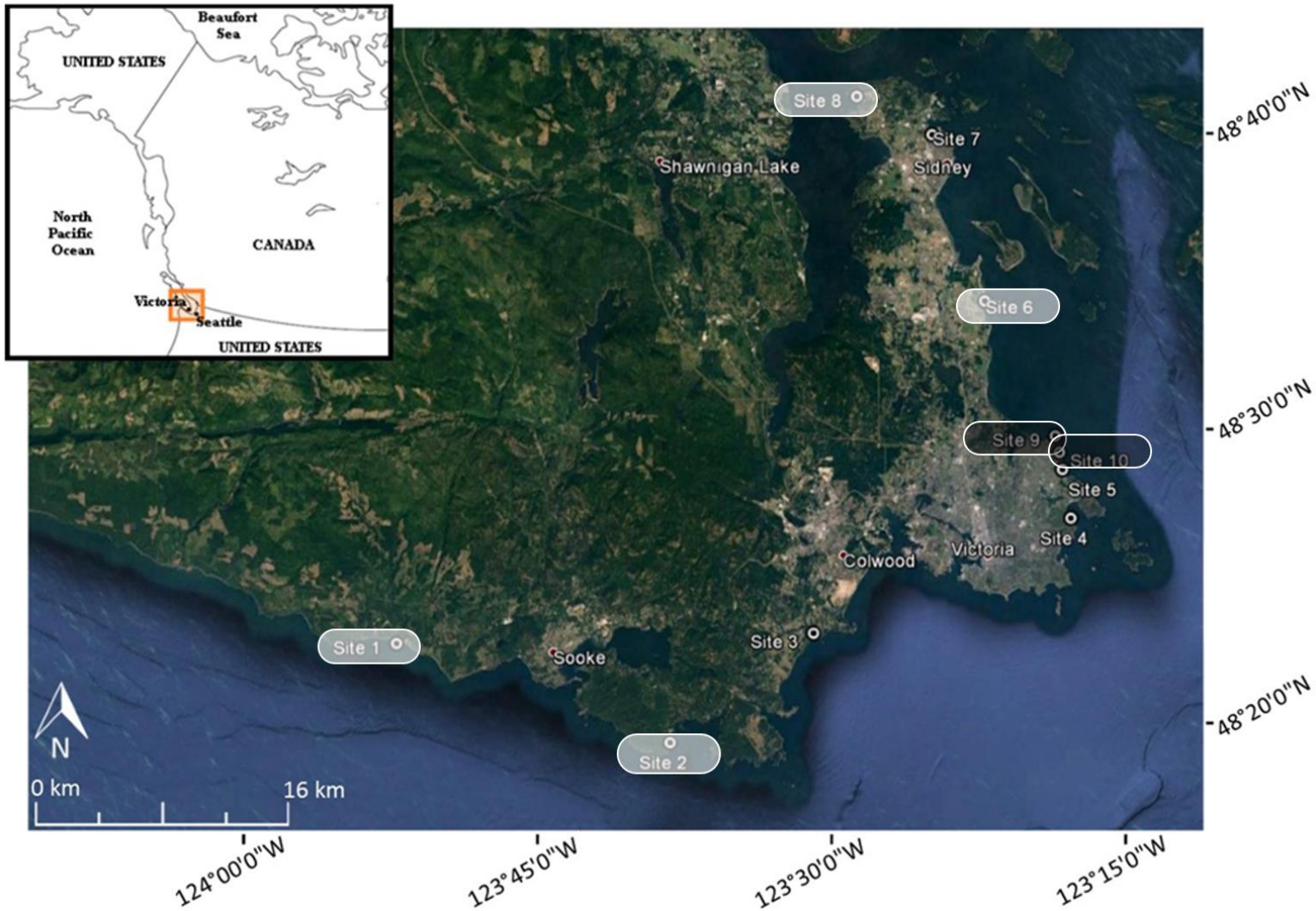

Figure 5.1 - Map showing W0 and W2 high retention shorelines and high retention strata. Light grey indicating shorelines with both high and low retention sediments, while dark grey indicates shorelines that have a stratum of high retention that span the whole length of the breach.

Coarser sediment (i.e. high retention) strata generally occurred at the surface, although one shoreline (Site 6 Plot 10) possessed a sub-surface stratum composed of coarse, high retention sediment. Such a stratum is not of immediate concern as it was overlaid with finer, low retention sediment. However, as shoreline sediments are highly mobile, fine-grained, low retention sediments may be redistributed, leaving behind heavier and coarser grain sizes with potentially high retention characteristics.

Identifying the boundaries between strata is important. As sediments transition from a coarse, high Ks, low retention surface stratum to a fine, low Ks, low retention subsurface stratum, it is likely that the characteristics required for sediment to be of high retention exist (Short *et al.* 2004). If such characteristics occur, oil will easily transmit through the surface strata to be retained within the transitional area.

5.3 Objective 3: To make recommendations to aid in emergency response planning and risk mapping for dilbit.

If dilbit is unweathered, its behaviour is similar to conventional heavy oil allowing for conventional response strategies to be employed (WO 2013, Harper *et al.* 2016, Laforest *et al.* 2017). However, as dilbit weathers, the sediment of maximum retention will become coarser and response efforts and strategies should reflect this. Initial response strategies should be placed on protecting shorelines with a Ks and effective grain size indicative of high W0 retention (coarse sand to small pebble) but should shift to high W2 retention as the spill temporally extends.

As a spill temporally extends, response strategies should change. Once past the initial 6 to 12-hour window in which dilbit is most similar to conventional heavy oils, focus should shift from coarse sands and fine pebble beaches to shorelines composed of coarser, higher retention sediments due to changing dilbit fluid properties. Weathered dilbit is more difficult to remobilize from a standardised surface when compared with unweathered dilbit (O'Briens, 2013). Remobilization strategies, such as flushing, may not be adequate or may need to be modified with weathered dilbit given its low Ks values and therefore mobility. The remobilization of weathered dilbit may require new remediation strategies, contrary to what was suggested by Laforest *et al.* (2017).

5.4 Limitations, recommendations, and extensions

5.4.1 Bit_Ex

Bit_Ex provided adequate information to designate sediments as being of high or low retention. A recommendation of this study is to increase the number of sediment classifications used in the future experiments to produce more robust retention predictions. As sediment grain-size increased, percent retention approximately fitted a Gaussian distribution, but was truncated at coarse sand for W0 dilbit. Increasing the number of sediments classifications, specifically for sediment finer than coarse sand for unweathered dilbit, would allow for more confident retention predictions in fine-grained sediment and for the designation of the finest penetrable sediment for unweathered dilbit. Additionally, both finer and coarser sediment should be tested for weathered dilbit to produce similar outcomes.

Increasing the range of sediment tested would allow for a more complete understanding of dilbit and sediment interactions, and would corroborate the finding that retention is normally distributed in accordance to sediment size (Figure 5.2 (A); (B). This finding states that as sediment size increases from the finest penetrable sediment, percent retention also

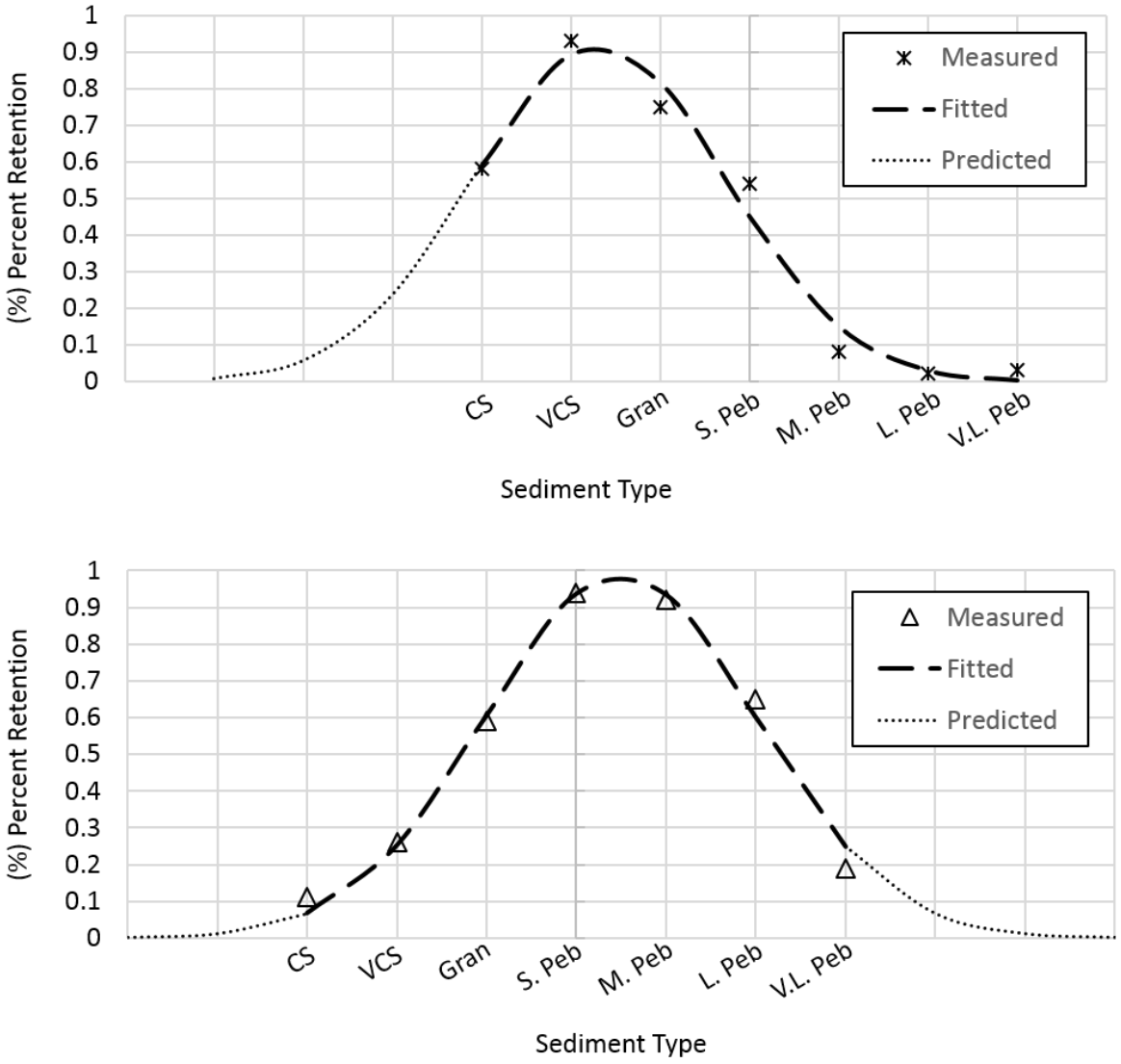

Figure 5.4 – Percent retention fitted to a Gaussian distribution: (A) one hour unweathered dilbit percent retention (root sum squared error 0.14); and, (B) one hour weathered dilbit percent retention.

increases until sediment of maximum retention is reached. Once the sediment grain sizes associated with maximum retention has been surpassed, percent retention decreases (Figure 5.2 (A); (B)). Such a trend was observed in weathered dilbit (Figure 5.2(B)) during Bit_Ex with more experiments required to confirm a similar pattern in unweathered dilbit (Figure 5.2 (A)).

5.4.2 Seasonal Considerations

As discussed in section 2.3, shorelines undergo constant change. One of the more dramatic changes occurs on an annual or seasonal basis, whereby storm surges alter the shoreline by moving sediments from high wave energy regions to quiescent areas of the shoreline. Given the importance of the effective grain size or d_{10} when predicting the ability of a shoreline to transmit and retain dilbit, and the prevalence of seasonal variations in shoreline sediments, seasonality should be a consideration when mapping regions of high and low dilbit retention risk. For example, a shoreline of low dilbit retention that is dominated by sand during the summer months (approximately June to August) shift to being composed of coarser sediments such a pebbles or cobbles, resulting in that same shoreline shifting to be a high dilbit retention shoreline. Shorelines in the Salish Sea and the Juan de Fuca Strait undergo continuous deposition, erosion, and sediment transportation.

5.4.3 Mapping implications

The current methodology for shoreline sediment mapping may be inadequate given the importance of stratification observed during this research. The present method for determining shoreline oil residency is largely done through aerial surveys via helicopter. Such methods have been instrumental in obtaining coarse scale oil retention patterns,

although they do not account for the effects of sediment stratification. This research showed that stratification is an important factor when predicting oil retention using Ks. Thus shoreline sediment stratigraphy and armouring, a common feature in coastal British Columbian shorelines (Harper *et al.* 2015, Sergy 2016) should be taken into consideration.

5.4.4 The use of the effective grain size to determine retention

The grain size distribution (GSD) of high retention sediments all showed bi, tri, or multi-modal distributions when sediment samples were assessed as a bulk uniform sample (Chapter 4). When shoreline strata were analysed independently, the tendency for sediment samples to have multiple modalities was substantially reduced and resulted in sediments having a higher degree of sorting and less skewness within GSD analysis. Sediments that were not stratified but showed multiple modalities were typical of low retention (e.g. Site 2 Plot 24 (Figure 4.23), and Site 5 plot 16 (Figure 4.41)).

If a stratum is isolated and a GSD analysis is performed, the effective grain size may be used to predict dilbit retention. When analysing Bit_Ex sediments, an approximate linear correlation between an increase of grain size d_{10} and weathered dilbit penetration (R^2= .89) was found. Also, an approximate logarithmic relationship between Ks and weathered dilbit retention (R^2=.72) was found when oil did not freely penetrate sediment columns. Employing statistical relationships such as these to predict fluid retention requires an understanding of shoreline hydraulics (described in Section 2.9) and the properties of the permeating fluid. Given that effective grain size is significant when estimating Ks (Cabalar and Akbulut 2016), and Ks influences retention, the effective grain size could be used as a

proxy to estimate dilbit retention. As such, a recommendation of this thesis would be to explore the relationship between effective grain size and dilbit/oil retention.

5.4.5 Broader application

The modified version of the Hazen Approximation (Equation 5.5) employed for this study could be applied to any oil with a known density and viscosity. The broad application of this method could improve preparedness for a spill of any hydrocarbon, extending beyond response to dilbit spills. Such efforts would streamline the response process by providing vital information regarding which shorelines are of high retention, allowing for responders to prioritise areas of the shoreline for treatment during a spill.

5.5 Summary

In summary, shoreline sediments indicative or high unweathered and weathered dilbit retention were uncommon. However, when individual strata were isolated and analysed in terms of their retention, it was found that the occurrence rate and distribution of high retention sediments increased. Upon analysing shorelines strata, two of the ten shorelines were entirely veneered with high retention sediments, while the remaining high retention plots were distributed amongst four other shorelines. Such findings demonstrate the importance of shoreline stratification when determining shoreline oil retention. Given the importance of shoreline stratification, current mapping techniques require modification or ground-truthing to verify their oil residence index rating. Finally, this study shows that coarse-grained sediments of initial low retention are of potential high retention as the spill event extends and the fluid properties of the dilbit changes. In the event of a dilbit spill, the above considerations could reduce its long-term impacts by minimising oil shoreline

retention and by reducing the environmentally invasive shoreline remediation techniques required to recover stranded oil.

References

AEUB (Alberta Energy and Utilities Board). 2015. Alberta's Reserves 2004 and Supply/Demand Outlook 2005-2014 (ST 98-2005). Calgary, AB.

Al-Zyoud, H., and Elloumi, F. 2017. Dynamics of Canadian Trade Pattern: A Time-Series Analysis. International Journal of Economics and Finance, **9**: 115-125.

Alrodini, K. 2015. Case Study Analysis of Oil Spill Cleanup Methods. M.A. Thesis, Sciences and Humanities, Ball State University, Muncie, Indiana.

Alyamani, M., and Şen, Z. 1993. Determination of Hydraulic Conductivity from Complete Grain-Size Distribution Curves. Ground Water, **31**: 551–555.

Ametepe, J.K. 1991. A Model Study of Longshore Transport. M.Sc. Thesis, Department of Civil Engineering, The University of British Columbia, Vancouver, B.C.

Argyrokastritis, I., and Kerkides, P. 2003. A Note to the Variable Sorptivity Infiltration Equation. Water Resources Management, **17**: 133–145.

ASTM:D3385-09. 2016. Standard Test Method for Infiltration Rates of Soils in Field Using Double-Ring Infiltrometer. *In* ASTM Standards International. ASTM Standards International. 1-7.

ASTM:D422−63. 2007. Standard Test Method for Particle-Size Analysis of Soils. *In* ASTM Standards International. ASTM Standards International. 1–8.

ASTM:D4700-15. 1999. Standard Guide for Soil Sampling From the Vadose Zone. *In* ASTM Standards International. ASTM Standards International. 1–16.

ASTM:D5126/D5126M-90. 2010. Standard Guide for the Comparison of Field Methods for Determining Hydraulic Conductivity in Vadose Zone. *In* ASTM Standards International. ASTM Standards International. 1-11.

Banerjee, D. 2012. Oil Sands, Heavy Oil, & Bitumen: From Recovery to Refinery. PennWell Corp., Tulsa, OK.

Barontini, S., Clerici, A., Ranzi, R., and Bacchi, B. 2005. Saturated Hydraulic Conductivity and Water Retention Relationships for Alpine Mountian Soils. *In* Climate and Hydrology in Mountain Areas. John Wiley & Sons, Edmonton, AB. 111-121,

Barrow, T.D., Bucheger, S., Cox, C., Farrington, J., Lehr, B., Maki, A., Pitt, R., Rauta, D., Rice, J., and Wiens, J.A. 2004. Behavior and Fate of Oil. *In* Oil in the Sea III: Inputs, Fates, and Effects, Third Edit. National Academy of Sciences Press. Washington, D.C.

Bascom, W. 1964. Waves and Beaches. Anchor Books, Garden City, N.Y.

Bear, J. 1972. Dynamics of Fluids in Porous Media. American Elsevier Publishing Company, Inc. Garden City, N.Y.

Beegle-Krause, C.J., and Lehr, W.J. 2015. Oceanographic and Meteorological Effects on Spilled Oil. *In* Handbook of Oil Spill Science and Technology. *Edited by* M. Fingas. Wiley Publishing Co., Edmonton, AB.

Bernier, J.C., Kelso, K.., Buster, N.A., Flocks, J.G., Miselis, J.L., and DeWitt, N.T. 2014. Sediment Data Collected in 2012 From the Northern Chandeleur Islands, Louisiana. U.S. Geological Survey Data Series 850, St. Petersburg, FL.

Bloomquist, D. 2001. Enhancement of Flordia Highways Using Results from an Improved Field Permeability Test Device. Florida Department of Transportation, Gainesville, FL.

Blott, S., and Pye, K. 2001. GRADISTAT: A Grain Size Distribution and Statistics Package for the Analysis of Unconsolidated Sediments. Earth Surface Processes and Landforms, **26**: 1237–1248.

Blott, S., and Pye, K. 2010. Gradistat V8: A Grain Size Distribution and Statistical Package for the Analysis of Unconsolidated Sediments by Sieving or Laser Granulometer. Berkshire, UK.

Brassington, R. 2007. Field hydrogeology. Wiley Publishing Co.West Sussex, UK.

Brokaw, A. 2012. Citing online sources: Top 5 exports: Canada| the economy| Minyanville's Wall Street. Available from http://www.minyanville.com/business-news/the-economy/articles/canada-exports-crude-NXY-CNOOC-NXY/9/11/2012/id/43892?page=full [accessed 12 June 2015].

Brown, H.M., Goodman, R.H., and Nicholson, P. 1991. The Evaporation of Heavy Oil Stranded on Shorelines (EC/EPS--93-01710). *In* Arctic and Marine Oilspill Program Technical Seminar; Edmonton, AB, **15**: 47-53.

Cabalar, A.F., and Akbulut, N. 2016. Evaluation of Actual and Estimated Hydraulic Conductivity of Sands with Different Gradation and Shape. SpringerPlus, **5**:1-16.

Carrier, W.D. 2003. Goodbye, Hazen; Hello, Kozeny-Carman. Journal of Geotechnical and Geoenvironmental Engineering, **129**: 1054–1056.

Chapuis, R., and Aubertin, M. 2003. Predicting the Coefficient of Permeability of Soils Using the Kozeny-Carmen Equation (EPM–RT–2003-03). Département des Génies Civil, Géologique et des Mines, Montreal, QB.

Chardón-Maldonado, P., Pintado-Patiño, J., and Puleo, J. 2015. Advances in Swash-Zone Research: Small-Scale Hydrodynamic and Sediment Transport Processes. Coastal Engineering, 1-18.

Cheng, N., Law, A., and Findikakis, A. 2000. Oil Transport in Surf Zone. Journal of Hydraulic Engineering, **126**: 803–809.

Chilingarian, G. 2011. Bitumens, Asphalts, and Tar Sands. Elsevier Scientific Publishing Company. Amsterdam, Netherlands.

Clark, P., and Mix, A. 2002. Ice Sheets and Sea Level of the Last Glacial Maximum. Quaternary Science Reviews, **21**: 1–7.

COE (Corps of Engineers). 1956. Relative Efficiency of Beach Sampling Methods. Technical memorandum No. 90. Washington, D.C.

Cooper, D. 2006. Floating Heavy Oil Recovery: Current State Analysis. US Coast Guard

Research and Development Center, SAIC Canada: Environmental Technologies Program, Ottawa, ONT.

Crosby, S., Fay, R., Groark, C., Kani, A., Smith, J., and Sullivan, T. 2013. Transporting Alberta's Oil Sands Products: Defining the Issues and Assessing the Risks. NOAA technical memorandum, Seattle, W.A.

Davidson-Arnott, R., MacQuarrie, K., and Aagaard, T. 2005. The Effect of Wind Gusts, Moisture Content and Fetch Length on Sand Transport on a Beach. Geomorphology, **68**: 115–129.

Davies, J.L. 1972. Geographic Variations in Coastal Developments. *Edited by* K.M. Clayton. Oliver & Boyd. Edinburgh, UK.

Deck, J.H. 2010. Hydraulic Conductivity, Infiltration, and Runoff from No-Till and Tilled Cropland. M.Sc. Thesis, Department of Environmental Engineering, The University of Nebraska, Lincoln, NE.

Detmer, D.M. 1995. Permeability, Porosity, and Grain-Size Distribution of Selected Pliocene and Quaternary sediments in the Albuquerque Basi. New Mexico Geology, 79–87.

Dew, W.A., Hontela, A., Rood, S.B., and Pyle, G.G. 2015. Biological Effects and Toxicity of Diluted Bitumen and its Constituents in Freshwater Systems. Journal of applied toxicology, **35**: 1219–27.

Dingman, S.L. 2002. Water in Soil: Infiltration and Redistribution. *In* Physical hydrology. Prentice Hall. 1–646.

Doerffer, J.W. 1992. Oil Spill Response in the Marine Environment. Pergamon Press, Gdansk. Terrytown, N.Y.

Downing, J. 1983. The coast of Puget Sound : Its Processes and Development. University of Washington Press. Seattle, W.A.

Dullien, F.A. 1979. Porous Media- Fluid Transport and Pore Structure. Academic Press Inc., Toronto, ONT.

Dunning, S. 2006. The Grain-Size Distribution of Rock Avalanche Deposits in Valley-Confined Settings. Italian Journal of Engineering Geology and Environment, **1**: 117–121.

EIA, (U.S. Energy Information Administration). 2014. EIA's U.S. Crude Oil Import Tracking Tool: Selected Sample Applications, U.S. Department of Energy, Washington, D.C.

Emmett, B., Hammond, M., Short, J., and Spies, R. 2011. Expert Opinion on Petroleum Tanker Accidents and Malfunctions in Browning Entrance and Principe Channel: Potential Marine Effects on Gitxaała Traditional Lands and Waters of a Spill During Tanker Transport of Bitumen from the Northern Gateway Pipeline Project (NGP). JFK Law Corporation, Counsel to Gitxaała First Nation, Vancouver, B.C.

Etkin, D.S., McCay, D.F., and Michel, J. 2007. Review of the State-Of-The-Art on Modeling Interactions Between Spilled Oil and Shorelines for the Development of Algorithms for Oil Spill Risk Analysis Modeling. US Department of the Interior Minerals Management Services & Environmental Research Consulting, Cortlandt Manor, N.Y.

Etkin, D.S., Michel, J., McCay, D., Boufadel, M., and Li, H. 2008. Development of a Practical Methodology for Integrating Shoreline Oil-Holding Capacity Into Spill Modeling. *In* Proceedings of the 31st Arctic and Marine Oilspill Program Technical Seminar. Calgary, AB, **31**: 564–583.

Etkin, D.S. 2015. Risk Analysis and Prevention. *In* Handbook of Oil Spill Science and Technology. *Edited by* M. Fingas. Wiley Publishing Co. Edmonton, AB.

Etkin, D.S., Joeckel, J., Walker, A., Scholz, D., Moore, C., Baker, C., Hatzenbuhler, D., Patton, R., Lyman, E., and Culpepper, D. 2015. Washington State 2014 Marine and Rail Oil Transportation Study. Washington State Department of Ecology. Seattle, WA.

Fetter, C.W. 2001. Applied Hydrology. Fourth Ed. Prentice-Hall Inc., New Jersey, N.J.

Fingas, M. 2006. The Density Behaviour of Heavy Oils in Freshwater: the Example of the Lake Wabamun Spill. Arctic and Marine Oilspill Program Technical Seminar, 1–21.

Fingas, M. 2013. The basics of oil spill cleanup. Third Ed. CRC Press Taylor & Francis Group. Boca Raton, FL.

Fingas, M. 2015a. Introduction to Spill Modeling. *In* Handbook of Oil Spill Science and

Technology. *Edited by* M. Fingas. Wiley Publishing Co. Edmonton, AB.
Fingas, M. 2015b. Estimation of Saturate, Aromatic, Resin and Asphaltene (SARA) Values From Readily-Available Oil Properties. *In* Proceedings of the Thirty-Eighth Arctic and Marine Oilspill Program Technical Seminar. Vancouver, BC. **38:** 193–206.
Fingas, M. 2015c. Introduction to Oil Chemistry and Properties. *In* Handbook of Oil Spill Science and Technology. *Edited by* M. Fingas. Wiley Publishing Co., Edmonton, AB.
Fingas, M. 2015d. Review of the Properties and Behaviour of Diluted Bitumens. *In* Proceedings of the Thirty-Eighth Arctic and Marine Oilspill Program Technical Seminar. Vancouver, BC. **38:** 470–494.
Fingas, M. 2015e. Handbook of Oil Spill Science and Technology. *In* Handbook of Oil Spill Science and Technology, John Wiley & Sons Inc., Edmonton, AB.
Floor, A. 2000. Oceanography: Waves. Available from http://www.seafriends.org.nz/oceano/waves.htm [accessed 25 February 2016].
Folk, R. 1974. Petrology of Sedimentary Rocks. Hemphill Publishing Company, Austin, TX.
Folk, R., and Ward, W. 1957. Brazos River Bar: A Study in the Significance of Grain Size Parameters. Journal of Sedimentary Research, **27**: 3–26.
Foster, L., Keller, P., McKee, B., and Ostry, A. 2010. The British Columbia Demographic Context. *In* British Columbia Atlas of Wellness. Western Geographical Press, Victoria, B.C.,
Freeze, A., and Cherry, J. 1979. Groundwater. Prentice-Hall, Inc., Englewood Cliffs, N.J.
French-McCay, D.P. 2004. Oil Spill Impact Modeling: Development and Validation. Environmental Toxicology and Chemistry, **23**: 2441–2456.
Geng, X., Boufadel, M.C., Lee, K., Abrams, S., and Suidan, M. 2014. Biodegradation of Subsurface Oil in a Tidally Influenced Sand Beach: Impact of Hydraulics and Interaction with Pore Water Chemistry. Water Resources Research, **51**: 3193–3218.
Gerhard, J.I., Pang, T., and Kueper, B.H. 2007. Time Scales of DNAPL Migration in Sandy Aquifers Examined Via Numerical Simulation. Ground Water, **45**: 147–157.
GOC (Government of Canada). 2013. Properties, Composition and Marine Spill Behaviour, Fate and Transport of Two Diluted Bitumen Products From the Canadian Oil Sands. Federal Government Technical Report En 84-96, Ottawa, ONT.
Google Inc. 2016. Google Earth. Available from http://www.google.com/earth/.
Green, W., and Ampt, G. 1911. Studies on Soil Physics: Part I.- The Flow of Air and Water Through Soils. Journal of Agricultural Science, **4**: 1–24.
Gregory, J., Dukes, M., Miller, G., and Jones, P. 2005. Analysis of Double-Ring Infiltration Techniques and Development of a Simple Automatic Water Delivery System. Applied Turfgrass Science, **12**: 1-7.
Gundlach, E. 1987. Oil-Holding Capacity and Removal Coefficients for Different Shoreline Types to Computer Simulated Spills in Coastal Water. *In* International Oil Spill Conference Proceedings, Vol. 1987, Narragansett, R.I., **1**, 451-457
Gunter, P. 2009. Challenges of Heavy Oil Response, Impacts: The Particularities of Heavy Oil Response. *In* Proceedings of Interspill. Marseille, France. 1-13.
Hajek, E., Huzurbazar, S., Mohrig, D., Lynds, R., and Heller, P. 2010. Statistical Characterization of Grain-Size Distributions in Sandy Fluvial Systems. Journal of Sedimentary Research, **80**: 184–192.
Hammecker, C., Razzouk, R., Maeght, J., and Grünberger, O. 2005. Water Infiltration in

Saline Sandy Soils. *In* Management of Tropical Sandy Soils for Sustainable Agriculture. Khon Kaen, Thailand. 474–478.

Harper, J. 1980. Seasonal Changes in Beach Morphology Along the B.C. Coast: National Research Council of Canada, Association Committee for Research on Shoreline Erosion and Sedimentation. *In* The Canadian Coastal Conference. Burlington, ONT, 136–150.

Harper, J., Sergy, G., and Sagayama, T. 1995. Surface Oil in Coarse Sediment Experiments (SOCSEX II). Victoria, B.C.

Harper, J.R., Laforest, S., and Sergy, G. 2015. Field Investigations of Intertidal Sediment Permeability Related to Spilled Oil Retention in British Columbia Shorelines. *In* Proceedings of the 38th Arctic and Marine Oilspill Program Technical Seminar.Vancouver, B.C. **38**: 1689–1699.

Harper, J., Sergy, G., Britton, L., and Kory, M. 2016. Diluted Bitumen Sediment Interaction Experiments; Bit_Ex. Ottawa, ONT. 1-88.

Hazen, A. 1911. Discussion of Dams on Sand Foundations. Transactions of the American Society of Civil Engineers, 1911, Vol. LXXIII, **3**: 190-207

HIFM (Hydramotion Innovations in Fluid Measurement). 2015. Viscosity Equivalents Chart. Available from Hydramotion Background Briefing V-03. York, England.

Hollebone, B. 2015. Physical Properties. *In* Handbook of Oil Spill Science and Technology. *Edited by* M. Fingas. Wiley Publishing Co. Edmonton, AB.

Hossain, S.Z. 2016. Laboratory investigation of Diluted Bitumen Trapping and Dissolution in Gravel. M.Sc. thesis, Department of Civil Engineering, Queen's University, Kingston, ONT.

Hubbard, B., and Glasser, N. 2005. Field Techniques in Glaciology and Glacial Geomorphology. John Wiley & Sons, Inc. New Jersey, N.J.

Hudak, P.F. 2005. Principals of Hydrogeology, Third Ed. CRC Press, Washington, D.C.

Humphrey, B., and Harper, J.R. 1993. Coarse Sediment Oil Persistence Laboratory Studies and Model EC/TDTS--94-02286. *In* Proceedings of the 16th Arctic and Marine Oil Spill Program Technical Seminar Victoria, BC., **16**: 1-10.

IEA (International Energy Agency), and OECD (Organisation for Economic Co-Operation and Development). 2016. Key World Energy Statistics. *In* International Energy Agency. Paris, France. 1-80.

Imhoff, P.T., Mann, A.S., Mercer, M., and Fitzpatrick, M. 2003. Scaling DNAPL Migration From the Laboratory to the Field. Journal of Contaminant Hydrology, **64**: 73–92.

ITC (International Trade Center). 2015. Trade Map - List of Products Exported by Canada. Available from http://www.trademap.org/Product_SelCountry_TS.aspx?nvpm=1%7C124%7C%7C%7C%7CTOTAL%7C%7C%7C2%7C1%7C1%7C2%7C2%7C1%7C1%7C1%7C [accessed 12 June 2015].

ITOPF (The International Tanker Owners Pollution Federation Limited). 2015. Oil Tanker Spill Statistics. Longdon, England. 1-20

James, T., Gowan, E., Hutchinson, I., Clague, J., Barrie, J., and Conway, K. 2009. Sea-Level Change and Paleogeographic Reconstructions, Southern Vancouver Island, B.C. Quaternary Science Reviews, **28**: 1200–1216.

Joeckel, J., Walker, A.H., Scholz, D., Hatzenbuhler, D.L., Lyman, E.J., and Patton, R.G.

2015. New Risks From Crude-By-Rail Transportation. *In* Proceedings of the 38th Arctic and Marine Oil Spill Program Technical Seminar. Vancouver, BC. **38**: 900–923.

Johnson, A. 1963. A Field Method for Measurement of Infiltration. United States Government Printing Office, Paper 1544-F, Washington, D.C.

Jury, W., and Horton, R. 2004. Soil Physics. Sixth Ed. John Wiley & Sons, Inc., New Jersey, N.J.

King, T., Robinson, B., Boufadel, M., and Lee, K. 2014. Flume Tank Studies to Elucidate the Fate and Behavior of Diluted Bitumen Spilled at Sea. Marine Pollution Bulletin, 1-6.

KM (Kinder Morgan). 2015. Kinder Morgan-TMX Expansion. Available from http://www.kindermorgan.com/pages/business/canada/tmep.aspx [accessed 12 June 2015].

Knödel, K., Lange, G., and Voigt, H.-J. 2007. Environmental Geology: Handbook of Field Methods and Case Studies. Springer. Berlin, Germany.

Laforest, S., Lambert, P., Harper, J., and Sergy, G. 2017. Meso-Scale Studies on the Penetration and Retention of Diluted Bitumen in Different Types of Shorelines, Northern British Columbia, Canada. *In* International Oil Spill Conference. Long Beach, CA, 1–18.

Laing, A., Gemmill, W., Magnusson, A., Burroughs, L., Reistad, M., Khandekar, M., Holthuijsen, L., Ewing, J., and Carter, D. 1998. Guide to Wave Analysis. 2 Ed. World Meteorological Organization (WMO-No. 702). Geneva, Switzerland.

Lee, K., Stoffyn-Egli, P., Tremblay, G.H., Owens, E.H., Sergy, G.A., Guénette, C.C., and Prince, R.C. 2003. Oil-Mineral Aggregate Formation on Oiled Beaches: Natural Attenuation and Sediment Relocation. Spill Science and Technology Bulletin, **8**: 285–296.

Li, Z., and Amorelli, A. 2016. Informing Choices for Meeting China's Energy Challenges. Springer, Berlin, Germany.

Lin, Q. 2015. Oil spill impact and recovery of coastal marsh vegetation. *In* Handbook of Oil Spill Science and Technology. *Edited by* M. Fingas. Wiley, Edmonton, AB. 477–982.

LO (Living Oceans). 2013. Taxpayers Would Foot Most of the Bill for a Spill. Available from http://www.livingoceans.org/media/news/taxpayers-would-foot-most-the-bill-spill?language=en [accessed 11 March 2016].

Masselink, G., and Hughes, M. 2003. Introduction to Coastal Processes & Geomorphology. Cambridge University Press, Cambridge, UK.

McGowan, E., Song, L., and Hasemyer, D. 2016. The Dilbit Disaster: Inside the Biggest Oil Spill You've Never Heard of. CreateSpace Independent Publishing Platform, Brooklyn, N.Y.

McKnight, D., Boufadel, M., Fingas, M., Hamilton, S., Harris, O., Hayes, J., Michel, J., Mitchelmor, C., Reed, D., Sussman, R., Valentine, D., Bem, D., Walt, D., Abruña, H., Barrish, J., Barteau, M., Brennecke, J., Buchanan, M., Christianson, D., Curtis, J., Eisenberg, R., Gellman, S., Glotzer, S., John, M., Ligler, F., Mills, S., Rossky, P., Swager, T., Mitchelmore, C., Reed, D., Sussman, R., Valentine, D., Friedman, D., Tran, C., Anderson, C., Brown, C., Mathona, N., Bem, D., Walt, D., Abruna, H., Barrish, J., Barteau, M., Brennecke, J., Buchanan, M., Christianson, D., Vurtis, J.,

Eisenberg, R., Gellman, S., Glotzer, S., John, M., Ligler, F., Mills, S., Powell, J., Rossky, P., and Swager, T. 2015. Spills of Diluted Bitumen From Pipelines: A Comparative Study of Environmental Fate, Effects, and Response. *Edited by* T. Leschine and M. Ladisch. National Academies Press. Washington, D.C.

Melalia, A.M. 1993. The Relation Between Soil Infiltration and Effective Porosity in Different Soils. Agricultural Water Management, **24**: 39–47.

Michel, J. 2011. Submerged Oil. *In* Oil Spill Science and Technology: Prevention, Response, and Cleanup. *Edited by* M. Fingas. Elsevier. Burlington, MA, 959–981.

Michel, J., Owens, E.H., Zengel, S., Graham, A., Nixon, Z., Allard, T., Holton, W., Reimer, P.D., Lamarche, A., White, M., Rutherford, N., Childs, C., Mauseth, G., Challenger, G., and Taylor, E. 2013. Extent and Degree of Shoreline Oiling: Deepwater Horizon Oil Spill, Gulf of Mexico, USA. PLOS One, **8**: 1–9.

MOE (Ministry of the Environment). 2015. Environmental Emergency Management Program-Burnaby Oil Spill. Available from http://www.env.gov.bc.ca/eemp/incidents/2007/burnaby_oil_spill_07.htm [accessed 20 May 2006].

Mohanty, B.P., Kanwar, R.S., and Everts, C.J. 1994. Comparison of Saturated Hydraulic Conductivity Measurement Methods for a Glacial-Till Soil. Soil Science Society of America Journal, **58**: 672-677.

Moldestad, M., Daling, S., and Leirvik, F. 2004. The Prestige Oil–Properties and Weathering at Sea. *In* Proceedings of Interspill, Trondheim, Norway. 1-15.

Mosher, D.C., and Hewitt, A.T. 2004. Late Quaternary Deglaciation and Sea-Level History of Eastern Juan de Fuca Strait, Cascadia. Quaternary International, **121**: 23–39.

Muñoz, J., Ancheyta, J., and Castañeda, L. 2016. Required Viscosity Values to Assure Proper Transportation of Crude Oil by Pipeline. ACS Paragon Plus Environment: Energy and Fuels,: 1-19.

Nimmo, J. 2004. Porosity and Pore Size Distribution. Encyclopedia of Soils in the Environment. Elsevier, London, Englad, **3**: 295–303.

Nimmo, J.R., Schmidt, K.M., Perkins, K.S., and Stock, J.D. 2009. Rapid Measurement of Field-Saturated Hydraulic Conductivity for Areal Characterization. Vadose Zone Journal, **8**: 142.

NRC (National Research Council). 2013. Effects of Diluted Bitumen on Crude Oil Transmission Pipelines. Committee for a Study of Pipeline Transportation of Diluted Bitumen; Transportation Research Board; Board on Energy and Environmental Systems; Board on Chemical Sciences and Technology; National Research Council (TRB Special Report 311). Washington, D.C.

NRPG (Nuka Research & Planning Group LLC.). 2013. West Coast Spill Response Study: Volume 3: World Class Oil Spill Prevention, Preparedness, Response & Recovery, Seldovia, AK.

Onur, E. 2014. Predicting the Permeability of Sandy Soils From Grain Size Distributions. M.Sc. thesis, Department of Geology, Kent State University, Kent, OH.

Owens, E. 1985. Factors Affecting the Persistence of Stranded Oil on Low Energy Shorelines. *In* International Oil Spill Conference. Aberdeen, U.K. 359-365.

Owens, E., Taylor, E., and Humphrey. 2008. The Persistence and Character of Stranded Oil on Coarse-Sediment Beaches. Marine pollution bulletin, **56**: 14–26.

Peterson, C., Rice, S., Short, J., Ester, D., Bodkin, J., Ballachey, B., and Irons, D. 2003.

Long-Term Ecosystem Response to the Exxon Valdez Oil Spill. Science, **302**: 2082–2086.

PGLEC (PGL Consultants Environmental). 2015. Potential Effects of Diluted Bitumen Spills on Salmonid Specis. PGL Consultants Environmental: Hearing Order OH-001-2014, Vancouver, B.C.

Philibert, D.A., Philibert, C.P., Lewis, C., and Tierney, K.B. 2016. Comparison of Diluted Bitumen (Dilbit) and Conventional Crude Oil Toxicity to Developing Zebrafish. Environmental Science and Technology, **50**: 6091–6098.

Philips, E.C., and Kitch, W.A. 2011. A Review of Methods for Characterization of Site Infiltration With Design Recommendations. 43rd Symposium on Engineering Geology and Geotechnical Engineering, Los Angeles, CA: 23–25.

Pliakas, F., and Petalas, C. 2011. Determination of Hydraulic Conductivity of Unconsolidated River Alluvium From Permeameter Tests, Empirical Formulas and Statistical Parameters Effect Analysis. Water Resour Manage, **25**: 2877–2899.

Polaris. 2013. A Comparison of the Properties of Diluted Bitumen Crudes With Other Oils (Ex5510-000026-CRK). Bainbridge Island, WA. 1–26.

Prins, M., Vriend, M., Nugteren, G., Vandenberghe, J., Lu, H., Zheng, H., and Weltje, G. 2007. Late Quaternary Aeolian Dust Input Variability on the Chinese Loess Plateau: Inferences From unmixing of loess grain-size records. Quaternary Science Reviews, **26**: 230–242.

Rawle, A. 2011. Basic Principles of Particle Size Analysis. Malvern Instruments Limited, Worcestershire, UK, 1-8

Rodríguez, J., and Uriarte, A. 2009. Laser Diffraction and Dry-Sieving Grain Size Analyses Undertaken on Fine and Medium Grained Sandy Marine Sediments: A Note. Journal of Coastal Research, **251**: 257–264.

Salarashayeri, A., and Siosemarde, M. 2012. Prediction of Soil Hydraulic Conductivity From Particle-Size Distribution. International Journal of Environmental, Chemical, Ecological, Geological and Geophysical Engineering, **6**: 16–20.

Santos, R., Loh, W., Bannwart, A., and Trevisan, O. 2014. An Overview of Heavy Oil Properties and its Recovery and Transportation Methods. Brazilian Journal of Chemical Engineering, **31**: 571–590.

Scheffers, A., Scheffers, S., and Kelletat, D. 2015. The Coastlines of the World with Google Earth: Understanding Our Environment. Springer, New York, N.Y.

Sergy, G. 2016. Response Guidance for Diluted Bitumen Spills Impacting Marine Shorelines of Northern British Columbia. Contract Report prepared by S3 Environmental and Coastal and Ocean Resources for Emergencies Science and Technology Section. Environment Canada, Ottawa, ONT. 1-54.

Sergy, G., Guénette, C., Owens, E., Prince, R., and Lee, K. 2003. In-Situ Treatment of Oiled Sediment Shorelines. Spill Science and Technology Bulletin, **8**: 237–244.

Shigenaka, G. 2011. Effects of Oil in the Environment. *In* Oil Spill Science and Technology: Prevention, Response, and Cleanup. Gulf Professional Publishing, Burlington, MA, 985–1024.

Short, J. 2013. Susceptibility of Diluted Bitumen Products from the Alberta Tar Sands to Sinking in Water. Juneau, AK

Short, J., Lindeberg, M., Harris, P., Maselko, J., Pella, J., and Rice, S. 2004. Estimate of Oil Persisting on the Beaches of Prince William Sound 12 Years After the Exxon

Valdez Oil Spill. Environmental Science and Technology, **38**: 19–25.
SLRoss. 2012. Meso-Scale Weathering of Cold Lake Bitumen/Condensate blend. National Energy Board, Calgary, AB.
Smith, K., and Mullins, C. 2000. Soil and Environmental Analysis: Physical Methods. 2nd Ed. CRC Press Taylor & Francis Group, Washington, D.C.
Spaulding, M.L. 1988. A State-Of-The-Art Review of Oil Spill Trajectory and Fate Modeling. Oil and Chemical Pollution, **4**: 39–55.
Sperry, J., and Peirce, J. 1995. A Model for Estimating the Hydraulic Conductivity of Granular Material Based on Grain Shape, Grain Size, and Porosity. Ground Water, **33**: 892–898.
Steers, J.A. 1969. Coast and Beaches. Oliver & Boyd, Edinburgh, UK.
Svensson, A. 2014. Estimation of Hydraulic Conductivity From Grain Size Analyses. M.Sc. thesis, Department of Civil and Environmental Engineering, Chalmers University of Technology, Göteborg, Sweden
TC (Transport Canada). 2013. A Review of Canada's Ship-Source Oil Spill Preparedness and Response Regime-Setting the Course for the Future. Tanker Saftey Panel Secretariat, Ottawa, ONT.
TC (Transport Canada). 2015. Trans Mountian Expansion Project Reply Evidence. National Energy Board, Ottawa, ONT.
Terich, T.A. 1987. Living With the Shore of Puget Sound and Georgia Strait. Duke University Press, Durham, WA.
Thomas, K. 1990. Beach-Surf Zone Morphology Along a Wave-Dominated Coast. PhD, Faculty of Marine Sciences, Cochin University of Science and Technology, Kochi, India.
Thomson, R. 1981. Juan de Fuca Strait. *In* Oceanography of the British Columbia Coast. Canadian Special Publication of Fisheries and Aquatic Science, Sidney, B.C.
TSBC (Transporation Saftey Board of Canada). 2014. Lac-Mégantic Runaway Train and Derailment Investigation Summary. Transportation Safety Board of Canada: Railway Investigation Report R13D0054, Ottawa, ONT, 1-12
Vereecken, H., Binley, A., Cassiani, G., Revil, A., and Titov, K. 2006. Applied Hydrogeophysics. *In* Applied Hydrogeophysics. Springer in cooperation with NATO Public Diplomacy Division. Petersburg, Russia, 1–9.
Viles, H., and Spencer, T. 1995. Coastal Problems: Geomorphology Ecology and Society at The Coast. Edward Arnold, London.
Wang, Z., Hollebone, B., Fingas, M., Fieldhouse, B., Sigouin, L., Landriault, M., Smith, P., Noonan, J., Thouin, G., and Weaver, J. 2003. Characteristics of Spilled Oils, Fuels, and Petroleum Products: Composition and Properties of Selected Oils. US Environmental Protection Agency Publication and National Exposure Research Laboratory, Research Triangle Park, N.C. 1–286.
WCMRC (Western Canada Marine Response Corporation). 2012. Western Canada Marine Response Corporation Information Handbook. Burnaby, BC
Winter, J., and Haddad, R. 2014. Ecological Impacts of Dilbit Spills: Considerations for Natural Resource Damage Assessment. *In* Proceedings of the 38th Arctic and Marine Oilspill Program Technical Seminar. Vancouver, B.C. **38**: 1-27.
WO (Witt O'Brien's). 2013. A Study of Fate and Behavior of Diluted Bitumen Oils on Marine Waters. Gainford, AB.

Workman, D. 2015. Canada's Top 10 Exports- World's Top Exports. Available from http://www.worldstopexports.com/canadas-top-exports/2502 [accessed 12 June 2015].

Worldatlas. 2016. Outlined map of North America, Map of North America. Available from http://www.worldatlas.com/webimage/countrys/namerica/naoutl.htm [accessed 11 March 2016].

Xia, Y., Li, H., Boufadel, M., and Sharifi, Y. 2010. Hydrodynamic Factors Affecting the Persistence of the Exxon Valdez Oil in a Shallow Bedrock Beach. Water Resources Management, **46**: 1–17.

Yapa, P. 2013. Modeling Oil Spills to Mitigate Coastal Pollution. *In* Handbook of Environmental Fluid Dynamics: Systems, Pollution, Modeling, and Measurements. *Edited by* H.J.S. Fernando. CRC Press Taylor & Francis Group. Washington, D.C.

Yorath, C. 2005. The geology of Southern Vancouver Island. Harbour Publishing Co. Ltd. Madeira Park, B.C